No universal support for solar glare as an evolutionary driver of malar stripes in falcons

Michelle Vrettos

Thesis presented for the degree of Master of Science
in the Fitzpatrick Institute of African Ornithology, Department of Biological Sciences, University of Cape Town

Supervisors: A/Prof. Arjun Amar, Dr. Chevonne Reynolds

August 2022

No universal support for solar glare as an evolutionary driver of malar stripes in falcons

Michelle Vrettos

Thesis presented for the degree of Master of Science in the Fitzpatrick Institute of African Ornithology, Department of Biological Sciences, University of Cape Town

Supervisors: A/Prof. Arjun Amar, Dr. Chevonne Reynolds

August 2022

PLAGIARISM DECLARATION

1. I know that plagiarism is wrong. Plagiarism is to use another's work and pretend that it is one's own.

2. I have used the Harvard convention for citation and referencing. Each contribution to, and quotation in, this report from the work(s) of other people has been attributed, and has been cited and referenced.

3. This thesis is my own work.

4. I have not allowed, and will not allow, anyone to copy my work with the intention of passing it off as his or her own work.

Name: Michelle Vrettos

Signature: Signed by candidate

Date: 29/08/2022

DEDICATION

This work is dedicated to my parents, Lyn and Basil Vrettos, for their endless support and encouragement throughout the challenges of completing my dissertation, and especially for their love and support during the turmoil and uncertainty of the COVID-19 lockdown. I would also like to dedicate this work to late Johan Schlebush, who provided me with invaluable opportunities to develop my science communication skills and share my research through involvement with BirdLife South Africa and the Cape Bird Club's Youth Education Programme, and who inspired me with his passion for nature and dedication to education and outreach.

ACKNOWLEDGEMENTS

With special thanks to A/Prof. Arjun Amar and Dr. Chevonne Reynolds for their oversight, guidance, and assistance with this project, as well as to A/Prof. Patrick Marais for his assistance in exploring automated methods of quantifying falcon malar stripe characteristics (despite these turning out to be unfeasible for this project). I would also like to extend special thanks to Kyle Walker and Mike J. McGrady for providing their photographs of Taita and Sooty Falcons upon request, and to Prof. Robert P. Freckleton, Prof. Håvard Rue, Prof. Finn Lindgren, A/Prof. Res Altwegg, and especially A/Prof. Russell Dinnage for assisting with the statistical analysis. I would also like to thank the curators and staff of the Macaulay Library at the Cornell Laboratory of Ornithology and the Global Biodiversity Information Facility photographic databases, and all the amateur observers and 'citizen scientists' who contributed their images to the web.

ABSTRACT

The paired dark malar or moustachial stripes of falcons (*Falco* spp.) are putatively adaptive plumage features whose function and evolutionary significance are poorly understood, and have rarely been investigated in published literature. A popular hypothesis for the function of falcon malar stripes is that they serve as antiglare devices, with the dark pigment absorbing vision-impeding solar glare and thereby improving the falcon's ability to visually detect and target prey in bright conditions. Correlative evidence from Peregrine Falcons (*Falco peregrinus*) provides support for this hypothesis, with a previous study finding that the size and prominence of malar stripes in this species correlate positively with solar radiation across the species' geographic range. In the present study, I extend the methodology used in this previous research to all extant species in the genus *Falco*, to determine both whether other falcon species display similar intraspecific trends, and whether differences in solar radiation conditions, in conjunction with species ecology, explain interspecific variation in falcon malar stripe characteristics. My results indicated that malar stripe characteristics were not positively related to solar radiation in the majority of species, with only the Peregrine Falcon showing reliable trends towards larger and darker malar stripes in individuals inhabiting regions of higher solar radiation. Likewise, solar radiation was not positively related to interspecific variation in falcon malar stripe characteristics, even after accounting for differences in body size, agility, prey base, and habitat between species. These results suggest that falcon malar stripes do not universally function as antiglare devices, at least in species other than the Peregrine Falcon. Malar stripes thus likely evolved in falcons for a different purpose (such as crypsis or social signaling), but may have become exapted for solar glare reduction in Peregrine Falcons owing to the species' cosmopolitan distribution and high degree of specialization on agile bird prey.

TABLE OF CONTENTS

1. INTRODUCTION

1.1. FUNCTIONS OF AVIAN COLOURATION PATTERNS: OVERVIEW

Avian colouration and markings serve multiple adaptive functions (Burtt 1981; Burtt 1986; Ortolani 1999; Bortolotti 2006; Pérez-Rodríguez et al. 2017; Romano et al. 2019). While hypotheses for the functions of such markings have typically focused on natural selection as the evolutionary driver behind colouration patterns (Bortolotti 2006), hypotheses involving socio-sexual functions, such as intraspecies communication and signalling, have recently begun to receive more attention in the literature (Bortolotti 2006; Pérez-Rodríguez et al. 2017). However, due to the complex physiological processes associated with pigmentation, colouration patterns may be subject to multiple, often opposing, selective forces (Cuthill et al. 2017; Gomes et al. 2018; Romano et al. 2019). The evolved plumage pattern of an individual or species may thus represent the outcome of tradeoffs between several biotic and abiotic pressures (Cuthill et al. 2017; Gomes et al. 2018; Romano et al. 2019). This is further complicated by both developmental factors (Price and Pavelka 2002; Bortolotti 2006) and pleiotropic effects of genes associated with pigmentation (Chakarov et al. 2008; Gangoso et al. 2011), which may promote or inhibit the evolution of particular integument colours or patterns (Price and Pavelka 2002; Bortolotti 2006; Romano et al. 2019). Thus, determining the functional significance of, or evolutionary drivers behind, particular bird colouration patterns or markings is frequently difficult (Cuthill et al. 2017; Gomes et al. 2018; Romano et al. 2019).

Burtt (1981; 1986) identifies four principal types of hypotheses for functions of animal colouration patterns: physical, optical, identity, and visual (Burtt 1981; 1986). Physical hypotheses purport that the functional or adaptive significance of the colouration pattern depends on the physical, chemical, or molecular properties of the pigments themselves, such as their radiation absorption spectra or strength of chemical bonds (Burtt 1981; 1986). For example, melanic feathers are considerably mechanically and structurally stronger than their unpigmented counterparts, and thus dark colouration or markings may help to protect the bird's integument from abrasive or ectoparasite damage (Barrowclough and Sibley 1980; Bergman 1982; Burtt 1986; Bonser 1995; Ward et al. 2002; Burtt and Ichida 2004). This has been advanced to explain the prevalence of black wing tips or trailing edges in birds with otherwise light plumage, such as gulls (Averill 1923; Bergman 1982), since feather wear is most pronounced in the outer primaries due to their continuous contact with airborne particles during flight (Bergman 1982; Burtt 1986). In keeping with this hypothesis, Barrowclough and Sibley (1980) found that the unpigmented primaries in a partial albino Yellow-rumped Warbler (*Dendroica coronata*) were smaller in length and area than the pigmented feathers, consistent with reduced resistance to feather wear (Barrowclough and Sibley 1980). Reduced risk of feather damage from dust and particulate matter has also been proposed to explain the prevalence of all-black plumage in birds inhabiting desert environments (Burtt 1986; Ward et al. 2002), as well as the greater frequency of dark-morph Swainson's Hawks (*Buteo swainsonii*) in drier areas (Amar et al. 2019).

Physical or metabolic benefits to melanisation are also hypothesised to underlie broad ecogeographical trends such as Gloger's and Bogert's rules (Gloger 1833; Bogert 1949; Burtt and Ichida 2004; Clusella-Trullas et al. 2007; Delhey 2018; Galván et al. 2018; Delhey 2019; Amar et al. 2019; Romano et al. 2019; Marcondes et al. 2020; Marcondes et al. 2021; Goldenberg et al. 2022). In its most common interpretation, Gloger's rule predicts that individuals occurring in wetter or more humid environments should be darker-coloured than those inhabiting drier environments (Gloger 1833; Rensch 1936; Delhey 2019; Marcondes et al. 2020; Marcondes et al. 2021). This is frequently attributed to increased parasite loads in wetter or more humid regions, with darker colouration expected to confer a selective advantage due to both protection against ectoparasite and bacterial damage (Burtt and Ichida 2004; Marcondes et al. 2020) and immune advantages pleiotropically linked to pigmentation (Chakarov et al. 2008; Gangoso et al. 2011; Lei et al. 2016). In a comparable manner, Bogert's rule predicts that darker individuals should be associated with colder environments (Bogert 1949; Clusella-Trullas et al. 2007). This is attributed to the heat- and light-absorbing properties of dark pigments, which increase the rate of heat transfer to the body and thus reduce the need for metabolic heat generation, thereby minimising the energetic costs of thermoregulation at low temperatures (Heppner 1970; Mosher and Henny 1976; Ellis 1984; Galván et al. 2018; Amar et al. 2019; Goldenberg et al. 2022). In keeping with both rules, Romano et al. (2019) found that Barn Owls (*Tyto alba* species complex) exhibit larger eumelanic breast spots and darker pheomelanin-based breast colouration in colder and rainier regions (Romano et al. 2019), while similar trends towards darker plumage in cool and wet conditions have also been observed intraspecifically in Variable Antshrikes (*Thamnophilus caerulescens*) (Marcondes et al. 2020), and interspecifically in ovenbirds (Furnariidae) (Marcondes et al. 2021) and Australian landbirds (Delhey 2018). The thermal benefits to dark colouration are also hypothesised to increase flight efficiency in birds with dark-coloured wings, as hotter wing surfaces result in reduced skin friction drag, and dark feather pigmentation therefore provides a selective advantage by increasing the rate at which the wing absorbs heat (Rogalla et al. 2019).

Optical hypotheses for animal colouration patterns propose that the pattern functions by affecting the animal's visibility to other individuals or species, for example by enhancing crypsis or deterring predators (Burtt 1986). For instance, Galeotti et al. (2003) argue that plumage polymorphism in accipitrid raptors may be explained by colouration serving a cryptic or background-matching function, with darker-coloured individuals experiencing greater hunting success in low light conditions due to their ability to camouflage against dark skies (Galeotti et al. 2003). This "light level-detectability hypothesis" (Galeotti et al. 2003; Amar et al. 2013; Tate et al. 2016) has been advanced to explain the reversed morph frequencies found in Black Sparrowhawks (*Accipiter melanoleucus*) in the Cape Peninsula, where ~75% of the population are dark or melanistic morphs, compared to the rest of the species' range, where the more typical white-chested morph dominates (Amar et al. 2013; Tate et al. 2016). Uniquely among southern African ecoregions, the Cape Peninsula experiences a winter rainfall regime, and thus melanistic Black Sparrowhawks may experience greater hunting success in this region during their winter breeding season due to enhanced crypsis in the low light conditions associated with rainfall and cloud cover (Amar et al. 2013; Tate et al. 2016). The opposite is expected to be true for white-chested morphs in summer rainfall regions, due to superior camouflage against bright or clear

winter skies (Amar et al. 2013; Tate et al. 2016). In keeping with this hypothesis, Tate et al. (2016) found that solar radiation or light levels predict spatial structuring of Black Sparrowhawk morph frequencies (Tate et al. 2016). The same study also found that melanistic morphs have greater hunting success in lower light conditions, whereas white-chested morphs are more successful in bright conditions (Tate et al. 2016). Background-matching has also been advanced to explain the association between dark plumage and forested environments in other species (Marcondes et al. 2020), and even as a potential driver behind Gloger's rule, as darker individuals presumably experience more effective crypsis in the low light conditions and dense vegetation cover associated with high rainfall and humidity (Zink and Remsen 1986; Delhey 2019; Marcondes et al. 2020; Marcondes et al. 2021).

Colouration patterns or markings may also enhance crypsis by disguising the bird's outline or obscuring key features, reducing detectability by predators or prey, or else by producing a disruptive effect that may disorient predators, prey, or ectoparasites (Stevens 2007; Caro et al. 2014). Such a function has been proposed for the head and breast markings in plovers (Charadriiformes: Charadriidae), which may serve as disruptive colouration to break up the outline of the bird or obscure the distinction between the bird and surrounding objects, thereby reducing detectability to predators (Graul 1973). This is corroborated by the observation that plover species that nest on discontinuous substrates tend to have dark breast bands, while those that nest on uniform substrates overwhelmingly lack breast bands (Graul 1973). Evidence from non-avian taxa likewise suggests a potentially disruptive role for high-contrast striping or banding markings, with pelage striping in zebras (Equidae) hypothesised to reduce visibility to biting flies such as tabanids and tsetse flies (Caro et al. 2014). Ectoparasite avoidance is also proposed by Chakarov et al. (2008) as a potential role for pale plumage colouration in Common Buzzard (*Buteo buteo*) nestlings, since tsetste flies and other haematophagous dipterans typically prefer landing on dark or black surfaces (Chakarov et al. 2008). Likewise, since eyes are a common target of visual search patterns, markings or patterning around the eyes may enhance crypsis by disguising the eye (Barlow 1972; Gavish and Gavish 1981; Josef 2017). Experiments using human observers (Gavish and Gavish 1981) found that the visual detectability of bird eyes is strongly reduced by the presence of dark markings which bisect or partially incorporate the eye, suggesting that these markings prevent visual detection of the eye by predators or prey (Gavish and Gavish 1981). This cryptic role for dark eye markings is corroborated by Barlow's (1972) observation that the angle of the eye-line in fish corresponds to body shape, with deep-bodied species with sloping foreheads typically exhibiting vertical eye-lines, while more elongate species exhibit horizontal eye-lines or longitudinal striping (Barlow 1972), consistent with the hypothesis that these markings serve to obscure the eye and break up the visual outline of the head, reducing visibility to predators (Barlow 1972). However, colouration may serve an even more dramatic optical function: in Barn Owls, white ventral plumage is associated with longer freezing times in prey and greater hunting success under full moon conditions, suggesting that reflectance of moonlight against the white feathers creates a "dazzle" effect that stuns or disorients prey (San-Jose et al. 2019).

Identity hypotheses for animal colouration patterns, in contrast, state that the colouration pattern functions in signalling some aspect of the animal's identity to potential mates, competitors, or

predators (Burtt 1986). For example, carotenoid-based colouration in passerines is hypothesised to signal male fitness or mate quality, with the size or brightness of red or yellow plumage patches serving as indicators of an individual's genetic quality, immune function, and body condition due the high metabolic costs involved in the synthesis of carotenoid pigments (Dale 2006; Cooney et al. 2019). Several studies on Great Tits (*Parus major*) have demonstrated that the white cheek patches function similarly as intraspecific signals of individual quality and social dominance, with brighter or more immaculate white cheek patches indicative of higher social status and greater individual fitness or quality (as more immaculate patches indicate reduced damage from conspecific aggression or ectoparasites) (Ferns and Hinsley 2004; Galván and Sanz 2007). Contrasting colouration patterns or markings adjacent to these visual signals, such as the black cap in American Goldfinches (*Carduelis tristis*) and the black facial mask in Great Tits (Ferns and Hinsley 2004; Galván and Sanz 2007), may likewise serve as 'amplifiers' which enhance the appearance of the quality-signalling colouration pattern, reducing perceptual errors by the signal receiver in assessing the true quality or appearance of the trait, or even producing an optical illusion which artificially boosts the perceived brightness or saturation of the quality-signalling colour (Dale 2006). Colouration or marking patterns may likewise function to communicate information regarding the bearer's sex, breeding strategy, or territoriality, or even enable individual recognition between mates, kin, or members of social groups (Dale 2006). However, colouration patterns and markings may also serve as forms of deceptive signalling: Negro et al. (2007) argue that the ocelli (eye-like patches) found on the back of the head in many raptor species may serve to signal the appearance of a "false face" to prey, thereby provoking a mobbing response and allowing the predator to flush out prey (Negro et al. 2007).

Visual hypotheses for animal colouration patterns refer to those in which the colouration pattern is hypothesised to aid the animal's own vision (Burtt 1986). For example, Ficken and Wilmot (1968) propose that the dark horizontal 'eye-lines' found in many insectivorous passerines, most notably the wood-warblers (Passeriformes: Parulidae), may serve as visual guides to enable the bird to aim at and strike fast-moving prey (Ficken and Wilmot 1968). A test of this hypothesis in North American songbirds found a strong correlation between the presence of dark eye-lines and a diet consisting of fast-moving prey, such as flying insects, while comparison of insectivorous vireos and warblers to granivorous sparrows likewise found facial markings to be consistently more complex in the former than in the latter (Ficken and Wilmot 1968; Ficken et al. 1971). Ficken et al. (1971) extend this hypothesis both to other bird groups that typically exhibit dark eye-lines and feed on fast-moving prey, such as grebes, mergansers, and herons, and to non-avian predators, such as pickerels, ranids, and tree snakes (Ficken et al. 1971). In particular, they argue that the slanting or angled eye-lines found in many waterbirds may serve as sighting lines on prey prior to diving, or correct for light refraction by the water to enable accurate targeting of underwater prey (Ficken et al. 1971). However, Ficken et al. (1971) also suggest that eye-lines may serve additional visual functions other than aiming at prey, with the rearward-facing eye-lines in European woodcocks (*Scolopax rusticola*) and subocular stripes in Eurasian bitterns (*Botaurus stellaris*) hypothesised to instead serve as "sighting lines" that enhance visual detection of predators (Ficken et al. 1971).

1.2. THE SOLAR GLARE HYPOTHESIS FOR THE FUNCTION OF DARK EYE MARKINGS

Dark markings around or under the eyes are frequently hypothesised to serve a visual function by reducing the obstructive effects of solar glare on vision (Ficken and Wilmot 1968; Ficken et al. 1971; Densley 1979; Ortolani 1999; De Broff and Pahk 2003; Bortolotti 2006; Josef 2017; Lebow 2020; Vrettos et al. 2021). Scattering of sunlight produces glare, which negatively interferes with vision by depositing additional, non-information-containing light onto the retinal image, reducing visual contrast between objects and thus compromising the subject's ability to detect detail and distinguish objects from the background (De Broff and Pahk 2003). This impedes the subject's ability to visually detect and target objects, and may especially impede the ability to track moving objects as their velocity relative to that of the subject increases or decreases (De Broff and Pahk 2003). Since dark surfaces and melanin pigments intrinsically absorb light, dark markings around or under the eyes may counteract these negative effects of solar glare on vision by absorbing excess sunlight, preventing it from being reflected into the eyes as glare (De Broff and Pahk 2003; Vrettos et al. 2021), and thereby increasing the animal's ability to discern and target food objects in bright conditions (Ficken and Wilmot 1968; Ficken et al. 1971; Ortolani 1999; De Broff and Pahk 2003; Bortolotti 2006; Josef 2017; Lebow 2020; Vrettos et al. 2021). This hypothesis, termed the "solar glare hypothesis" by Vrettos et al. (2021), thus purports that dark eye markings serve as an adaptation to increase foraging efficiency in animals inhabiting bright environments (Ficken and Wilmot 1968; Ficken et al. 1971; Densley 1979; Ortolani 1999; Bortolotti 2006; Josef 2017; Lebow 2020; Vrettos et al. 2021).

Correlative and experimental evidence from a variety of animal taxa provides support for this hypothesis. For example, Ficken et al. (1971) noted that dark patches or stripes around the eyes are disproportionately found in bird and mammal species that inhabit bright environments, such as deserts and open water (Ficken et al. 1971). Similarly, Ortolani (1999) argued that the dark eye-patches and facial masks found in many mammalian carnivores are likely to serve a glare-reducing function, based on the observation that such markings are associated with species that occur in riparian habitats (where glare is likely to be highest due to reflection off the water surface), and exhibit crepuscular behaviour (and thus forage at the time of day when the sun is directly parallel to the visual field, likewise increasing glare) (Ortolani 1999). However, this was contested by Newman et al. (2005), who argued that these markings were more likely to serve an aposematic or predator-deterring function (Newman et al. 2005). Burtt (1986) found that the eye-lines and upper mandibles of wood-warbler (Parulidae) species that inhabit bright environments are consistently darker-coloured than would be predicted based on the colouration of other body surfaces that are outside the visual field, consistent with selection for darker colouration in regions around or below the eyes (Burtt 1986). Burtt (1984) also found that painting the upper mandibles of Willow Flycatchers (*Empidonax trailli*) with lightening polish caused the birds to shift their foraging behaviour to more shaded locations, mimicking the natural foraging behaviour of species with naturally light-coloured bills, while the proportion of commuting ("give-up") flights when foraging in sunlight was also significantly higher among experimental birds than in dark-billed controls (Burtt 1984). Yosef et al. (2012) observed similar trends in

Masked Shrikes (*Lanius nubicus*), in which birds with white-painted facial masks hunted facing away from the sun more frequently than did those with natural black masks, and also exhibited reduced hunting efficiency in sunlight compared to control birds, although their hunting success recovered after removal of the white paint (Yosef et al. 2012). Quantitative measurements of the amount of irradiance reflected into the eyes of avian museum specimens under natural light conditions (Lebow 2020) likewise showed a significant relationship between the size and position of dark facial patches and reduction in irradiance, both when the eye faced directly into the sun and when it was rotated up to 45º away from the sun (Lebow 2020). Ophthalmological studies in humans likewise corroborate the efficacy of dark eye or under-eye markings in reducing negative effects of solar glare on vision: De Broff and Pahk (2003) found that application of commercially available "eye black" grease, such as that worn by athletes, significantly improved human subjects' sensitivity to contrast and detail and ability to track moving objects in bright sunlight conditions (De Broff and Pahk 2003).

1.3. THE SOLAR GLARE HYPOTHESIS IN THE CONTEXT OF FALCON MALAR STRIPES

Falcons are diurnal raptors in the genus *Falco* (Falconiformes: Falconidae). A characteristic feature of species in this genus is the presence of paired dark vertical stripes extending below the eyes, termed malar or moustachial stripes (Ferguson-Lees and Christie 2001; Bortolotti 2006; Josef 2017; Vrettos et al. 2021). These stripes vary considerably in size and colour both between and within falcon species, and have even been used as diagnostic characteristics to define geographic races in Peregrine Falcons (*Falco peregrinus*) (White and Boyce 1988). Falcon malar stripes are frequently claimed to function as antiglare devices (Bortolotti 2006; Josef 2017; Vrettos et al. 2021), but this hypothesis has received little attention in the scientific literature, and has never been tested interspecifically (Vrettos et al. 2021). Like other diurnal raptors, falcons rely predominantly on vision to hunt, and as a result exhibit highly developed visual faculties (Hirsch 1982; Jones et al. 2007; Mitkus et al. 2018; Potier et al. 2020). Falcons are also notable for their speed and agility: most species exhibit long, pointed wings for rapid flight in pursuit of agile prey, while the Peregrine Falcon is commonly regarded as the fastest living terrestrial animal species, as it is able to reach up to 320 km/h in aerial stoops or dives in pursuit of prey (Ferguson-Lees and Christie 2001). Thus, solar glare may be expected to provide a significant hindrance to the ability of falcons to locate and target prey, as their heavy reliance on vision, fast hunting speeds, and diurnal lifestyles mean that they must effectively discriminate and target fast-moving objects in bright sunlight as their own velocity relative to the object increases rapidly (Vrettos et al. 2021).

Bortolotti (2006) argued that the solar glare hypothesis was unlikely to explain the evolutionary and functional significance of falcon malar stripes (Bortolotti 2006). This is because, per Bortolotti (2006), interspecific differences in malar stripe characteristics appear to suggest a relationship with solar radiation opposite to that expected under the solar glare hypothesis, with species inhabiting brighter environments exhibiting smaller and paler malar stripes, or even

lacking them entirely (Bortolotti 2006). In particular, Bortolotti (2006) noted that the Saker Falcon (*Falco cherrug*), which occurs in desert habitats, has narrow and pale malar stripes, while the Orange-breasted (*F. deiroleucus*) and Bat Falcons (*F. rufigularis*), both tropical forest species, have solid black malar plumage (Bortolotti 2006). However, Vrettos et al. (2021) argued that Bortolotti's example does not consider that phylogenetic differences are likely to underlie much of the interspecific variation in malar stripe characteristics among falcons, while ecological differences between species, such as body size and diet, may also affect the strength of selection for glare-reducing facial markings (Vrettos et al. 2021). As Vrettos et al. (2021) argue, the Saker Falcon feeds largely on mammals and typically catches its prey on the ground, whereas Orange-breasted and Bat Falcons specialize in hunting agile, aerial prey (Vrettos et al. 2021), and therefore presumably experience stronger selection for adaptations that increase their ability to track and target moving objects visually while looking directly into the sun (Vrettos et al. 2021). Thus, Vrettos et al. (2021) argue, solar radiation, phylogeny, and species ecology need to be considered synergistically when assessing the predictions of the solar glare hypothesis between species (Vrettos et al. 2021).

Vrettos et al. (2021) undertook a correlative test of the solar glare hypothesis in the most widespread falcon species, the Peregrine Falcon (*Falco peregrinus*). They found that intraspecific variation in malar stripe characteristics in this species was consistent with the predictions of the hypothesis, with populations inhabiting regions of higher solar radiation exhibiting wider and darker malar stripes, and overall darker or more hooded heads (Vrettos et al. 2021). The authors tested the solar glare hypothesis using web-sourced, 'citizen science' photographs of Peregrine Falcons taken across the species' geographic range, with a total of 2197 individual birds analysed (Vrettos et al. 2021). For each bird in each photograph, the length, width, extent of plumage contiguity with the hood (i.e., extent of dark plumage in the area between the malar stripe and the hood), and prominence of the malar stripe were quantified subjectively according to visual scales, with birds assigned scores of 1-10 based on the size and prominence of their malar stripes (Vrettos et al. 2021). Relationships between malar stripe characteristics and climatic conditions (average annual solar radiation, average annual rainfall, and minimum average daily temperature) were then assessed using climatic data extracted from Google Earth Engine (Gorelick et al. 2017) for the coordinate location of each photograph. The authors found that solar radiation was a stronger predictor of geographic variation in malar stripe characteristics than were rainfall or temperature, and that all measures of malar stripe characteristics except length were positively related to solar radiation (Vrettos et al. 2021). These relationships were also found to be robust to the inclusion of both migratory and restored (hybrid) populations in the dataset, suggesting that the geographic trends in Peregrine Falcons towards larger and darker malar stripes in regions of higher solar radiation are strong enough to overcome these potentially disrupting effects (Vrettos et al. 2021). While this evidence is purely correlative and does not conclusively demonstrate that malar stripes in Peregrine Falcons serve a glare-reducing function, the trends found in this species are strongly suggestive of solar glare reduction being a major evolutionary driver of malar stripe characteristics in falcons (Vrettos et al. 2021).

1.4. RESEARCH AIMS

In the present study, I aim to extend the methodology and analysis presented by Vrettos et al. (2021) to all extant species in the genus *Falco*, to determine whether a) the intraspecific trends found in the Peregrine Falcon are reflected in other falcon species, and b) whether the solar glare hypothesis provides a plausible explanation for the evolution and function of falcon malar stripes across species. According to the predictions of the solar glare hypothesis, it is expected that the same trend of increasing malar stripe size and prominence with increasing solar radiation should be observed for most species (potentially excluding those with very restricted ranges, such as island endemics), and that there should also be positive interspecific relationships between average malar stripe size and prominence and average solar radiation, such that species which inhabit brighter environments exhibit larger and darker malar stripes after controlling for spatial effects and phylogeny.

In keeping with Vrettos et al.'s (2021) argument that differences in species ecology may affect the relative strength of selection on malar stripe characteristics under the solar glare hypothesis (with the benefits of glare-reducing malar stripes expected to be greatest for species that specialize in hunting fast, agile aerial prey in open environments), I also aim to test whether species traits relevant to the solar glare hypothesis, namely body size, hand-wing index, prey preference, hunting style, and habitat openness, are related to malar stripe characteristics across species, and whether adjusting for differences in these traits affects interspecific relationships with solar radiation. It is expected that fast-moving falcons and those specialized for hunting agile aerial prey in open environments should show stronger within-species relationships between solar radiation and malar stripe size and prominence, as well as exhibiting larger and darker malar stripes on average, relative to slower-moving or more generalist feeders and species inhabiting forested environments.

2. METHODS

2.1. PHOTOGRAPH SELECTION

I obtained photographs of adult falcons from two online 'citizen science' observation databases, the Macaulay Library at the Cornell Laboratory of Ornithology (https://www.macaulaylibrary.org) and the Global Biodiversity Information Facility (GBIF) (https://www.gbif.org). I performed a separate database search for each species, treating the Barbary Falcon (*Falco* (*peregrinus*) *pelegrinoides/babylonicus*) as a distinct species owing to its unresolved and contentious taxonomic position (Ferguson-Lees and Christie 2001; Fuchs 2015; McClure et al. 2020). In contrast, I treated the Eurasian Merlin, *Falco* (*columbarius*) *aesalon*, as conspecific with the North American Merlin for the purpose of this analysis, *contra* Fuchs (2015), largely because the taxonomy used by the databases did not permit separate queries for the two taxa. I thus obtained photographs for a total of 39 falcon taxa. For the Macaulay Library searches, observations were filtered to include only photographic observations and were ranked from highest to lowest quality (according to user ratings). If fewer than 10 000 observations were available for the species, I exported the metadata for all observations from the site as a single .csv file. However, since the Macaulay Library allows only the top 10 000 observations from each search query to be exported, this was not feasible for species for which there were over 10 000 photographs available. Thus, for these species, I split the database search by location, with separate searches performed for each country or island in which the species occurs, and the metadata from each of these searches downloaded as separate .csv files. For the GBIF searches, observations were filtered to include only photographic observations made by a human observer, and the metadata for all observations exported as a Darwin Core Archive (.zip file). I then merged the downloaded datasets from the Macaulay Library and GBIF, and filtered this combined dataset to exclude all photographs tagged as Juvenile or Immature. I also removed all photographs lacking location information. However, in the case of photographs that had textual location information available but no embedded GPS coordinates, the GPS coordinates of the general area were sourced from Google Maps and added to the photograph metadata.

I then converted the photograph datasets for each species into spatial point data frames using the R package sp (Pebesma and Bivand 2005), with the GPS coordinates of the photographs projected onto a generic world map projection using the World Geodetic System (WGS84) map projection system. For all non-sedentary species except the Peregrine Falcon, I clipped the spatial points data frames to include only observations that fell within the species' breeding and resident ranges, using species distribution map files downloaded from BirdLife International (2020) to define these species ranges (Table S1, Table S2). This was done to ensure that photographs depicting wintering or passage migrants, as well as out-of-range or vagrant birds, were excluded from analysis. For the Peregrine Falcon, I instead clipped the spatial points data frame to include observations that fell within the species' breeding, resident, passage, and/or wintering ranges, since the species distribution map provided by BirdLife International did not

reflect the true extent of the species' breeding range (for example, the map depicted the entire African continent as part of the species' wintering range only, despite the existence of a distinct African-breeding race (*Falco peregrinus minor*) (Hustler 1983; Jenkins 2000; Simmons et al. 2008; Töpfer et al. 2019; McPherson et al. 2020)). For the Eleonora's Falcon (*F. eleonorae*) and Sooty Falcon (*F. concolor*), which have highly restricted breeding ranges and for which few photographs were available, a 100 km buffer was added around the breeding range prior to clipping (Table S1). In the case of migratory species whose breeding and nonbreeding ranges overlap, photographs taken within the region(s) of overlap were then filtered by date to include only photographs taken within the migrant population's breeding season (based on information from Ferguson-Lees and Christie (2001) and Birds of the World (Billerman et al. 2020)), to exclude all wintering migrant birds (Table S1, Table S2). Birds identified by the photographer as belonging to sedentary or resident subspecies were excluded from this filtering process (Table S2). If fewer than 1500 photographs were available for the species after filtering, I then downloaded all available photographs. If more than 1500 photographs were available, however, I drew a random sample of up to 1000 photographs from the data frame, with a minimum distance constraint of 20 km specified to minimise the chance of pseudoreplication or geographically biased sampling (Table S1). I then downloaded the selected photographs for each species and filtered them manually to remove those of insufficient quality for analysis, as well as any depicting dead birds, nests, or eggs only. Photographs depicting misidentified falcons were reassigned to the correct species, or removed from the dataset, in the case of misidentified non-*Falco* raptors. For species in which juvenile or immature birds could be reliably distinguished from adults based on plumage characteristics (based on identification guides provided in Ferguson-Lees and Christie (2001) and Birds of the World (Billerman et al. 2020) (Table S3)), I also removed any photographs depicting non-adult birds from the dataset. I also sexed all individuals, for species in which males and females could be reliably distinguished using plumage characteristics (Table S3). To minimise pseudoreplication, I also removed photographs from the dataset if they were taken at the same GPS location and within a month of a previous photograph depicting the same species. However, photographs taken on similar dates and at the same or similar GPS locations were retained in the dataset if the birds depicted in the photographs could be reliably determined to be different individuals (e.g., if they were different subspecies or sexes, or identifiable based on colour rings or plumage characteristics). For species for which there were still > 1500 unsampled photographs available from the larger dataset following initial sampling, this sampling and filtering process was repeated multiple times until a total of 1000 photographs, or the maximum number of photographs for the species, was reached.

For all species represented by fewer than 100 photographs following this sampling and filtering process, additional images were sourced manually from Flickr (https://www.flickr.com), Oiseaux (https://www.oiseaux.net), BirdGuides (https://www.birdguides.com), and the African and Oriental Bird Club Image Databases (https://africanbirdclub.org/afbid and https://www.orientalbirdimages.org, respectively) (Table S1). As in the initial sampling process, I obtained only photographs taken within the breeding or resident range of the species (and within the migrant breeding season, for species in which the ranges of migratory and resident populations overlap), and excluded all images that were taken at the same GPS location and within a month of a photograph already in the dataset. For the Sooty Falcon and the Taita Falcon

(*F. fasciinucha*), for which very few online photographs were available, additional photographs for analysis were also provided by private photographers via email correspondence (see Acknowledgements for details).

2.2. MALAR STRIPE ANALYSIS

I analysed malar stripe characteristics using a subjective visual scoring method adapted from Vrettos et al. (2021). Prior to scoring, all photographs were cropped to include only the head of the bird (if a photograph included multiple birds, these were cropped and saved separately, and treated as separate observations), to remove any location context provided by the bird's immediate surroundings which could introduce unconscious observer bias. I then pooled the cropped photographs into a single folder and shuffled them into a random order, to ensure that I was not immediately aware of the geographic location or even species of any of the birds during the scoring process. I then visually scored the malar stripe of each photographed bird according to a set of visual scoring guides adapted from Vrettos et al. (2021). Following Vrettos et al. (2021), I quantified the following three aspects of the malar stripe:

Length: The vertical or dorsoventral extent of the malar stripe, measured from the base of the bird's eye to the base of the neck (Figure 1).

Width: The horizontal or anterior-posterior extent of the malar stripe, measured from the nare to the ear coverts (Figure 1).

Contiguity with the hood: The extent of plumage continuity or "contiguity" between the malar stripe and the hood, measured as the amount of dark plumage in the region immediately posterior to the stripe, or between the stripe and the hood (Figure 1).

However, to measure malar stripe prominence, I split the Prominence variable used by Vrettos et al. (2021) into two variables, which I scored separately:

Darkness: The (achromatic) value or intensity of the malar stripe, measured by converting the image to greyscale and subjectively estimating the tonal value of the stripe (Figure 1).

Solidity: The approximate density of dark feathers within the area bounded by the malar stripe, or the apparent tonal uniformity of the stripe (Figure 1).

Each of the variables was scored on an eleven-point visual scale (based on the ten-point visual scales used by Vrettos et al. (2021), with a 0 score added to account for birds lacking the feature in question or for which no score could be assigned), with higher scores representing more positive values (larger, darker, or more solid malar stripes) (Figure 2). Birds that completely lacked malar stripes were given scores of 0 for all variables. Since some species, most notably the Fox (*Falco alopex*), Greater (*F. rupicoloides*) , Grey (*F. ardosiaceus*), and Dickinson's Kestrels (*F. dickinsoni*), lacked clearly definable malar stripes, and since visual measurement of the malar stripe was difficult for birds with uniformly or near-uniformly dark plumage (e.g.,

Sooty Falcons, male Amur (*F. amurensis*) and Red-footed Falcons (*F. vespertinus*), and dark-morph Eleonora's Falcons), all birds were also assigned a binary score based on the uniformity of their plumage colouration (0 = non-uniform plumage, 1 = uniform plumage) (Table S1). This was done to enable these birds to be removed from the dataset and the analysis repeated on this reduced dataset to determine whether inclusion of uniform birds affected the results. Following Vrettos et al. (2021), the angle of the bird's head and degree of plumage distortion in each photograph were also scored according to a visual scale (Figure 3), to account for any visual distortion which could influence assessment of the malar stripe.

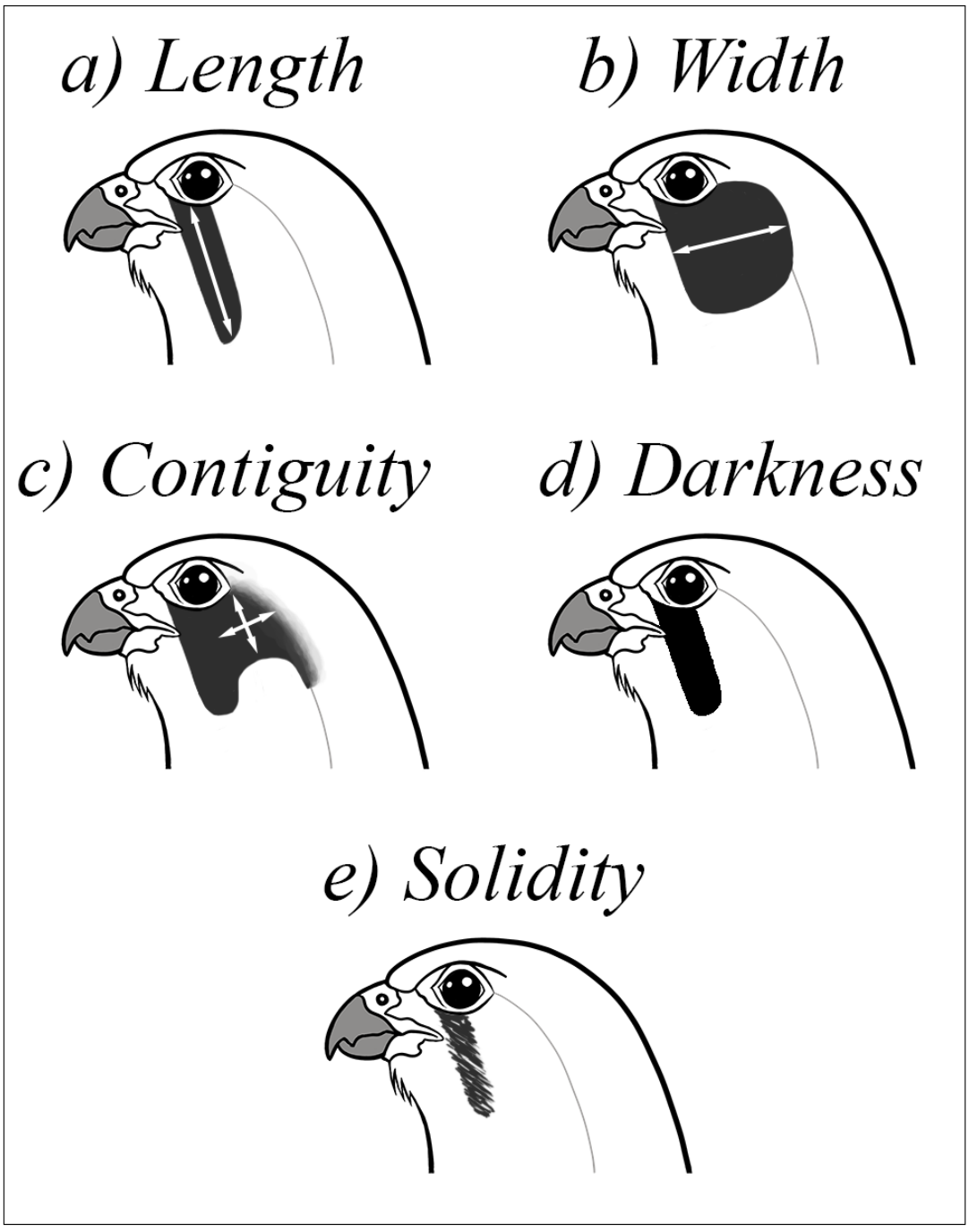

Figure 1. Illustration of the five malar stripe variables quantified in this study, namely **(a)** malar stripe length, **(b)** malar stripe width, **(c)** contiguity of the malar stripe width the hood, **(d)** malar stripe darkness, and **(e)** malar stripe solidity. Scoring variables and categories were adapted from those used by Vrettos et al. (2021).

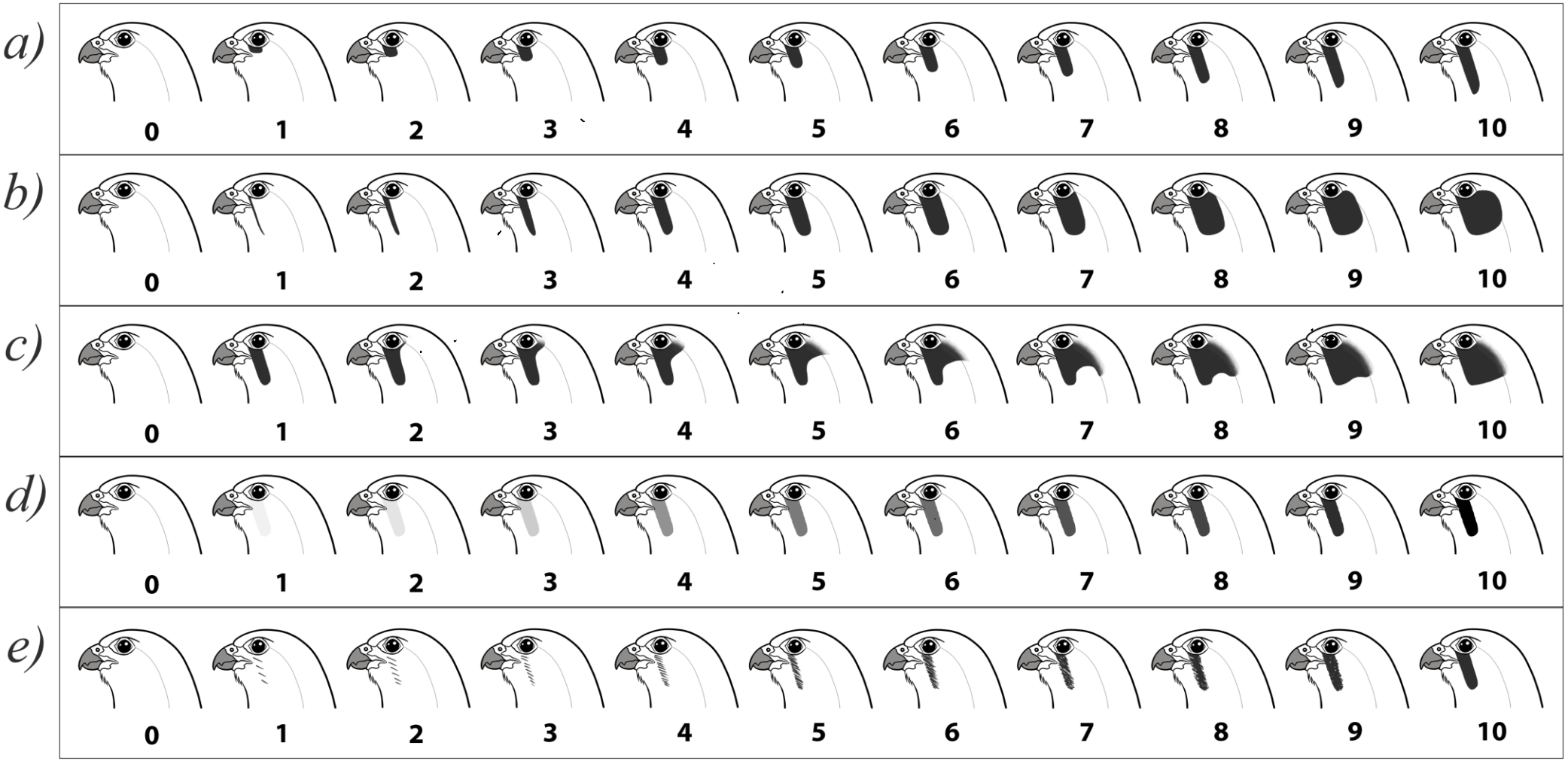

Figure 2. Eleven-point visual scales used to quantify variation in **(a)** malar stripe length, **(b)** malar stripe width, **(c)** contiguity of the malar stripe with the hood, **(d)** malar stripe darkness, and **(e)** malar stripe solidity in web-sourced photographs of falcons. Scoring variables and categories were adapted from those used by Vrettos et al. (2021).

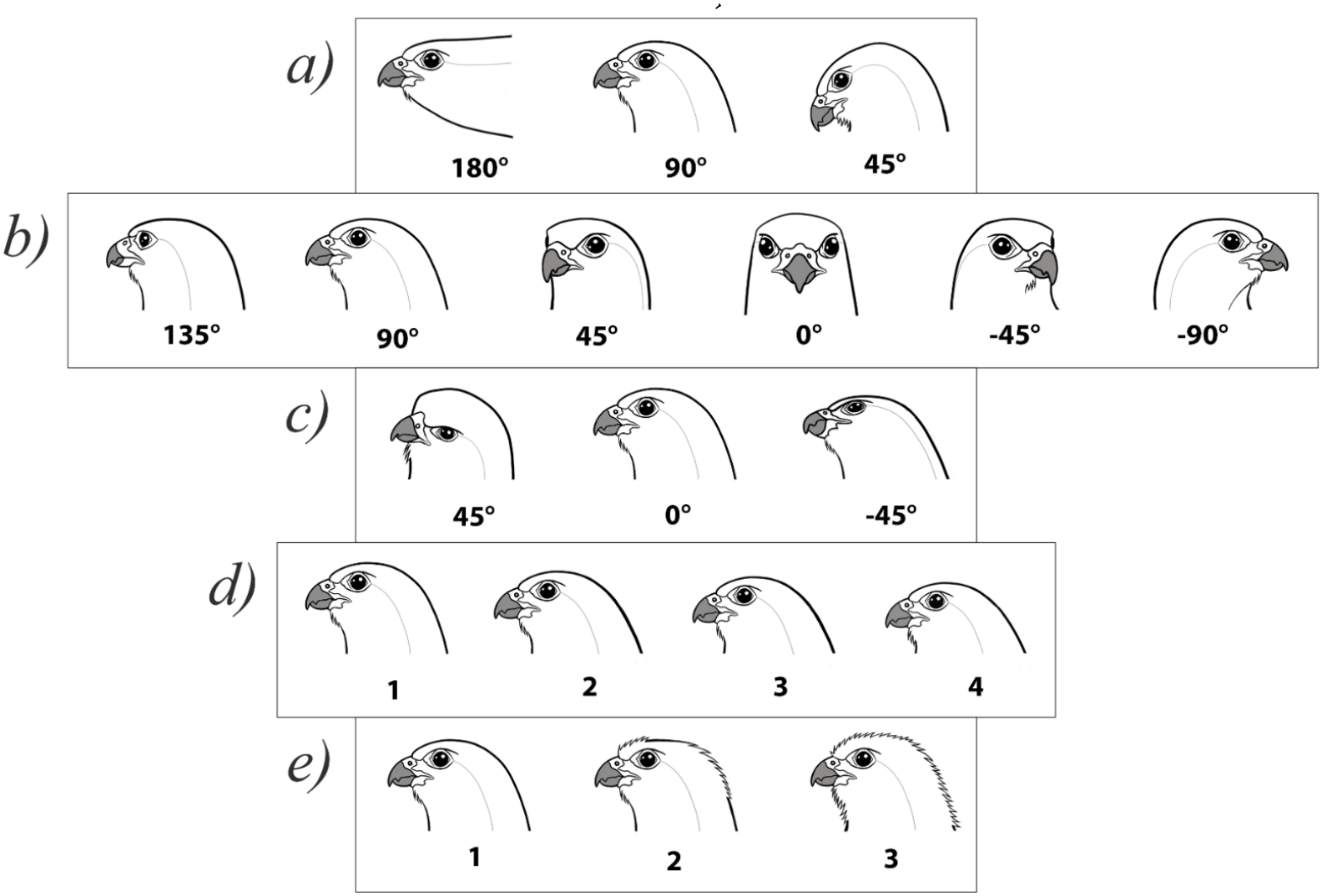

Figure 3. Illustration of and visual scales used to quantify and score head angle and degree of plumage distortion in web-sourced photographs of falcons, used to control for any potential visual distortion of the malar area which could influence assessment of malar stripe characteristics. Head angle variables scored include **(a)** head orientation in terms of pitch rotation, or rotation around the horizontal axis; (**b)** head orientation in terms of yaw rotation, or rotation around the vertical axis; and (**c)** head orientation in terms of roll rotation, or rotation around the anterior-posterior axis. Plumage distortion variables scored include (**d)** degree of plumage distortion as a result of vertical feather compression due to the bird sitting slumped or hunched, and (**e)** degree of plumage distortion as a result of ptiloerection. Scoring variables and categories were adapted from those used by Vrettos et al. (2021).

2.3. SOLAR RADIATION DATA

I extracted solar radiation data for each photograph GPS location from the TerraClimate dataset (Abatzoglou et al. 2018) using Google Earth Engine (Gorelick et al. 2017). The TerraClimate dataset provides monthly climate and climatic water balance data for global terrestrial surfaces at a spatial resolution of 4 km^2 (Abatzoglou et al. 2018). Since selective pressures exerted by environmental or climatic conditions are likely to be strongest during the breeding season (Amar et al. 2013; Tate et al. 2016), and since many of the species and populations represented in the analysis were migratory, I extracted solar radiation data only for the six-month period encompassing or containing the breeding season for each species, in most cases the spring-summer period. Prior to data extraction, I thus divided the photograph metadata into two datasets, one containing all species which breed between March and August (boreal summer breeders), and one containing species which breed between September and February (austral summer breeders) (Table S4). In the case of species with breeding populations both above and below the equator, all observations taken above 10º N or below 10º S were assigned to the boreal or austral datasets, respectively, while observations taken within the 10º N – 10º S equatorial band were assigned to whichever dataset was more suitable based on the breeding phenology of equatorial populations of the species (based on breeding season information provided in Ferguson-Lees and Christie (2001) and Birds of the World (Billerman et al. 2020)) (Table S4). If the breeding season of a species or population overlapped these two date ranges (for example, for species which breed between December and June), the species or population was assigned to whichever dataset exhibited the greater degree of overlap with the breeding season (Table S4). However, if the breeding season overlapped both date ranges equally, or if equatorial populations of the species exhibited latitudinal heterogeneity in their breeding phenology, observations were instead assigned to each dataset based on whether they lay above or below the equator, or other appropriate latitude cutoff for the species (Table S4). For both datasets, mean monthly downward surface shortwave radiation (hereafter solar radiation) (W/m^2) values were then extracted for the relevant six-month period over a 30-year-time scale (1991-2020). Monthly values were then averaged over each six-month period to obtain a single solar radiation value for each GPS point, representing the 30-year average for the relevant species' breeding period at that location.

2.4. SPECIES TRAIT DATA

For each of the 39 falcon taxa analysed, I collated data on five biometric and ecological traits – body mass, hand-wing index (HWI), prey, hunting style, and habitat - from Ferguson-Lees and Christie (2001), Roberts Birds of Southern Africa (Hockey et al. 2005), BirdLife International (2020), and AVONET (2022). Body mass (g) and hand-wing index (HWI) estimates were sourced from the AVONET database, based on literature values provided by Dunning (2008) and Sheard et al. (2020), respectively. However, for the Peregrine and Barbary Falcons, I instead independently calculated body mass estimates from Ferguson-Lees and Christie (2001) and

Dunning (2008) by averaging the values reported for different subspecies and sexes, since the AVONET estimates were based on analysis that treated the two taxa as conspecific (Dunning 2008). Body mass and HWI were used as proxies for falcon speed and agility, based on the observation that smaller body size enables raptors to hunt smaller, more agile prey, and the fact that higher hand-wing index is associated with increased flight efficiency, and therefore higher specialization for an active, aerial lifestyle (Sheard et al. 2020). To model prey preference, I assigned all species a score of 1-4 based on the proportion of birds in the diet (such that higher scores were assigned to species that exhibited a greater degree of specialization on bird prey), based on diet descriptions provided in Ferguson-Lees and Christie (2001) (Table S5). However, since Ferguson-Lees and Christie (2001) treated the Rock Kestrel (*Falco rupicolus*) as conspecific with the Common Kestrel (*F. tinnunculus*), I estimated a separate score for the former species based on descriptions of its diet in Roberts Birds of Southern Africa (Hockey et al. 2005) (Table S5). Similarly, I used the descriptions of hunting behaviour for each species provided in Ferguson-Lees and Christie (2001) to score the frequency of aerial hunting behaviour for each species on a scale of 1-4, with the highest score assigned to species that hunt predominantly by aerial chasing (Table S5), once again sourcing behaviour descriptions for the Rock Kestrel from Roberts Birds of Southern Africa (Hockey et al. 2005). To model habitat use, I converted the habitat descriptions provided in BirdLife International (2020) and Ferguson-Lees and Christie (2001) into scores of 1-5, in which species associated with more open habitats received higher scores (Table S5). As in the previous examples, I used the habitat description provided in Roberts Birds of Southern Africa (Hockey et al. 2005) to assign a score to the Rock Kestrel. I used this system over the habitat classification system provided in the AVONET database (Tobias et al. 2016) since that was based on relative habitat use across all bird species and assigned all falcon species the same score, and was therefore not useful for modelling differences in habitat use between falcon species.

2.5. STATISTICAL ANALYSIS

To analyse relationships between malar stripe characteristics, solar radiation, and species traits, I constructed Bayesian generalized linear mixed models (GLMMs) using R-INLA (Rue et al. 2009; Lindgren and Rue 2015). This approach uses the integrated nested Laplace approximation (INLA) method to estimate posterior distributions of model parameters, including latent random effects such as spatial dependence (Rue et al. 2009; Dinnage et al. 2020). Since solar radiation is a spatially varying variable, and thus the solar radiation values exhibited spatial autocorrelation (Dinnage et al. 2020), and since the species themselves were not phylogenetically independent, it was necessary to account for both spatial and phylogenetic effects in these models. I thus used the ‘spatiophylogenetic’ approach developed by Dinnage et al (2020), in which phylogenetic structure is incorporated into the model in the form of a precision matrix describing the inverse of the phylogenetic covariance between species pairs (Dinnage et al. 2020), while spatial effects are modelled using a stochastic partial differential equation (SPDE) approach, based on projection of the latitude and longitude coordinates of each datapoint onto a triangulated spatial

mesh (Lindgren and Rue 2015; Dinnage et al. 2020). Phylogenetic information was provided in the form of a multilocus consensus tree derived from Fuchs et al. (2015), which I converted into a variance-covariance matrix using the R package ape (Paradis and Schliep 2019) and then standardized by dividing by the matrix determinant raised to the power of 1/39 (i.e., 1 divided by the number of species in the phylogeny) (Dinnage et al. 2020). To model the spatial effect, I converted the latitude and longitude coordinates of the observations into locations on a spherical spatial mesh representing the globe surface, in which all datapoints were represented by a set of weights representing the distance to the three nearest mesh points (Dinnage et al. 2020). Following Dinnage et al. (2020), I used the default INLA prior (a Gaussian prior with mean = 0 and variance = 100) for the fixed effects, while for the spatial and phylogenetic random effects I used the same priors used by Dinnage et al. (2020), except for the mesh smoothness parameter, for which I used a value of 3/2 (indicating exponential smoothing) to account for the global coverage and clustered (non-random) spatial distribution of the data. For additional notes on the statistical models, see the supplementary material.

Since I was interested in assessing both interspecific and intraspecific relationships with solar radiation simultaneously, I used a contextual effects or "within-between" approach to model the solar radiation predictor (van de Pol and Wright 2009; Dinnage et al. 2018). In this approach, the predictor term is decomposed into a within-group (in this case, within-species) term, calculated by centering all individual values for the group on the group mean, or subtracting the group mean from each individual value, and a between-group (here between-species) term, representing the group (species) mean (van de Pol and Wright 2009; Dinnage et al. 2018). This method thus allowed simultaneous estimation of both the average within-species relationship across all species, and the between-species relationship, or the relationship between the species means. For each malar stripe (response) variable, I constructed three sets of models: a) a simple model, containing only the within-species and between-species solar radiation terms as fixed predictors; b) a set of additive models, containing the two solar radiation terms along with each of the trait variables; and c) interactive models, containing a first-order interaction between each solar radiation term and each of the trait variables. To account for any multicollinearity between the trait variables, I assessed these one at a time, such that each additive and interactive model contained only one trait variable along with the two solar radiation predictors. Models were fit with both phylogenetic and spatial random effects, along with random slope and intercept terms for each species, allowing estimation of separate relationships between malar stripe characteristics and solar radiation for each species. For species which exhibited considerable sexual dichromatism in facial plumage (i.e., the Common Kestrel, Lesser Kestrel (*Falco naumanni*), Amur Falcon, and Red-footed Falcon), males and females were coded as different species, allowing the model to estimate a different random slope for each sex and therefore preventing sex differences from biasing or obscuring relationships between malar stripe characteristics and solar radiation. Each model was also fit on both the full dataset and a subset of the data with uniform-plumaged birds removed, to assess whether the inclusion of birds that lacked clearly definable malar stripes affected the relationships observed. The head angle and plumage distortion variables were also included in all models as fixed effects to control for any effect of these on the response. All response and fixed effect variables were also standardized prior to model fitting to enable direct comparison between effect sizes. The body mass estimates

were also log-transformed prior to analysis to increase their normality and reduce potential outlier effects.

Predictor variables were considered to have a substantial effect on the response if the 95% credible interval for the marginal posterior distribution of the parameter did not overlap zero, or only marginally overlapped zero (Dinnage et al. 2020). Likewise, interactions between solar radiation and the trait variables were considered to be present only if the 95% credible interval for the marginal posterior distribution of the interaction term did not or only marginally overlapped zero (Dinnage et al. 2020). Since the trait variables were all measured at the species level, and the random slope estimates for each species were therefore not expected to vary between models, only the random slopes from the simple (solar radiation only) models were interpreted; species were considered to exhibit substantial relationships with solar radiation if the 95% credible intervals for the marginal posterior distributions of their random slopes did not substantially overlap zero (Dinnage et al. 2020). To model phylogenetic and spatial signal in malar stripe characteristics, and to assess the relative influences of the spatial and phylogenetic effects on the response variables, I followed Dinnage et al. (2020)'s method of calculating the standard deviation for both parameters, representing the predicted deviation from the average malar stripe value for each individual based on its phylogenetic or spatial position (Dinnage et al. 2020).

To corroborate the results of the INLA models, and to enable direct comparison with the results of Vrettos et al. (2021), I then extracted only those species that exhibited substantial relationships between malar stripe characteristics and solar radiation (95% credible intervals for the marginal posterior distributions of the random slope estimates did not or only marginally overlapped zero). I then used the nlme package (Pinhiero and Bates 2022) to construct Generalised Least Squares (GLS) linear regression models assessing the relationships between solar radiation and the malar stripe variables for these species, incorporating spatial effects using an exponential spatial autocorrelation structure (Dormann et al. 2007). The results of these models were then compared to those of the random slope models to determine the degree of congruence between frequentist and Bayesian estimates of the relationships for these species.

3. RESULTS

3.1. PHOTOGRAPH DATA

In total, I analysed 10 606 photographs, depicting 10 906 individual birds. The sample sizes varied widely between the species, with only four species represented by the maximum 1000 photographs, while 14 (over a third of the species in the dataset) were represented by fewer than 100 (Table 1). Nevertheless, usable photographs were obtained for all 39 species for which data were collected. The most well-represented species in the dataset were the American Kestrel (*Falco sparverius*) (1023 individuals), Peregrine Falcon (1013 individuals), Common Kestrel (1007 individuals), and Merlin (1003 individuals), while the most poorly represented species was the Taita Falcon (only 11 individuals) (Table 1). All major geographic regions were roughly equally represented in the dataset, albeit with a slight geographic bias towards North America, with 2134 observations from Africa (19.6% of the total dataset), 1578 from Asia (14.5%), 1707 from Europe (15.7%), 3170 from North America (29.1%), 1091 from South America (10.0%), and 1226 from Australasia (11.2%) (Figure 4). The best-represented countries were the United States and Canada, accounting for 1471 (13.5%) and 945 (8.7%) observations respectively, for a cumulative 22.15% of the total dataset. The time frame represented by the dataset was 1976-2021, although the bulk of the photographs (8823, or 80.9% of the total dataset) were taken post-2015; in contrast, only 18 (0.2%) were taken prior to 2000.

The majority of the birds in the dataset (7560, or 69.3% of all individuals) were unsexed. For the remaining 3346 birds, sex information was either provided by the photographer, or could be determined based on plumage characteristics (in the case of sexually dichromatic species) or contextual information (e.g., in the case of photographs depicting copulating pairs). Among these, there were nearly twice as many male as female birds, with 2124 males (19.5% of the total dataset, and 63.5% of all sexed birds) compared to 1222 females (11.2% of the total dataset, and 36.5% of all sexed birds). Birds with uniformly dark plumage accounted for 11.4% (N = 1238) of the individuals in the dataset, and 20.5% (N = 8) of the species (Table S1).

Table 1. Sample sizes (both number of photographs and number of individual birds) for each of the 39 falcon species in this study.

Species	Number of Photographs	Number of Individuals
American Kestrel (*Falco sparverius*)	1000	1023
Peregrine Falcon (*Falco peregrinus*)	1000	1013
Common Kestrel (*Falco tinnunculus*)	1000	1007
Merlin (*Falco columbarius*)	1000	1003
Bat Falcon (*Falco rufigularis*)	524	546
Red-necked Falcon (*Falco chicquera*)	514	546
Aplomado Falcon (*Falco femoralis*)	498	544
Lesser Kestrel (*Falco naumanni*)	419	444
Grey Kestrel (*Falco ardosiaceus*)	400	408
Orange-breasted Falcon (*Falco deiroleucus*)	368	380
Eurasian Hobby (*Falco subbuteo*)	349	351
Rock Kestrel (*Falco rupicolus*)	338	345
Brown Falcon (*Falco berigora*)	301	303
Lanner Falcon (*Falco biarmicus*)	278	292
Greater Kestrel (*Falco rupicoloides*)	255	274
Australian Kestrel (*Falco cenchroides*)	252	255
Prairie Falcon (*Falco mexicanus*)	246	246
Australian Hobby (*Falco longipennis*)	209	210
New Zealand Falcon (Kārearea) (*Falco novaeseelandiae*)	201	208
Red-footed Falcon (*Falco vespertinus*)	176	187
Madagascar Kestrel (*Falco newtoni*)	170	177
Eleonora's Falcon (*Falco eleonorae*)	118	121
Laggar Falcon (*Falco jugger*)	105	114
Dickinson's Kestrel (*Falco dickinsoni*)	107	111
Black Falcon (*Falco subniger*)	108	110
Saker Falcon (*Falco cherrug*)	95	96
Gyrfalcon (*Falco rusticolus*)	86	90
Barbary Falcon (*Falco (peregrinus) pelegrinoides*)	64	64
Spotted Kestrel (*Falco moluccensis*)	58	61
African Hobby (*Falco cuvierii*)	54	55
Amur Falcon (*Falco amurensis*)	50	52
Fox Kestrel (*Falco alopex*)	47	48
Grey Falcon (*Falco hypoleucos*)	43	47
Oriental Hobby (*Falco severus*)	40	41
Sooty Falcon (*Falco concolor*)	33	34
Banded Kestrel (*Falco zoniventris*)	33	33
Seychelles Kestrel (*Falco araeus*)	27	29
Mauritius Kestrel (*Falco punctatus*)	26	26
Taita Falcon (*Falco fasciinucha*)	11	11
Total	**10606**	**10906**

a)

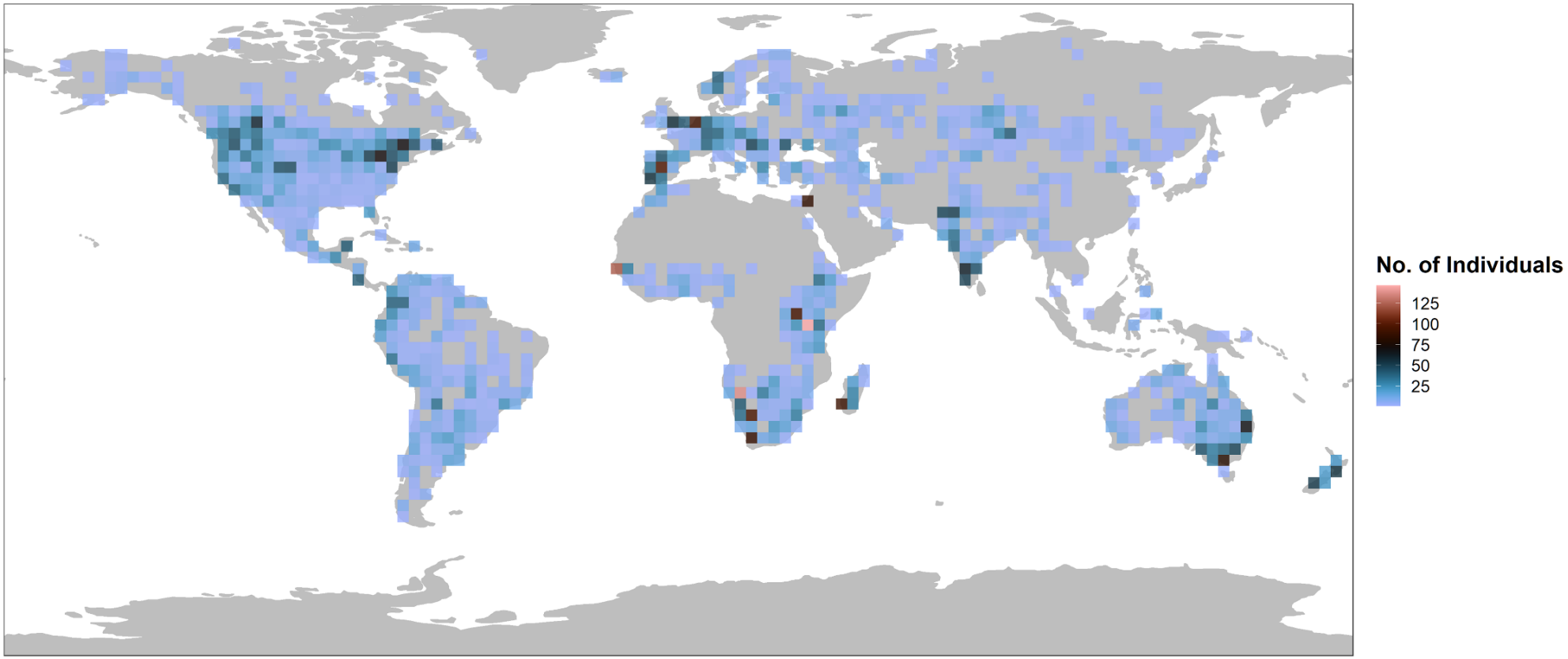

Figure 4a. Geographical distribution of the photographic observations used in this study, represented as the density of individual birds per 3 x 3 degree longitude/latitude grid square. Maps were constructed using the R package ggplot2 (Wickham 2016).

b)

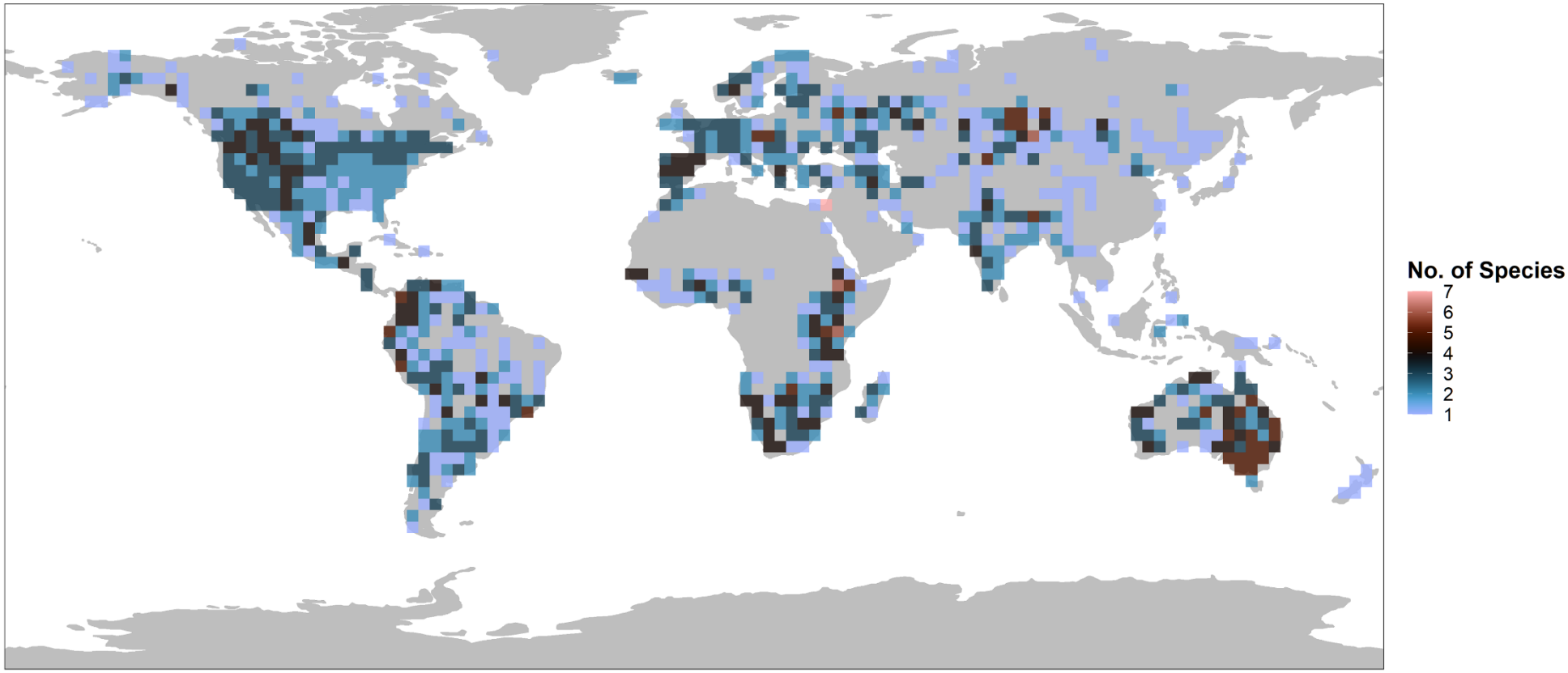

Figure 4b. Geographical distribution of the photographic observations used in this study, represented as the density of falcon species per 3 x 3 degree longitude/latitude grid square. Maps were constructed using the R package ggplot2 (Wickham 2016).

3.2. DESCRIPTIVE STATISTICS

Malar stripe scores were highly variable across species, although most demonstrated the same general interspecific pattern, with the highest mean scores exhibited by the Orange-breasted Falcon, Bat Falcon, and Oriental Hobby (*Falco severus*), and the lowest by the Dickinson's and Grey Kestrels (Figure 5). The exception to this trend was malar stripe length, with the Peregrine Falcon, Laggar Falcon (*Falco jugger*), and Prairie Falcon (*F. mexicanus*) exhibiting the longest malar stripes on average (Figure 5). Across all species, malar stripe length, darkness and solidity were all skewed towards higher values, with median values of 8 for all variables, and mean values of 7.9 (± 2.1), 7.7 (± 2.1), and 7.6 (± 2.5), respectively; in contrast, the width and contiguity scores were skewed towards lower values, with mean and median values of 4.7 (± 2.2) and 4, and 3.2 (± 2.7) and 2, respectively (Figure 5).

a)

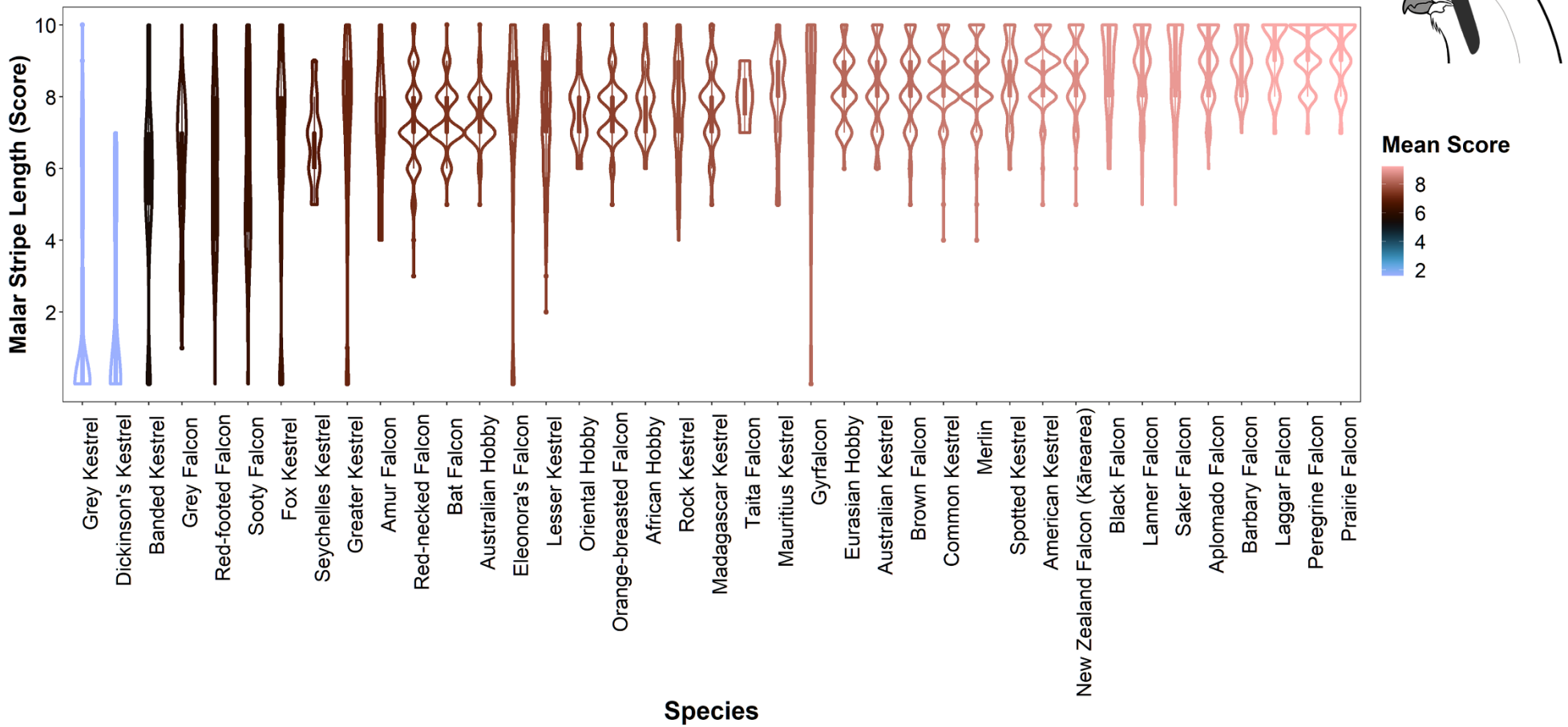

Figure 5a. Distribution of malar stripe length scores for each of the 39 falcon species in this study, with colours representing the mean score for each species. Species are arranged in ascending order of mean malar stripe length score. Plots were constructed using the R package ggplot2 (Wickham 2016).

b)

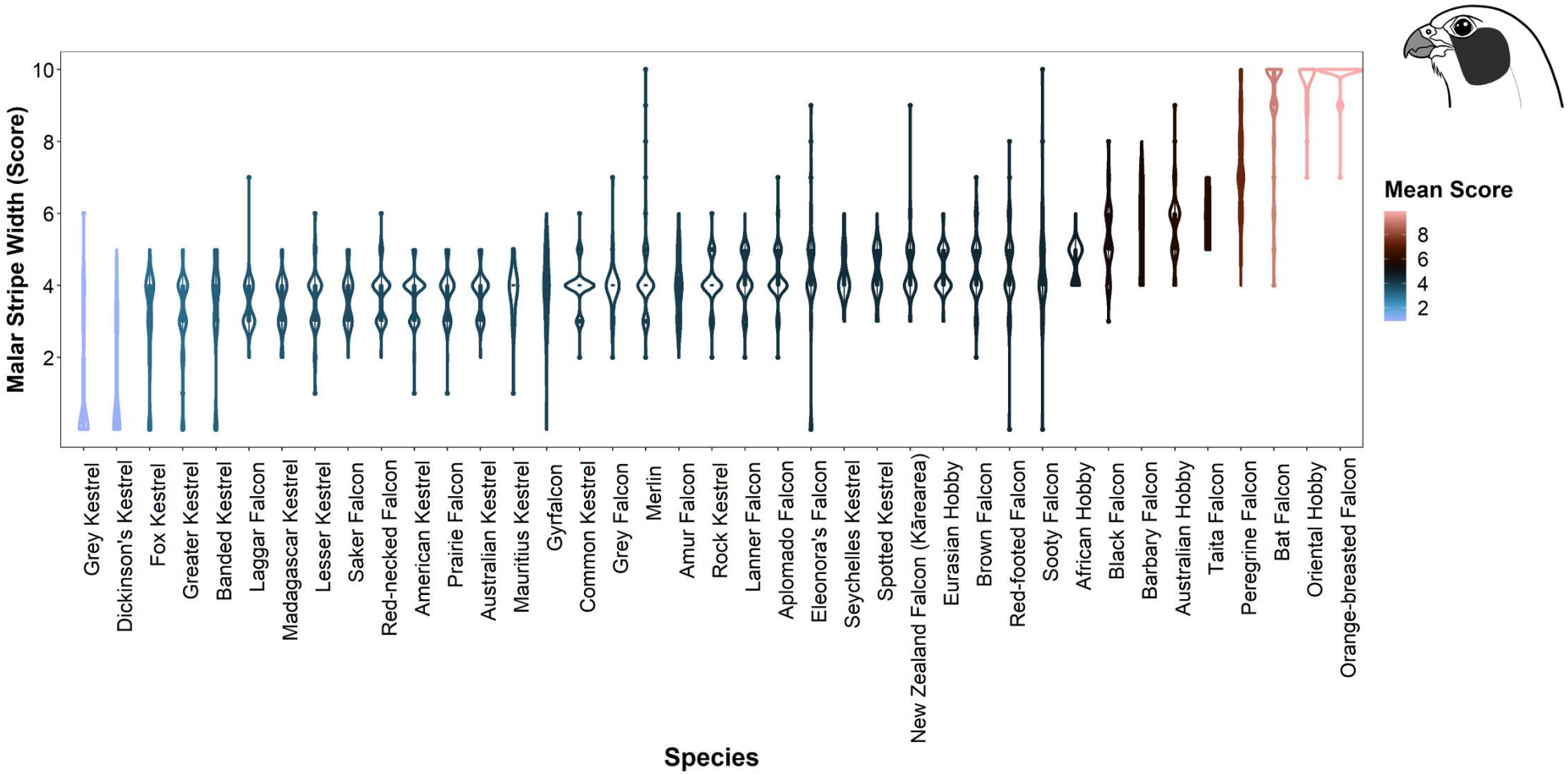

Figure 5b. Distribution of malar stripe width scores for each of the 39 falcon species in this study, with colours representing the mean score for each species. Species are arranged in ascending order of mean malar stripe width score. Plots were constructed using the R package ggplot2 (Wickham 2016).

c)

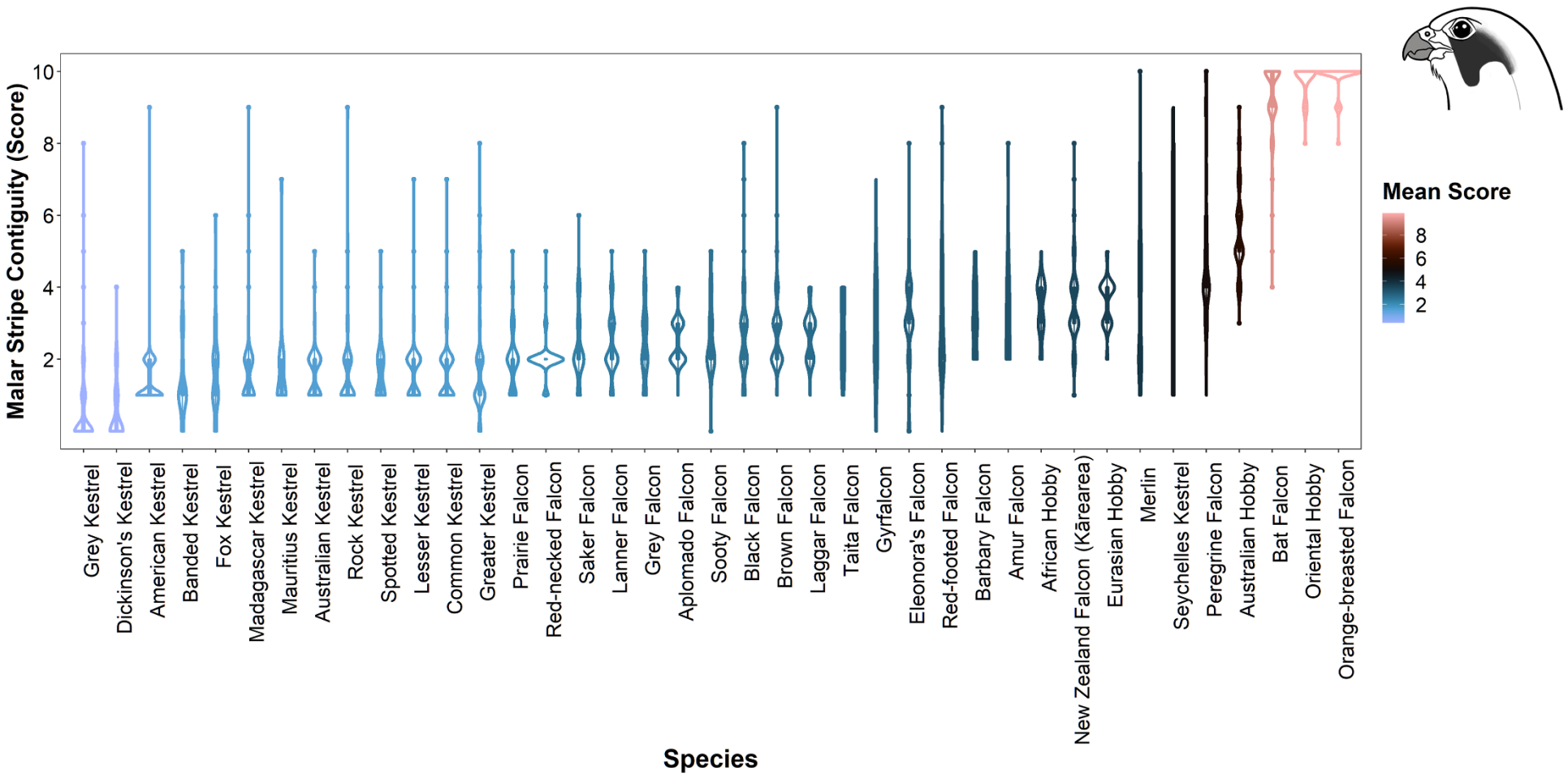

Figure 5c. Distribution of malar stripe contiguity scores for each of the 39 falcon species in this study, with colours representing the mean score for each species. Species are arranged in ascending order of mean malar stripe contiguity score. Plots were constructed using the R package ggplot2 (Wickham 2016).

d)

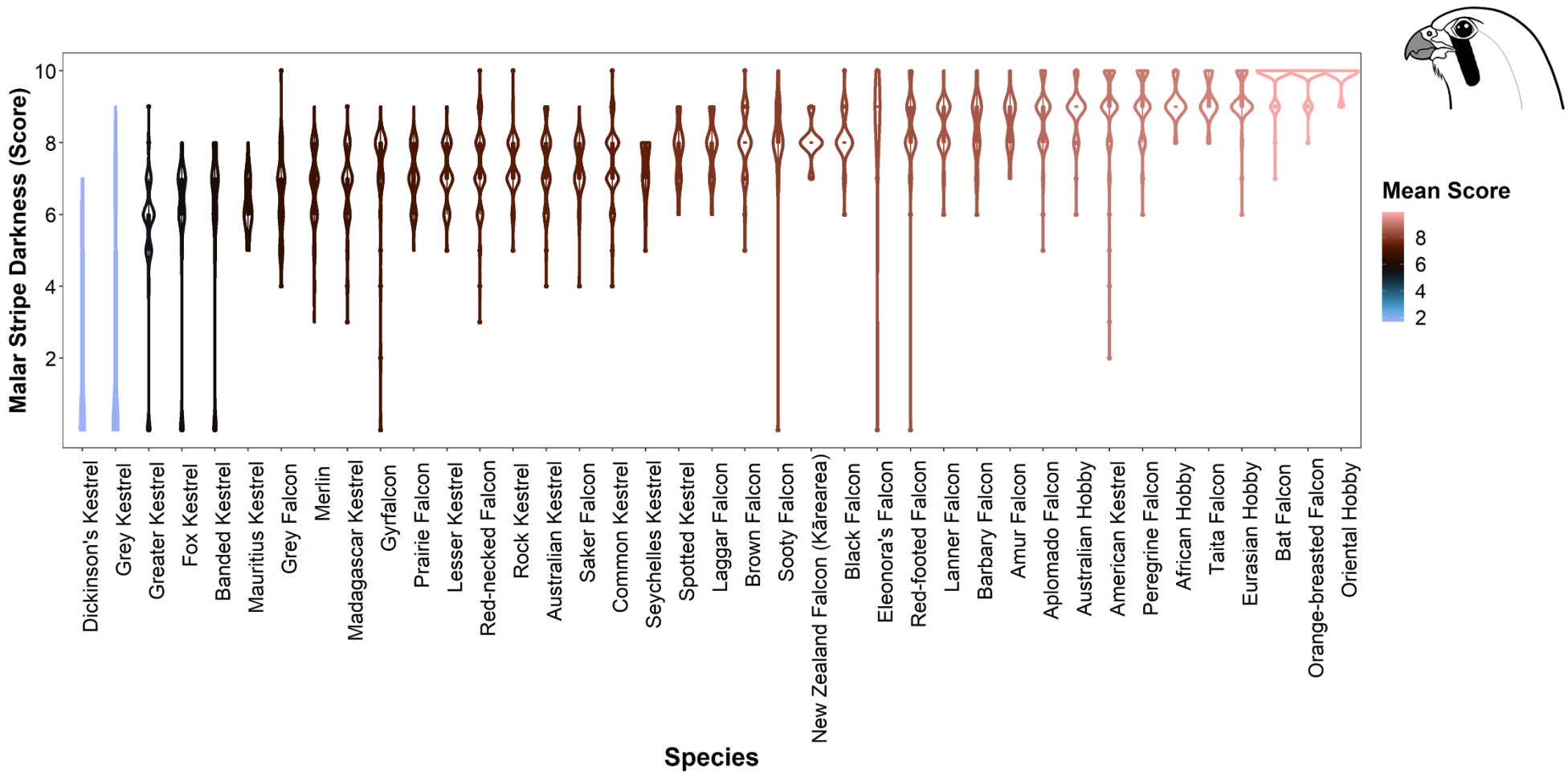

Figure 5d. Distribution of malar stripe darkness scores for each of the 39 falcon species in this study, with colours representing the mean score for each species. Species are arranged in ascending order of mean malar stripe darkness score. Plots were constructed using the R package ggplot2 (Wickham 2016).

e)

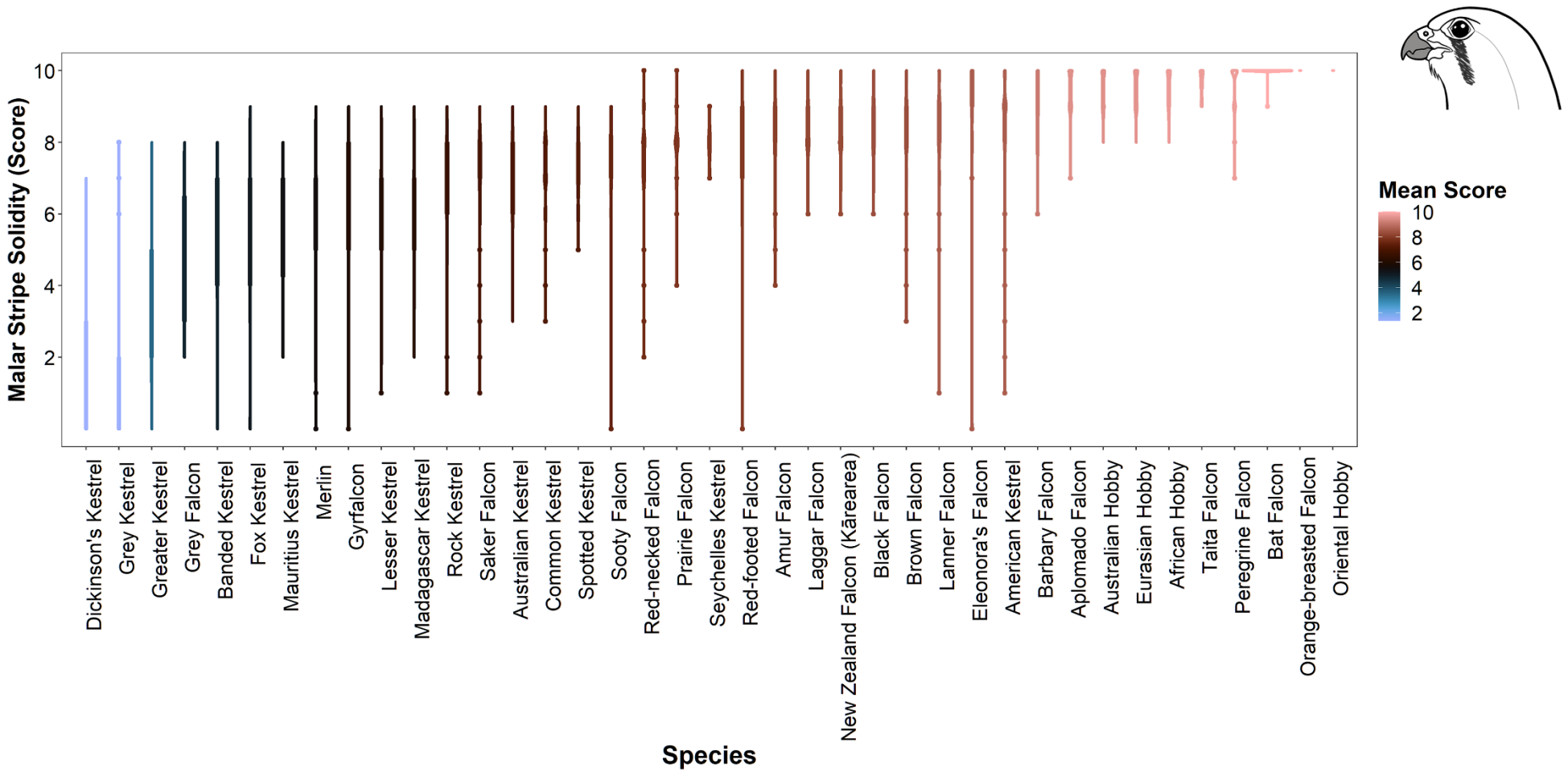

Figure 5e. Distribution of malar stripe solidity scores for each of the 39 falcon species in this study, with colours representing the mean score for each species. Species are arranged in ascending order of mean malar stripe solidity score. Plots were constructed using the R package ggplot2 (Wickham 2016).

Most of the malar stripe variables were only moderately correlated with each other, with Pearson's correlation coefficients < 0.65 (Table 2). However, width and contiguity were very strongly correlated (r = 0.82), as were darkness and solidity (r = 0.85) (Table 2). For this reason, the contiguity and solidity variables were omitted from further analysis.

Table 2. Pairwise correlations between the five malar stripe variables quantified in this study (length, width, contiguity with the hood, darkness, and solidity). Variable pairs that exhibited substantial correlation (r > 0.7) are bolded. Correlations were calculated using the R package PerformanceAnalytics (Peterson and Carl 2019).

Variable	**Correlation coefficient (r)**				
	Length	**Width**	**Contiguity**	**Darkness**	**Solidity**
Length		0.33	0.15	0.62	0.55
Width	0.33		**0.82**	0.64	0.63
Contiguity	0.15	**0.82**		0.46	0.46
Darkness	0.62	0.64	0.46		**0.85**
Solidity	0.55	0.63	0.46	**0.85**	

Most of the species trait variables were likewise uncorrelated or only mildly correlated (|r| < 0.4), with the notable exception of prey and hunting style, which exhibited a strong positive correlation (r = 0.86) (Table 3). Hunting style was thus omitted from further analysis. The trait variables were likewise uncorrelated with solar radiation, with the absolute values of all Pearson's correlation coefficients < 0.3 (Table 3).

Table 3. Pairwise correlations between solar radiation and the six species trait variables analysed in this study (body mass, HWI, prey preference, hunting style, and habitat openness). Variable pairs that exhibited substantial correlation (r > 0.7) are bolded. Correlations were calculated using the R package PerformanceAnalytics (Peterson and Carl 2019).

Variable	**Correlation coefficient (r)**					
	Solar Radiation (W/m^2)	**Body Mass (g)**	**HWI**	**Prey (Score)**	**Hunting Style (Score)**	**Habitat (Score)**
Solar Radiation (W/m^2)		0.04	0.19	-0.16	-0.14	0.27
Body Mass (g)	0.04		0.22	0.37	0.31	0.02
HWI	0.19	0.22		-0.01	-0.01	0.34
Prey (Score)	-0.16	0.37	-0.01		**0.86**	-0.39
Hunting Style (Score)	-0.14	0.31	-0.01	**0.86**		-0.35
Habitat (Score)	0.27	0.02	0.34	-0.39	-0.35	

3.3. RELATIONSHIPS BETWEEN MALAR STRIPE CHARACTERISTICS, SOLAR RADIATION, AND SPECIES TRAITS

Between species, malar stripe characteristics appeared largely unrelated to solar radiation, with the 95% credible intervals of the between-species parameters for both length and darkness overlapping zero in the simple models (Table 4, Figure 6). However, for malar stripe width, the 95% credible interval was negative and did not overlap zero, suggesting narrower malar stripes in falcon species inhabiting regions of higher solar radiation (Table 4, Figure 6). Most of these relationships were not meaningfully influenced by the addition of body mass, HWI, prey preference, or habitat to the models, or by the addition of interaction terms between solar radiation and any of these trait variables (Table 4, Figure 6). The only exceptions were the between-species relationship between solar radiation and malar stripe width, whose 95% credible interval overlapped zero after the addition of habitat (although the inclusion of an interaction term with habitat recovered the negative relationship observed in the solar radiation only model (Table 4, Figure 6)), and the between-species relationship between solar radiation and malar stripe darkness, whose 95% credible interval was negative and did not overlap zero after the addition of an interaction term with body mass, despite neither the body mass parameter or the interaction term having a substantial effect (Table 4, Figure 6).

Within species, the models suggested neutral to negative effects of solar radiation on malar stripe characteristics, with the 95% credible intervals for length and width substantially overlapping zero in the simple models (Table 4, Figure 6). However, for malar stripe darkness, the 95% credible interval was negative and did not overlap zero, suggesting that falcons tend to exhibit intraspecific trends towards paler malar stripes in regions of higher solar radiation (Table 4, Figure 6). These relationships were not meaningfully influenced by the addition of interaction terms (Table S6, Figure 6).

The additive models suggested no effect of body mass, HWI, prey preference, or habitat on malar stripe size or darkness, with the 95% credible intervals for all terms substantially overlapping zero for all malar stripe variables (Table 5, Figure 6). However, when an interaction between habitat and the between-species solar radiation parameter was included, the relationship between habitat and malar stripe width was negative, suggesting narrower malar stripes in falcon species inhabiting more open habitats (Table 5, Figure 6).

There was moderate evidence for interactions between the trait variables and solar radiation. For malar stripe length, the interactive models identified a positive interaction between body mass and the between-species solar radiation parameter, indicating that the effect of solar radiation on malar stripe length was more positive between larger-bodied species than between smaller species, despite the overall relationship across species being negligible (Table 6, Figure 6). Likewise, for malar stripe width, there was a positive interaction between the between-species solar radiation parameter and habitat, meaning that the negative effect of solar radiation on malar stripe width was less pronounced between species inhabiting more open habitats, and likewise that the negative effect of habitat openness on malar stripe width was less pronounced in regions of higher solar radiation (Table 6, Figure 6). However, for malar stripe darkness, there was a

marginally negative interaction between body mass and the within-species solar radiation parameter, suggesting that the intraspecific trend towards paler malar stripes in regions of higher solar radiation was stronger for smaller species (Table 6, Figure 6).

Table 4. Marginal posterior means, standard deviations, and 95% credible intervals of the solar radiation parameters in the simple, additive, and interactive INLA models for each malar stripe variable, along with the standard deviations of the phylogenetic and spatial random effects in the simple models, showing only the most relevant results. Fixed effects which demonstrated a substantial effect on the response (95% credible intervals do not or only marginally overlap zero) are bolded.

Variable	Variable Type	Mean	SD	0.025	0.975
Length					
Phylogenetic Effect (SD)	Random	0.462	0.827	0.350	0.634
Spatial Effect (SD)	Random	0.056	0.013	0.033	0.084
Solar Radiation (Within Species)	Fixed	-0.032	0.038	-0.108	0.042
Solar Radiation (Between Species)	Fixed	-0.043	0.071	-0.184	0.097
+ Body Mass		-0.033	0.076	-0.183	0.117
+ HWI		-0.035	0.072	-0.179	0.108
+ Prey		-0.039	0.074	-0.185	0.107
+ Habitat		-0.039	0.073	-0.183	0.105
+ Interaction with Body Mass		-0.101	0.084	-0.266	0.064
+ Interaction with HWI		-0.004	0.081	-0.164	0.154
+ Interaction with Prey		-0.017	0.076	-0.168	0.133
+ Interaction with Habitat		-0.047	0.074	-0.192	0.098
Width					
Phylogenetic Effect (SD)	Random	0.537	0.976	0.410	0.729
Spatial Effect (SD)	Random	0.241	0.038	0.175	0.239
Solar Radiation (Within Species)	Fixed	-0.028	0.035	-0.097	0.041
Solar Radiation (Between Species)	**Fixed**	**-0.177**	**0.074**	**-0.323**	**-0.033**
+ Body Mass		**-0.206**	**0.081**	**-0.366**	**-0.046**
+ HWI		**-0.173**	**0.075**	**-0.322**	**-0.026**
+ Prey		**-0.171**	**0.075**	**-0.319**	**-0.024**
+ Habitat		-0.140	0.076	-0.291	0.010
+ Interaction with Body Mass		**-0.233**	**0.089**	**-0.409**	**-0.057**
+ Interaction with HWI		**-0.159**	**0.082**	**-0.321**	**0.000**
+ Interaction with Prey		**-0.162**	**0.083**	**-0.325**	**0.000**
+ Interaction with Habitat		**-0.183**	**0.071**	**-0.323**	**-0.043**
Darkness					
Phylogenetic Effect (SD)	Random	0.533	1.029	0.421	0.714
Spatial Effect (SD)	Random	0.224	0.027	0.176	0.283
Solar Radiation (Within Species)	**Fixed**	**-0.084**	**0.042**	**-0.168**	**-0.002**
Solar Radiation (Between Species)	Fixed	-0.100	0.071	-0.241	0.040
+ Body Mass		-0.131	0.079	-0.287	0.025
+ HWI		-0.108	0.074	-0.253	0.036
+ Prey		-0.095	0.073	-0.239	0.047
+ Habitat		-0.069	0.076	-0.220	0.081
+ Interaction with Body Mass		**-0.175**	**0.087**	**-0.347**	**-0.005**
+ Interaction with HWI		-0.096	0.081	-0.258	0.062
+ Interaction with Prey		-0.107	0.080	-0.265	0.050
+ Interaction with Habitat		-0.085	0.076	-0.237	0.065

Table 5. Marginal posterior means, standard deviations, and 95% credible intervals of the species trait parameters in the additive and interactive INLA models for each malar stripe variable. Fixed effects which demonstrated a substantial effect on the response (95% credible intervals do not or only marginally overlap zero) are bolded.

Variable	Variable Type	Mean	SD	0.025	0.975
Length					
Body Mass	Fixed	0.104	0.125	-0.144	0.349
+ Interaction Term (Within Species)		0.041	0.137	-0.230	0.313
+ Interaction Term (Between Species)		0.233	0.150	-0.064	0.529
HWI	Fixed	-0.066	0.111	-0.286	0.153
+ Interaction Term (Within Species)		-0.063	0.116	-0.292	0.165
+ Interaction Term (Between Species)		-0.051	0.115	-0.278	0.176
Prey	Fixed	0.129	0.146	-0.156	0.417
+ Interaction Term (Within Species)		0.121	0.143	-0.158	0.403
+ Interaction Term (Between Species)		0.139	0.137	-0.129	0.410
Habitat	Fixed	-0.017	0.093	-0.199	0.166
+ Interaction Term (Within Species)		-0.014	0.098	-0.206	0.179
+ Interaction Term (Between Species)		-0.026	0.111	-0.244	0.193
Width					
Body Mass	Fixed	-0.110	0.133	-0.373	0.152
+ Interaction Term (Within Species)		-0.113	0.133	-0.375	0.149
+ Interaction Term (Between Species)		-0.042	0.163	-0.364	0.279
HWI	Fixed	-0.028	0.122	-0.268	0.213
+ Interaction Term (Within Species)		-0.025	0.122	-0.265	0.216
+ Interaction Term (Between Species)		-0.019	0.125	-0.264	0.228
Prey	Fixed	0.133	0.144	-0.148	0.418
+ Interaction Term (Within Species)		0.130	0.143	-0.150	0.415
+ Interaction Term (Between Species)		0.140	0.148	-0.147	0.435
Habitat	Fixed	-0.150	0.099	-0.345	0.043
+ Interaction Term (Within Species)		-0.148	0.099	-0.345	0.047
+ Interaction Term (Between Species)		**-0.401**	**0.106**	**-0.607**	**-0.191**
Darkness					
Body Mass	Fixed	-0.123	0.133	-0.384	0.138
+ Interaction Term (Within Species)		-0.125	0.130	-0.382	0.131
+ Interaction Term (Between Species)		-0.012	0.159	-0.324	0.301
HWI	Fixed	0.057	0.120	-0.178	0.293
+ Interaction Term (Within Species)		0.058	0.119	-0.176	0.293
+ Interaction Term (Between Species)		0.064	0.121	-0.175	0.303
Prey	Fixed	0.121	0.139	-0.151	0.397
+ Interaction Term (Within Species)		0.120	0.139	-0.153	0.396
+ Interaction Term (Between Species)		0.116	0.141	-0.159	0.396
Habitat	Fixed	-0.121	0.097	-0.311	0.069
+ Interaction Term (Within Species)		-0.121	0.096	-0.310	0.068
+ Interaction Term (Between Species)		-0.205	0.117	-0.436	0.027

Table 6. Marginal posterior means, standard deviations, and 95% credible intervals of the interaction terms between the solar radiation parameters and species trait variables in the interactive INLA models for each of the malar stripe variables. Terms for which a substantial interaction was found (95% credible intervals do not or only marginally overlap zero) are bolded.

Interaction Term	Mean	SD	0.025	0.975
Length				
Solar Radiation (Within Species) * Body Mass	-0.051	0.037	-0.124	0.022
Solar Radiation (Between Species) * Body Mass	**0.088**	**0.043**	**0.003**	**0.174**
Solar Radiation (Within Species) * HWI	0.012	0.041	-0.070	0.093
Solar Radiation (Between Species) * HWI	-0.078	0.084	-0.243	0.088
Solar Radiation (Within Species) * Prey	-0.023	0.039	-0.101	0.053
Solar Radiation (Between Species) * Prey	-0.062	0.088	-0.237	0.109
Solar Radiation (Within Species) * Habitat	-0.011	0.036	-0.082	0.060
Solar Radiation (Between Species) * Habitat	0.024	0.089	-0.152	0.198
Width				
Solar Radiation (Within Species) * Body Mass	-0.039	0.030	-0.099	0.020
Solar Radiation (Between Species) * Body Mass	0.031	0.044	-0.056	0.117
Solar Radiation (Within Species) * HWI	0.030	0.035	-0.039	0.100
Solar Radiation (Between Species) * HWI	-0.040	0.085	-0.208	0.129
Solar Radiation (Within Species) * Prey	-0.015	0.035	-0.084	0.053
Solar Radiation (Between Species) * Prey	-0.025	0.094	-0.213	0.157
Solar Radiation (Within Species) * Habitat	0.009	0.032	-0.054	0.072
Solar Radiation (Between Species) * Habitat	**0.340**	**0.086**	**0.169**	**0.509**
Darkness				
Solar Radiation (Within Species) * Body Mass	**-0.068**	**0.036**	**-0.139**	**0.002**
Solar Radiation (Between Species) * Body Mass	0.053	0.043	-0.032	0.138
Solar Radiation (Within Species) * HWI	0.014	0.043	-0.070	0.098
Solar Radiation (Between Species) * HWI	-0.029	0.084	-0.195	0.138
Solar Radiation (Within Species) * Prey	-0.014	0.042	-0.098	0.069
Solar Radiation (Between Species) * Prey	0.033	0.091	-0.146	0.211
Solar Radiation (Within Species) * Habitat	-0.009	0.039	-0.085	0.067
Solar Radiation (Between Species) * Habitat	0.115	0.093	-0.069	0.298

a)

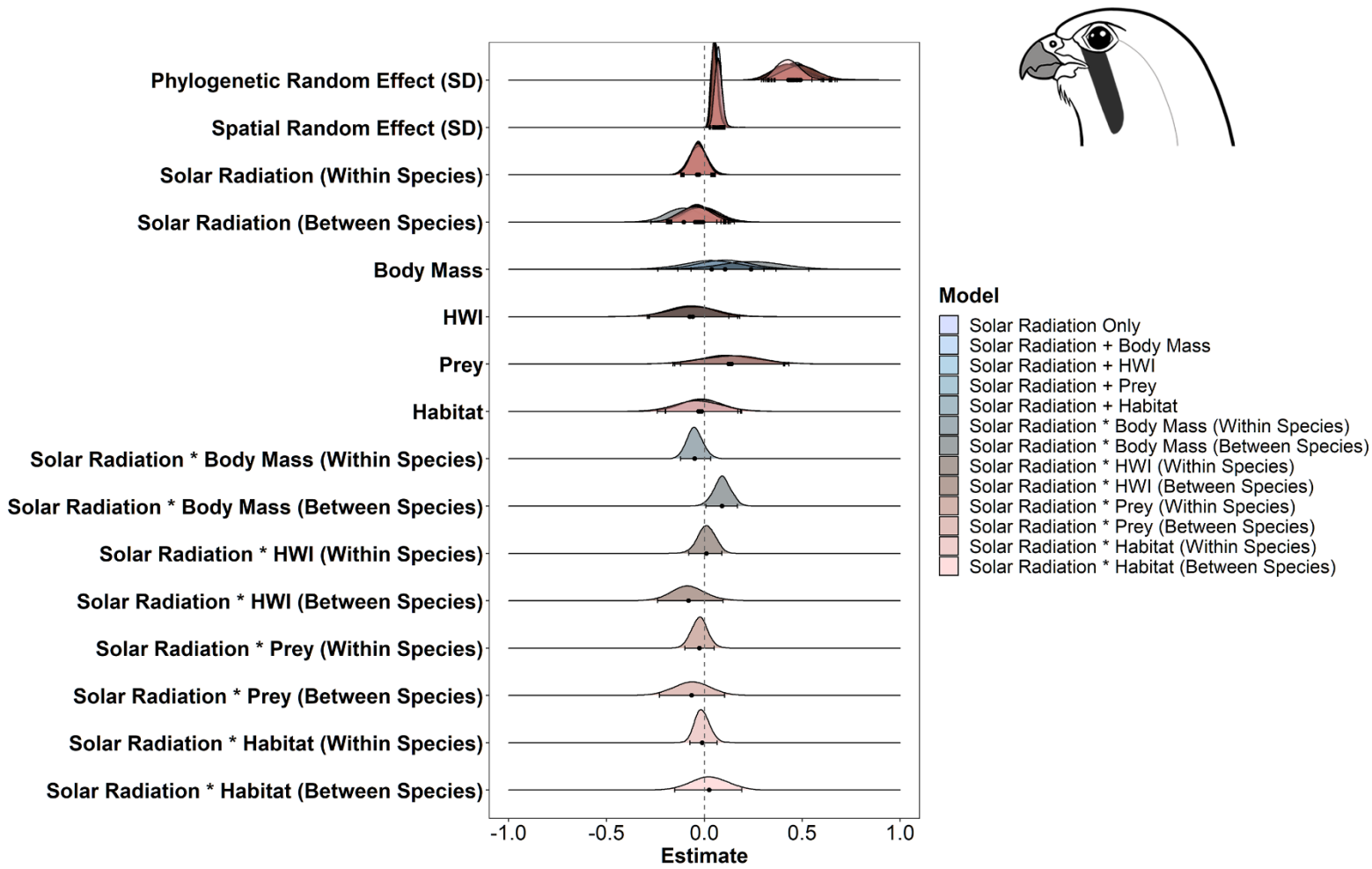

Figure 6a. Marginal posterior probability distributions of the fixed effects and the standard deviations of the phylogenetic and spatial random effects in the INLA models for malar stripe length, colour coded according to model specification. Since all fixed effect variables were standardized prior to model fitting, these coefficients are comparable to one another. Plots were created using the R package phyr (Li et al. 2020).

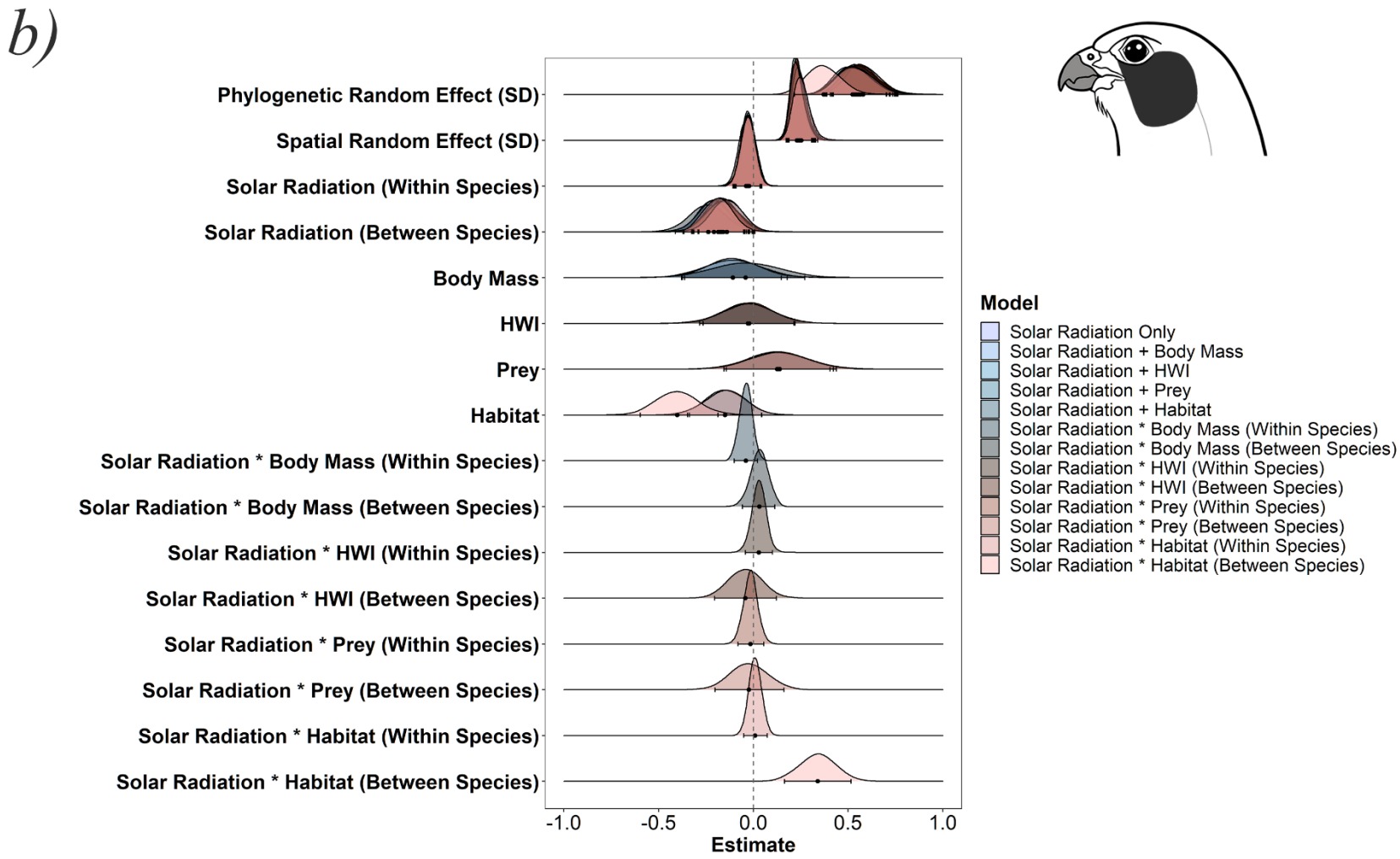

Figure 6b. Marginal posterior probability distributions of the fixed effects and the standard deviations of the phylogenetic and spatial random effects in the INLA models for malar stripe width, colour coded according to model specification. Since all fixed effect variables were standardized prior to model fitting, these coefficients are comparable to one another. Plots were created using the R package phyr (Li et al. 2020).

c)

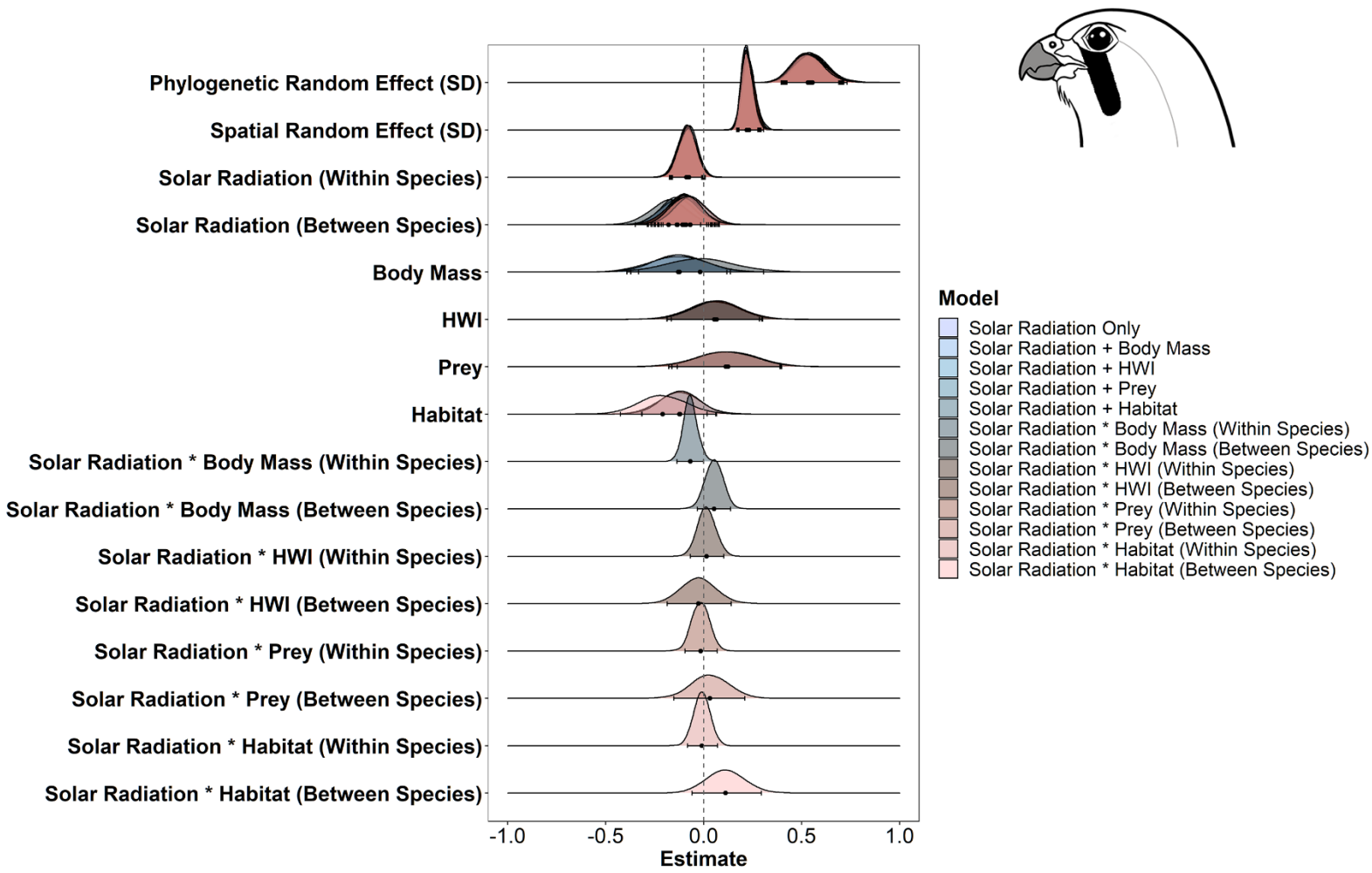

Figure 6c. Marginal posterior probability distributions of the fixed effects and the standard deviations of the phylogenetic and spatial random effects in the INLA models for malar stripe darkness, colour coded according to model specification. Since all fixed effect variables were standardized prior to model fitting, these coefficients are comparable to one another. Plots were created using the R package phyr (Li et al. 2020).

Phylogeny explained a greater amount of the variation in malar stripe characteristics than did spatial position, with the phylogenetic effect roughly twice the magnitude of the spatial effect for malar stripe width and darkness, and nearly eight times that of the spatial effect for malar stripe length, in the simple models (Table 4, Figure 6). The phylogenetic effect was roughly equal in magnitude for all malar stripe variables, albeit slightly higher for width and darkness than for length (Table 4, Figure 6), while the spatial effect was less consistent, with malar stripe width and darkness exhibiting spatial effects roughly four times larger than that for malar stripe length (Table 4, Figure 6). The phylogenetic and spatial effects were largely unaltered by the addition of species trait variables or interaction terms to the models (Table S6, Figure 6); however, the exception was the model involving an interaction term between habitat and the between-species solar radiation parameter for malar stripe width, in which the estimated phylogenetic effect was much lower than that in the simple model due to the strong explanatory power of the interaction term (Table S6, Figure 6).

All three of the malar stripe variables exhibited moderate phylogenetic signal (Figure 7). For all three variables, the phylogenetic effect was driven largely by the clade consisting of the Dickinson's and Grey Kestrels, which exhibited considerably shorter, narrower, and paler malar stripes than any other species (Figure 7). The phylogenetic effect for malar stripe width also appeared to be affected strongly by the clade consisting of the Orange-breasted and Bat Falcons, which exhibited wider than average malar stripes, while the phylogenetic effect for most other clades and species was negligible (Figure 7). The Peregrine Falcon-hierofalcon clade also exhibited consistently longer than average malar stripes (Figure 7), while malar stripes were consistently darker than average in the Orange-breasted-Bat Falcon clade, and consistently paler than average in the basal kestrels (Figure 7).

The estimated ranges of the spatial effect differed widely between the malar stripe variables, with the simple models identifying a marginal posterior mean range of 17.30 decimal degrees for malar stripe length, 82.91 decimal degrees for malar stripe width, and 41.94 decimal degrees for malar stripe darkness. The models thus suggested a relatively local-scale pattern of spatial clustering in the length of falcon malar stripes, with spatial covariance between datapoints decaying to very low values only after approximately 17 decimal degrees, while the pattern for falcon malar stripe width was extremely large-scale, and spatial covariance between malar stripe width values effectively negligible at an intra-hemispheric (< ~83 degree) level. Malar stripe darkness exhibited a range of spatial covariance intermediate between these two extremes, with spatial clustering operating at a mean range of ~42 degrees, or at a roughly continental scale.

Removing birds with uniform plumage from the dataset only mildly affected the results, with the bulk of trends unchanged (Table S7-S9, Figure S1). However, the negative relationship between solar radiation and intraspecific variation in malar stripe darkness disappeared after the removal of uniform birds (95% credible intervals substantially overlapped zero), while the negative interspecific relationship between solar radiation and malar stripe width was also less consistently observed in the reduced models, with the 95% credible intervals of the between-species solar radiation parameter overlapping zero in the bulk of the models (Table S7-S8, Figure S1). The reduced models also identified a positive relationship between malar stripe

length and body mass (i.e., longer malar stripes in larger species), as well as a negative interaction between body mass and the within-species solar radiation parameter (indicating that the intraspecific effect of solar radiation on malar stripe length was more negative in smaller species) (Table S8-S9, Figure S1). Removing birds with uniform plumage from the analysis also reduced the magnitude of the estimated phylogenetic effect for all malar stripe variables, and increased that of the spatial effect (Table S7, Figure S1). For malar stripe width, including an interaction term between habitat and the between-species solar radiation parameter also resulted in a greater reduction in the magnitude of the estimated phylogenetic effect after the removal of uniform birds from the dataset, with this model demonstrating a virtually negligible effect of phylogeny on malar stripe width (Table S7, Figure S1).

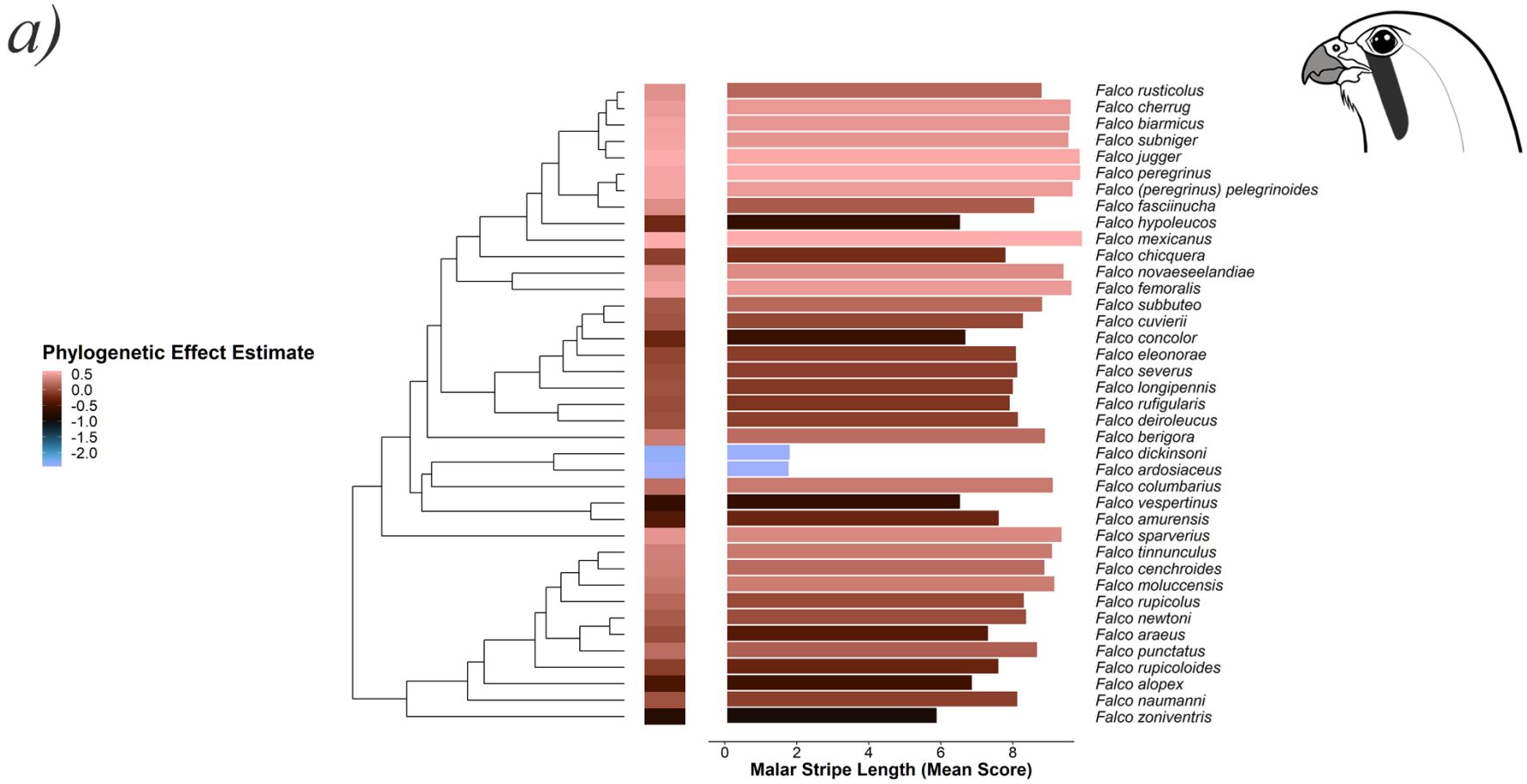

Figure 7a. Phylogeny for the 39 *Falco* species analysed in this study, with terminal branches coloured according to the predicted deviation from the average malar stripe length value for each species based purely on its phylogenetic position in the simple (solar radiation only) INLA model, used as a measure of phylogenetic signal in each malar stripe variable. Bar lengths and colours represent the average malar stripe length score for each species. Plots were constructed based on a multilocus consensus tree derived from Fuchs (2015) using the R package ggtree (Yu et al. 2017).

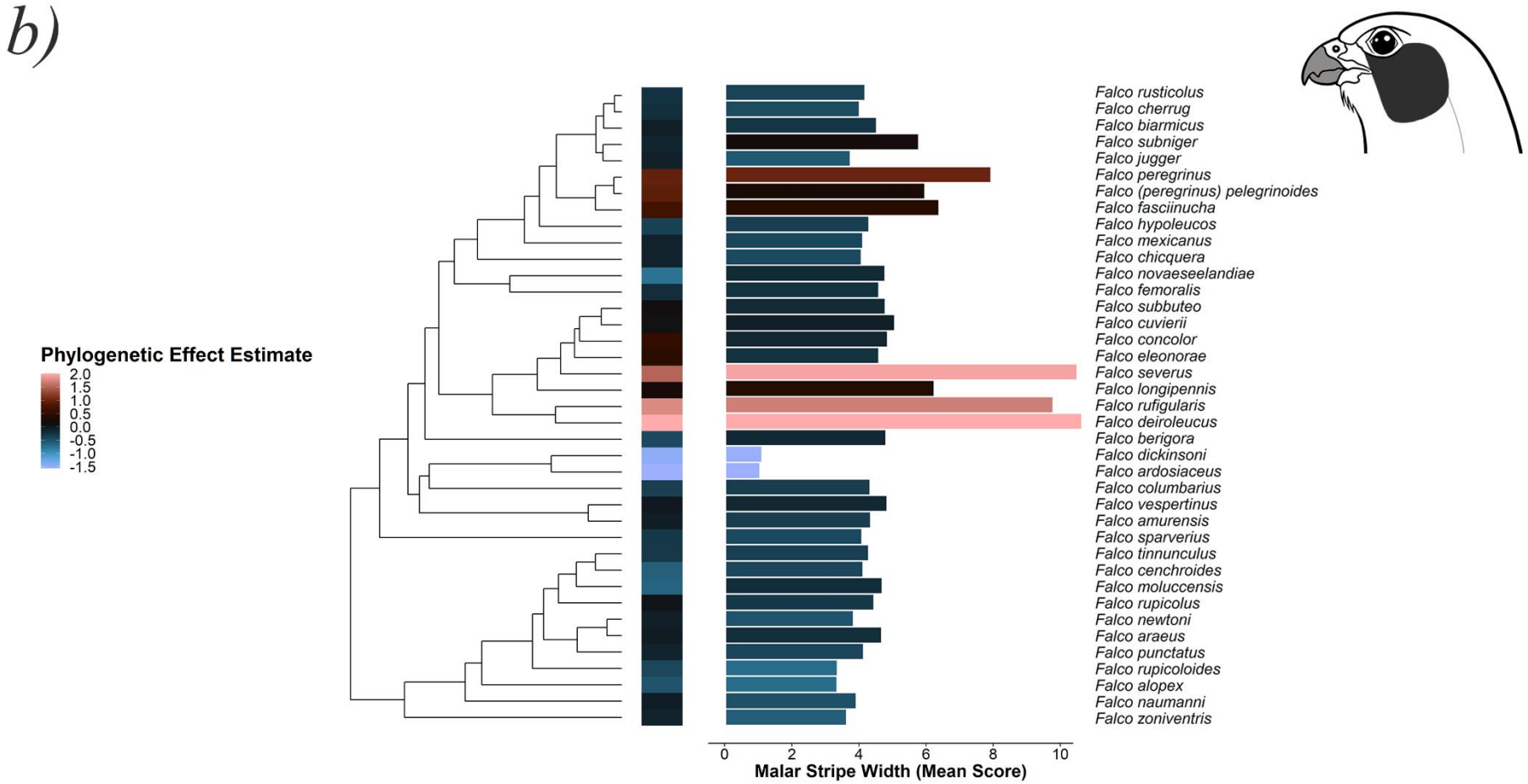

Figure 7b. Phylogeny for the 39 *Falco* species analysed in this study, with terminal branches coloured according to the predicted deviation from the average malar stripe width value for each species based purely on its phylogenetic position in the simple (solar radiation only) INLA model, used as a measure of phylogenetic signal in each malar stripe variable. Bar lengths and colours represent the average malar stripe width score for each species. Plots were constructed based on a multilocus consensus tree derived from Fuchs (2015) using the R package ggtree (Yu et al. 2017).

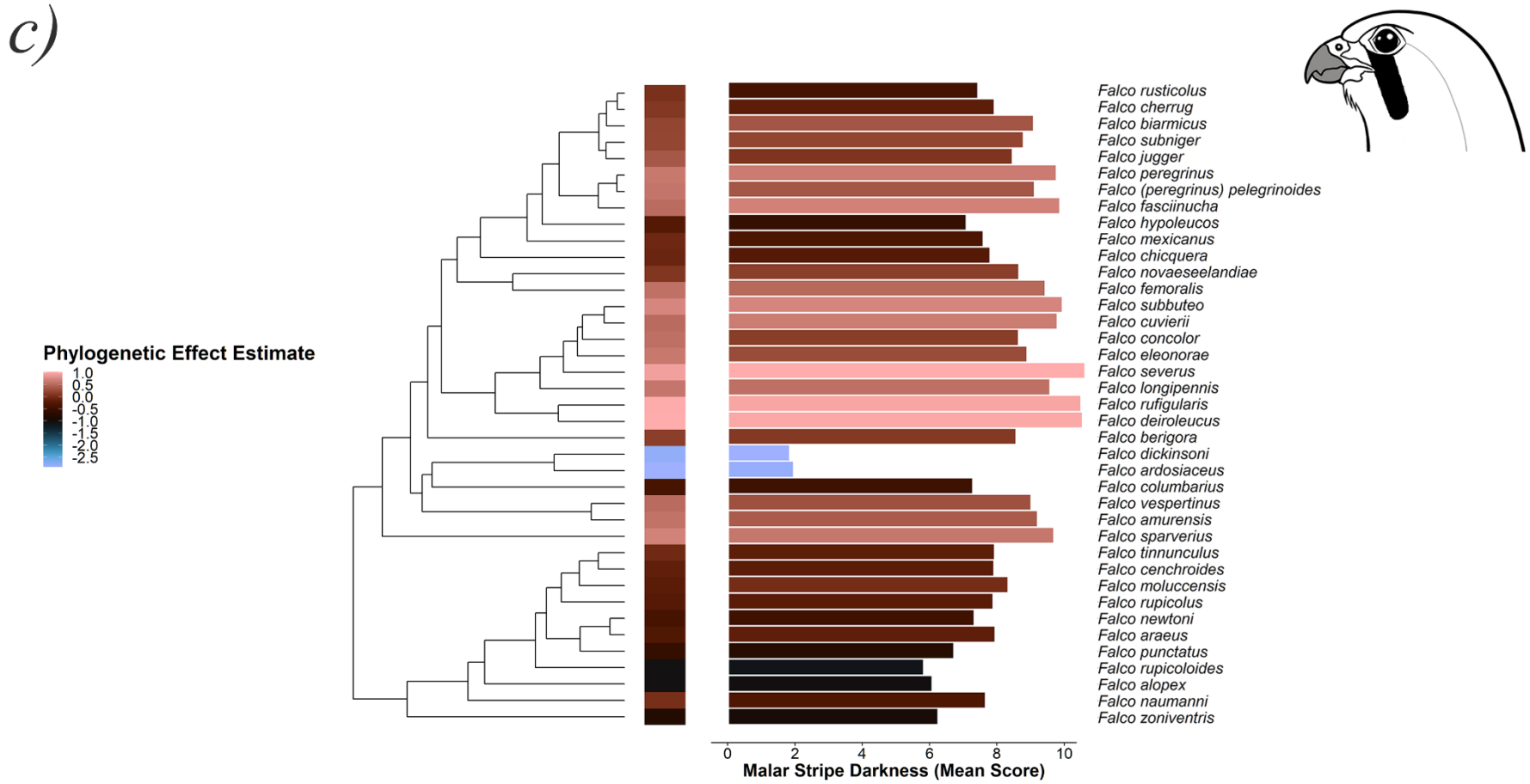

Figure 7c. Phylogeny for the 39 *Falco* species analysed in this study, with terminal branches coloured according to the predicted deviation from the average malar stripe darkness value for each species based purely on its phylogenetic position in the simple (solar radiation only) INLA model, used as a measure of phylogenetic signal in each malar stripe variable Bar lengths and colours represent the average malar stripe score for each species. Plots were constructed based on a multilocus consensus tree derived from Fuchs (2015) using the R package ggtree (Yu et al. 2017).

The majority of species showed no meaningful intraspecific relationships between solar radiation and malar stripe characteristics, with the 95% credible intervals for most of the random slope estimates overlapping zero (Table 7). Six of the 39 species did show substantial intraspecific relationships between solar radiation and malar stripe characteristics, although the relationships were positive in only half of these, with three species instead showing negative relationships between malar stripe characteristics and solar radiation (Table 7).

Negative relationships between malar stripe characteristics and solar radiation were observed in the Eleonora's Falcon and the Madagascar Kestrel (*Falco newtoni*), with the former species exhibiting negative relationships between solar radiation and both malar stripe length and darkness (i.e., a trend towards shorter and paler malar stripes in regions of higher solar radiation), while for the latter species, this negative trend was observed for malar stripe darkness only (Table 7). In contrast, the Dickinson's Kestrel and Rock Kestrel exhibited positive relationships between malar stripe characteristics and solar radiation, with substantial trends observed for both malar stripe length and darkness in the Dickinson's Kestrel (i.e., longer and darker malar stripes in regions of higher solar radiation), and for malar stripe darkness only in the Rock Kestrel (Table 7).

Only two species, the Peregrine Falcon and the Gyrfalcon (*Falco rusticolus*), exhibited relationships between solar radiation and all three malar stripe variables (Table 7). In the Peregrine Falcon, relationships between malar stripe characteristics and solar radiation were consistently positive, with the 95% credible intervals for the random slope estimates for length and width not overlapping zero (Table 4), and for darkness only marginally overlapping zero at the 2.5^{th} percentile (Table 7). In contrast, in the Gyrfalcon the relationships were consistently negative, with the 95% credible intervals for the random slope estimates shifted away from zero for all variables (Table 7).

The results of the species-specific GLS models largely corroborated these random slope trends. The models found strong evidence for positive relationships between solar radiation and all three malar stripe variables in the Peregrine Falcon (Table 8, Figure 8), and for negative relationships in the Gyrfalcon (Table 8, Figure 8). Peregrine Falcons thus exhibited larger (longer/wider) and darker malar stripes in regions of higher solar radiation, while Gyrfalcons exhibited smaller (shorter/narrower) and paler malar stripes (Table 8, Figure 8). In contrast, Madagascar Kestrels exhibited paler malar stripes in regions of higher solar radiation, but demonstrated only weak evidence ($0.05 < p < 0.1$) for negative relationships between solar radiation and malar stripe length and width, in keeping with the random slope trends (Table 8, Figure 8). However, the relationships found for the Dickinson's Kestrel, Eleonora's Falcon, and Rock Kestrel were not replicated in the GLS models, with the GLS analysis indicating no evidence for relationships between solar radiation and malar stripe length or darkness in the Dickinson's Kestrel (Table 8, Figure 8), and only weak evidence for negative relationships between solar radiation and these variables in the Eleonora's Falcon and Rock Kestrel ($0.05 < p < 0.1$) (Table 8, Figure 8).

Table 7. Means, standard deviations and 95% credible intervals for the marginal posterior probability distributions of the INLA random slope estimates for the relationships between malar stripe characteristics and solar radiation in each species. Variables and species in which one or more substantial relationships were found (95% credible intervals do not or only marginally overlap zero) are bolded.

Species	Random Slope Estimate											
	Length				Width				Darkness			
	Mean	**SD**	**0.025**	**0.975**	**Mean**	**SD**	**0.025**	**0.975**	**Mean**	**SD**	**0.025**	**0.975**
Red-footed Falcon												
Male	0.187	0.134	-0.075	0.453	-0.052	0.102	-0.254	0.148	0.063	0.132	-0.196	0.323
Female	0.036	0.140	-0.239	0.312	-0.027	0.107	-0.237	0.182	-0.018	0.137	-0.288	0.250
Dickinson's Kestrel	**0.179**	**0.079**	**0.023**	**0.335**	0.098	0.063	-0.026	0.222	**0.228**	**0.083**	**0.067**	**0.391**
Laggar Falcon	0.150	0.095	-0.037	0.338	0.123	0.076	-0.026	0.273	0.036	0.100	-0.159	0.231
Peregrine Falcon	**0.087**	**0.041**	**0.007**	**0.169**	**0.073**	**0.036**	**0.002**	**0.144**	**0.086**	**0.045**	**-0.002**	**0.174**
Black Falcon	0.077	0.081	-0.083	0.236	0.010	0.064	-0.115	0.135	0.053	0.082	-0.108	0.215
Red-necked Falcon	0.067	0.051	-0.032	0.167	0.016	0.043	-0.069	0.100	0.051	0.055	-0.056	0.158
African Hobby	0.052	0.109	-0.162	0.266	0.011	0.082	-0.150	0.173	0.100	0.107	-0.108	0.311
Rock Kestrel	0.045	0.062	-0.077	0.168	0.060	0.051	-0.040	0.160	**0.153**	**0.065**	**0.026**	**0.281**
Aplomado Falcon	0.043	0.043	-0.042	0.129	-0.005	0.039	-0.082	0.071	0.076	0.048	-0.018	0.171
Australian Kestrel	0.041	0.059	-0.075	0.158	-0.011	0.051	-0.111	0.090	0.048	0.065	-0.079	0.176
Seychelles Kestrel	0.036	0.213	-0.380	0.459	0.010	0.192	-0.369	0.389	0.014	0.231	-0.441	0.471
Common Kestrel												
Male	0.028	0.043	-0.055	0.112	0.042	0.037	-0.031	0.116	0.037	0.046	-0.054	0.129
Female	0.061	0.045	-0.027	0.149	0.050	0.038	-0.026	0.126	0.044	0.048	-0.050	0.138
Lesser Kestrel												
Male	0.027	0.061	-0.092	0.147	0.047	0.049	-0.049	0.144	-0.039	0.063	-0.163	0.085
Female	0.135	0.077	-0.016	0.287	0.071	0.059	-0.045	0.187	-0.028	0.077	-0.178	0.122
Orange-breasted Falcon	0.024	0.047	-0.069	0.117	0.006	0.043	-0.077	0.090	0.049	0.054	-0.056	0.155
Merlin	0.022	0.045	-0.066	0.111	-0.024	0.040	-0.102	0.055	-0.037	0.050	-0.135	0.061
Bat Falcon	0.021	0.044	-0.067	0.109	-0.043	0.040	-0.122	0.037	0.073	0.051	-0.026	0.173
Greater Kestrel	0.014	0.049	-0.081	0.110	0.067	0.042	-0.015	0.150	0.064	0.053	-0.040	0.169
Spotted Kestrel	0.014	0.132	-0.246	0.273	-0.060	0.105	-0.266	0.146	-0.000	0.135	-0.265	0.264
Taita Falcon	0.013	0.168	-0.317	0.343	-0.012	0.135	-0.277	0.253	-0.053	0.170	-0.388	0.279
Mauritius Kestrel	0.011	0.213	-0.408	0.431	0.008	0.193	-0.373	0.389	-0.009	0.232	-0.469	0.449

Table 7. cont.

Oriental Hobby	0.002	0.126	-0.246	0.251	0.114	0.105	-0.092	0.321	0.099	0.133	-0.162	0.362
Saker Falcon	0.001	0.141	-0.276	0.277	0.007	0.110	-0.210	0.224	0.080	0.141	-0.200	0.358
Lanner Falcon	0.000	0.047	-0.093	0.093	0.027	0.041	-0.053	0.108	0.075	0.052	-0.026	0.177
Australian Hobby	-0.006	0.065	-0.133	0.121	0.055	0.054	-0.050	0.161	0.056	0.069	-0.079	0.191
Barbary Falcon	-0.007	0.133	-0.269	0.253	0.010	0.102	-0.190	0.209	0.044	0.131	-0.212	0.301
Grey Falcon	-0.008	0.177	-0.348	0.347	-0.003	0.144	-0.287	0.281	-0.006	0.181	-0.362	0.350
Eurasian Hobby	-0.009	0.049	-0.105	0.087	0.028	0.041	-0.052	0.110	0.069	0.052	-0.032	0.172
Fox Kestrel	-0.010	0.112	-0.230	0.209	-0.027	0.084	-0.192	0.139	0.047	0.109	-0.167	0.261
Amur Falcon												
Male	-0.023	0.174	-0.368	0.319	-0.038	0.144	-0.322	0.245	-0.034	0.180	-0.390	0.319
Female	-0.093	0.187	-0.465	0.271	0.161	0.161	-0.149	0.484	0.018	0.199	-0.369	0.406
American Kestrel	-0.031	0.042	-0.115	0.053	-0.022	0.037	-0.095	0.057	0.040	0.046	-0.051	0.132
Banded Kestrel	-0.033	0.184	-0.397	0.328	-0.168	0.157	-0.482	0.135	-0.146	0.194	-0.535	0.230
Brown Falcon	-0.037	0.055	-0.146	0.071	-0.026	0.048	-0.121	0.069	0.014	0.061	-0.105	0.135
New Zealand Falcon (Kārearea)	-0.038	0.104	-0.244	0.167	-0.018	0.092	-0.200	0.163	-0.006	0.119	-0.240	0.228
Prairie Falcon	-0.053	0.064	-0.177	0.072	-0.011	0.051	-0.111	0.090	-0.046	0.065	-0.174	0.083
Sooty Falcon	-0.067	0.184	-0.431	0.292	0.028	0.157	-0.279	0.337	-0.019	0.194	-0.402	0.363
Grey Kestrel	-0.094	0.054	-0.200	0.011	-0.034	0.046	-0.125	0.056	-0.044	0.059	-0.160	0.071
Madagascar Kestrel	-0.096	0.087	-0.268	0.075	-0.044	0.072	-0.186	0.098	**-0.218**	**0.095**	**-0.406**	**-0.032**
Eleonora's Falcon	**-0.328**	**0.115**	**-0.556**	**-0.105**	-0.084	0.088	-0.257	0.088	**-0.329**	**0.116**	**-0.559**	**-0.102**
Gyrfalcon	**-0.445**	**0.116**	**-0.675**	**-0.221**	**-0.415**	**0.010**	**-0.613**	**-0.221**	**-0.685**	**0.134**	**-0.951**	**-0.426**

Table 8. Results of GLS models analysing the relationships between malar stripe characteristics and solar radiation in the species whose random slope estimates demonstrated an effect of solar radiation (95% credible intervals of their marginal posterior probability distributions did not or only marginally overlapped zero). Species and variables for which evidence for a relationship was found ($p < 0.05$, 95% confidence interval does not overlap zero) are bolded.

Model	Log Likelihood	Residual standard error	Residual df	Solar Radiation					
				Mean	SE	95% CI Lower	95% CI Upper	t	p
Peregrine Falcon									
Length	**-1294.003**	**0.867**	**1007**	**0.165**	**0.028**	**0.111**	**0.219**	**5.991**	**< 0.001**
Width	**-1350.475**	**0.919**	**1007**	**0.252**	**0.029**	**0.195**	**0.310**	**8.582**	**< 0.001**
Darkness	**-1403.006**	**0.974**	**1007**	**0.171**	**0.031**	**0.110**	**0.232**	**5.473**	**< 0.001**
Gyrfalcon									
Length	**-113.847**	**0.912**	**83**	**-0.431**	**0.116**	**-0.658**	**-0.204**	**-3.714**	**< 0.001**
Width	**-106.754**	**0.792**	**83**	**-0.585**	**0.092**	**-0.765**	**-0.404**	**-6.356**	**< 0.001**
Darkness	**-107.569**	**0.802**	**83**	**-0.590**	**0.094**	**-0.774**	**-0.407**	**-6.306**	**< 0.001**
Madagascar Kestrel									
Length	-240.418	0.941	170	-0.143	0.073	-0.286	0.000	-1.965	0.051
Width	-244.510	0.965	170	-0.124	0.075	-0.271	0.023	-1.659	0.099
Darkness	**-238.745**	**0.934**	**170**	**-0.306**	**0.072**	**-0.448**	**-0.164**	**-4.224**	**< 0.001**
Eleonora's Falcon									
Length	-165.894	0.958	114	-0.190	0.097	-0.380	0.000	-1.965	0.052
Width	-166.233	0.961	114	-0.152	0.097	-0.342	0.038	-1.566	0.120
Darkness	-164.512	0.954	114	-0.181	0.099	-0.374	0.013	-1.831	0.070
Rock Kestrel									
Length	-462.480	0.925	338	-0.012	0.051	-0.112	0.088	-0.242	0.809
Width	-481.706	0.982	338	-0.065	0.054	-0.172	0.041	-1.201	0.230
Darkness	-480.695	0.975	338	0.091	0.054	-0.014	0.197	1.694	0.091
Dickinson's Kestrel									
Length	-147.928	0.919	104	0.049	0.100	-0.146	0.245	0.495	0.622
Width	-145.767	0.900	104	0.076	0.097	-0.114	0.267	0.785	0.435
Darkness	-145.581	0.898	104	0.091	0.097	-0.099	0.282	0.937	0.351

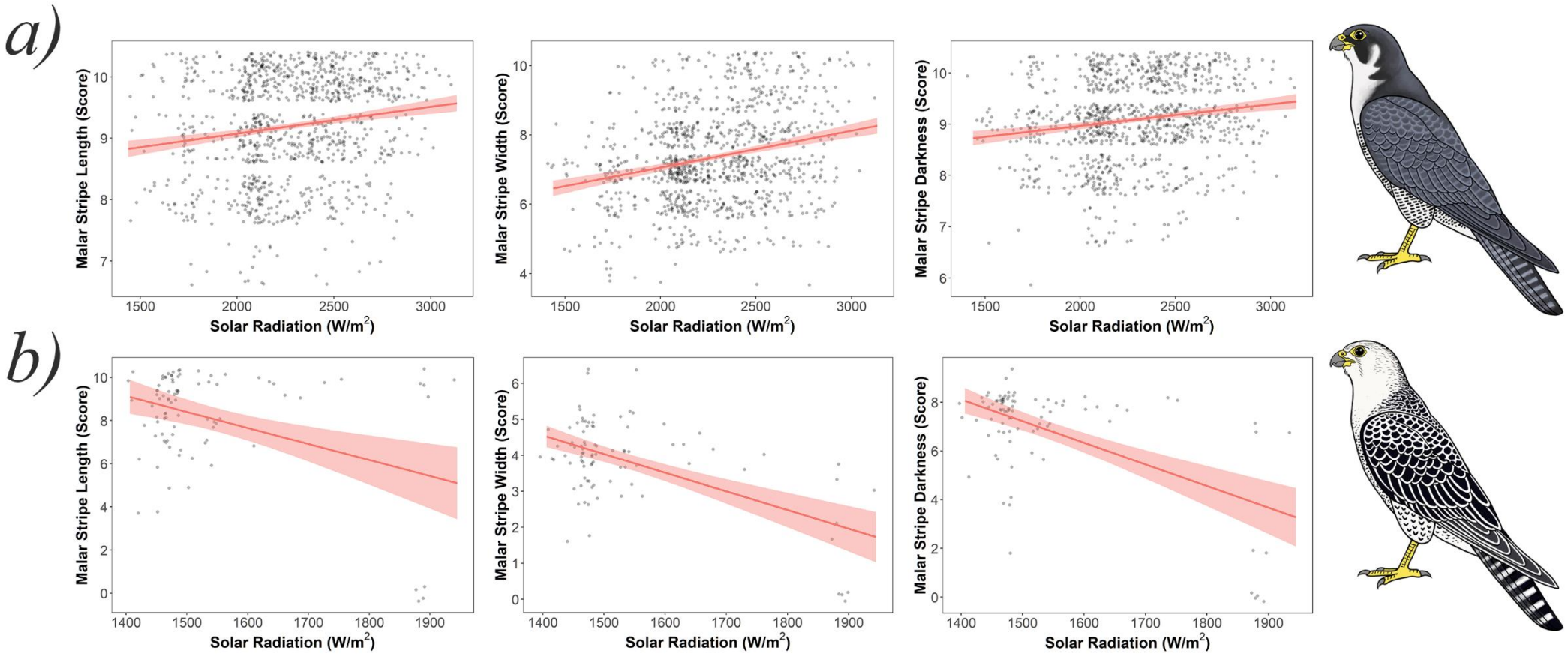

Figure 8a-b. Relationships between solar radiation (W/m^2) and malar stripe characteristics in the GLS models for the **(a)** Peregrine Falcon and **(b)** Gyrfalcon. Shaded bands represent 95% confidence intervals; pink shaded bands represent relationships for which substantial evidence was found ($p < 0.05$), black shaded bands represent relationships for which only weak evidence was found ($0.5 \leq p < 0.1$), and blue shaded bands represent relationships for which no evidence was found ($p \geq 0.1$). Datapoints are shown with a 10% jitter to aid interpretation. Plots were constructed using the R package ggplot2 (Wickham 2016).

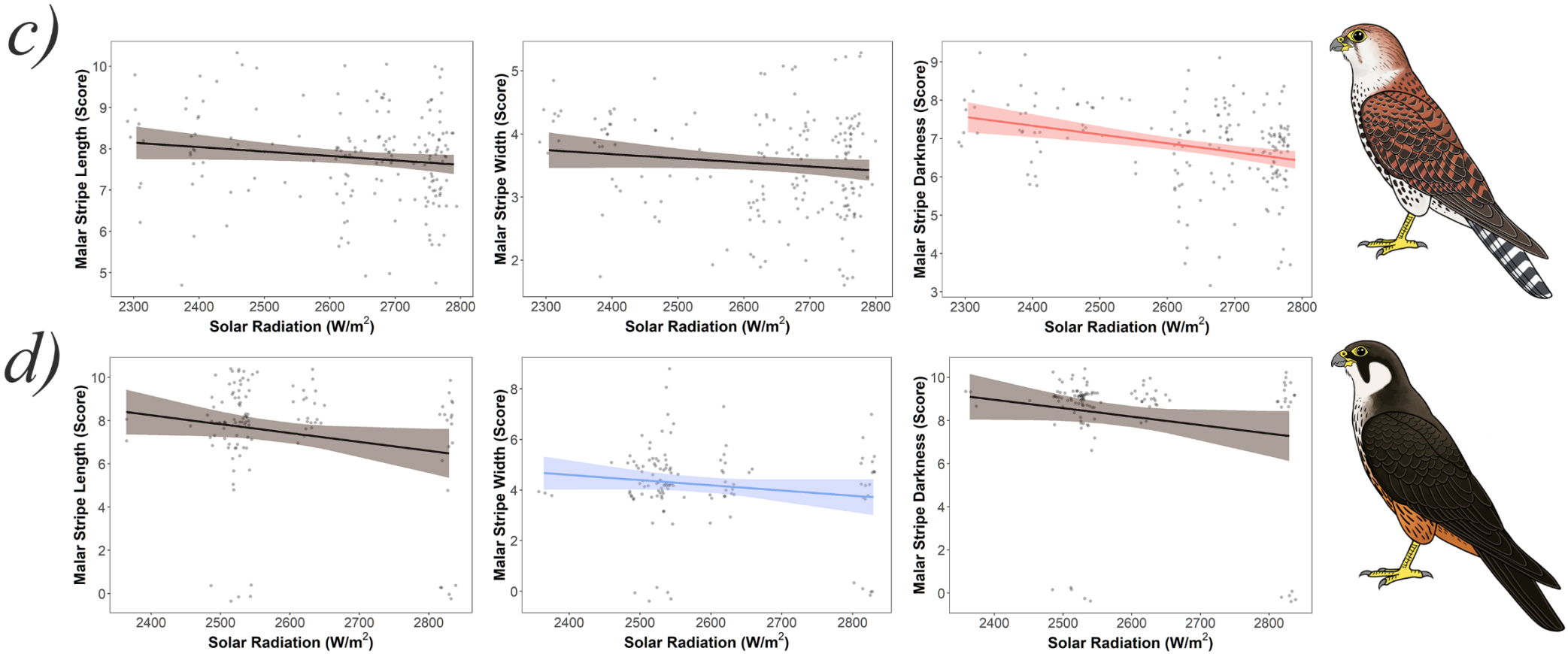

Figure 8c-d. Relationships between solar radiation (W/m^2) and malar stripe characteristics in the GLS models for the **(c)** Madagascar Kestrel and **(d)** Eleonora's Falcon. Shaded bands represent 95% confidence intervals; pink shaded bands represent relationships for which substantial evidence was found ($p < 0.05$), black shaded bands represent relationships for which only weak evidence was found ($0.5 \leq p < 0.1$), and blue shaded bands represent relationships for which no evidence was found ($p \geq 0.1$). Datapoints are shown with a 10% jitter to aid interpretation. Plots were constructed using the R package ggplot2 (Wickham 2016).

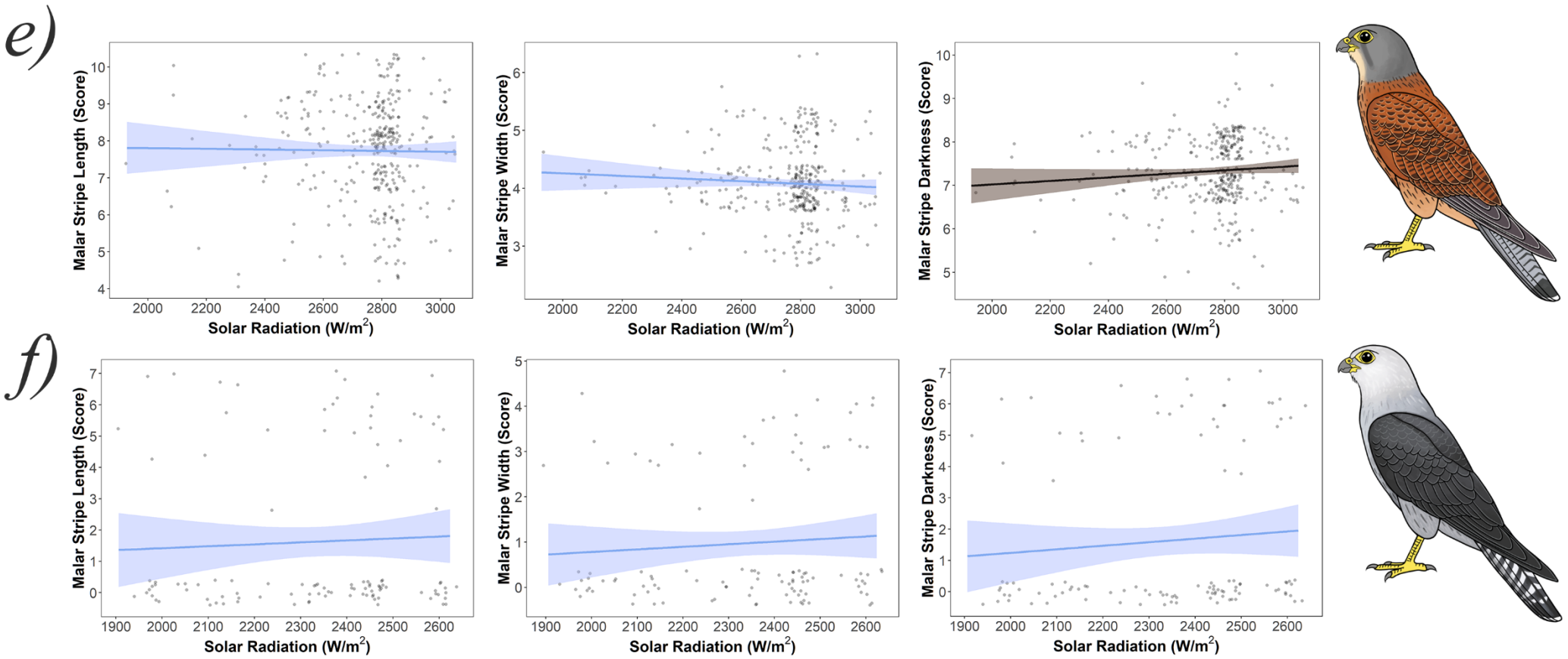

Figure 8e-f. Relationships between solar radiation (W/m^2) and malar stripe characteristics in the GLS models for the **(e)** Rock Kestrel and **(f)** Dickinson's Kestrel. Shaded bands represent 95% confidence intervals; pink shaded bands represent relationships for which substantial evidence was found ($p < 0.05$), black shaded bands represent relationships for which only weak evidence was found ($0.5 \leq p < 0.1$), and blue shaded bands represent relationships for which no evidence was found ($p \geq 0.1$). Datapoints are shown with a 10% jitter to aid interpretation. Plots were constructed using the R package ggplot2 (Wickham 2016).

4. DISCUSSION

4.1. EVIDENCE FOR SOLAR RADIATION AS A DRIVER OF FALCON MALAR STRIPES

I did not find consistent evidence that falcon malar stripe characteristics vary positively with solar radiation, either intra- or interspecifically. Most of the 39 species studied exhibited no intraspecific relationships between malar stripe size or prominence and average solar radiation during the breeding season, and, while the models suggested that there was an association between solar radiation and malar stripe width at the interspecific level, as well as a general trend for malar stripe darkness to vary with solar radiation within species, these relationships were negative in direction, such that species and individuals inhabiting regions of higher solar radiation exhibited narrower and paler malar stripes, respectively.

These findings contradict the trends found by Vrettos et al. (2021). These authors found strong positive relationships between solar radiation and malar stripe size and prominence in Peregrine Falcons, suggesting that solar radiation is a potential evolutionary driver of malar stripe characteristics in this species. However, my findings in the present study suggest that these relationships found in Peregrine Falcons are not reflected in other species, or across falcons generally. The findings of the present study are also inconsistent with the predictions of the solar glare hypothesis, and suggest that solar glare reduction is not a major selective pressure affecting malar stripe evolution in falcons, corroborating Bortolotti (2006).

The interspecific relationships found between solar radiation and malar stripe characteristics were also largely unaffected by controlling for differences in body mass, HWI, prey preference, or habitat between species, disconfirming Vrettos et al. (2021)'s hypothesis that differences in species ecology may underlie differences in the response of malar plumage to solar glare between species. Indeed, most of the biometric and ecological traits expected to be strong predictors of malar stripe size and prominence (body mass, HWI, and dependence on bird prey) were unrelated to malar stripe characteristics, while habitat openness exhibited a relationship with malar stripe width opposite to that expected under the solar glare hypothesis, with species with wider malar stripes associated with more closed or forested habitats (which experience reduced solar glare and low natural light levels due to shading from the canopy (Zink and Remsen 1986; Delhey 2019; Marcondes et al. 2020; Marcondes et al. 2021)). These results provide further evidence against the solar glare hypothesis for the evolution and function of falcon malar stripes, and suggest that malar stripes do not serve to enhance visual detection or targeting of agile prey (Vrettos et al. 2021).

However, there was some evidence that the effect of solar radiation on falcon malar stripe characteristics varies with both body size and habitat. The effects of body size were opposite to those expected under the solar glare hypothesis, with smaller species exhibiting more negative relationships between solar radiation and malar stripe darkness (i.e., stronger trends towards

paler malar stripes in regions of higher solar radiation) intraspecifically, and less positive relationships between solar radiation and malar stripe length interspecifically. Ficken et al. (1971) argued that smaller species should experience greater selective benefits from adaptations that aid in prey capture, due to both the smaller size of their prey-catching apparatus, and the greater speed and agility of their prey (Ficken et al. 1971). Thus, the trends observed here suggest that prey size and agility do not positively influence malar stripe characteristics, providing further evidence against malar stripes functioning as visual adaptations to enable targeting of agile prey (Vrettos et al. 2021). However, the direction of the habitat effect was consistent with the predictions of the solar glare hypothesis, with species inhabiting more open habitats experiencing more positive (i.e., less strongly negative) effects of solar radiation on malar stripe width, and species inhabiting regions of higher solar radiation likewise experiencing weaker or less negative relationships between malar stripe width and habitat openness. This could suggest that solar glare reduction is a positive evolutionary driver of malar stripe size in falcons, but that its effect is modulated by those of other, opposing selective pressures, such as habitat crypsis or parasite avoidance, which may exert selection for overall darker plumage in dimmer or more forested environments, and/or lighter plumage in brighter or more open environments (Galeotti et al. 2003; Chakarov et al. 2008; Amar et al. 2013; Tate et al. 2016). However, the fact that I did not observe any other interspecific relationships consistent with the predictions of the solar glare hypothesis, and that the majority of species likewise showed no intraspecific trends, perhaps suggests that such a tradeoff between solar glare reduction and other selective pressures is unlikely.

Intraspecific relationships between malar stripe characteristics and solar radiation were observed for six species: the Peregrine Falcon, Gyrfalcon, Eleonora's Falcon, Dickinson's Kestrel, Rock Kestrel, and Madagascar Kestrel. In three of these species (the Gyrfalcon, Eleonora's Falcon, and Madagascar Kestrel), the relationships were negative, with only three species (the Peregrine Falcon, Dickinson's Kestrel, and Rock Kestrel) exhibiting trends towards larger and/or darker malar stripes in regions of higher solar radiation. However, the positive relationships observed for the Dickinson's and Rock Kestrels were not replicated in the GLS analysis, suggesting that the findings for these species were not particularly robust, and that malar stripe characteristics in these species are not strongly influenced by solar radiation. Indeed, the Dickinson's Kestrel typically lacks clearly definable malar stripes (Ferguson-Lees and Christie 2001), and thus the relationships observed for this species may simply have been spurious trends driven by the small number of statistically outlying birds which received non-zero scores, since photographs were scored with the observer blind to species. This is corroborated by the fact that, of the 111 Dickinson's Kestrels in the dataset, 78 (~70%) received zero scores for all malar stripe variables. Thus, of the 39 species studied, only the Peregrine Falcon exhibited reliable trends towards larger and darker malar stripes in regions of higher solar radiation. The relationships found were largely consistent with those found by Vrettos et al. (2021), with the exception that the former study found that only the width and prominence of the malar stripe were related to solar radiation, while malar stripe length was unrelated to any climatic variables (Vrettos et al. 2021); however, in the present study, all three malar stripe variables (length included) were positively related to solar radiation. This discrepancy may potentially be explained by the fact that in this study I used a revised form of the visual scoring system developed by Vrettos et al. (2021)

adapted for use with multiple species, whose scoring categories may have been more sensitive to individual intraspecific differences, or provided more accurate estimates of the variation in malar stripe characteristics between individuals or species. Alternately, this revised scoring system may have controlled more effectively for visual distortion of the malar area caused by the angle or position of the bird's head in the photograph (Vrettos et al. 2021).

Of the three species that exhibited negative intraspecific relationships between malar stripe characteristics and solar radiation, only those for the Gyrfalcon and Madagascar Kestrel were reliably replicated in the GLS analysis, with only weak evidence for relationships between malar stripe characteristics and solar radiation in the Eleonora's Falcon. The negative relationships observed for the Eleonora's Falcon appeared to be driven by the presence of dark-morph birds, most of which lacked clearly definable malar stripes and thus received scores of zero; this is corroborated by the fact that removing these birds from analysis caused the weak relationship between solar radiation and malar stripe length to disappear, despite dark-morph birds accounting for only 10 (~8%) of the Eleonora's Falcons in the dataset (Table S10). Removing dark-morph birds from the analysis also reversed the direction of the weak relationship between solar radiation and malar stripe darkness, with birds with darker malar stripes associated with regions of higher solar radiation (Table S10). This is potentially indicative of a relationship between light environment and morph frequencies or plumage darkness opposite to that observed in the Black Sparrowhawk, with a higher proportion of melanistic birds and/or birds with overall darker plumage in regions of higher solar radiation (Amar et al. 2013; Tate et al. 2016). However, the fact that only weak evidence ($p > 0.05$) was obtained for these trends, and that the species was represented by a fairly small sample size ($N = 121$, with $N = 10$ dark-morph birds), mean that these findings should be interpreted with caution. More robust negative relationships between malar stripe characteristics and solar radiation were observed for the Gyrfalcon and Madagascar Kestrel, with the Gyrfalcon demonstrating strong negative relationships between solar radiation and all three malar stripe variables (i.e., smaller and paler malar stripes in regions of higher solar radiation), while the Madagascar Kestrel demonstrated such a trend for malar stripe darkness only. However, as in the Eleonora's Falcon, the negative relationships observed for the Gyrfalcon appeared to be driven largely by the small number ($N = 4$) of all-white birds which received zero scores for all malar stripe variables; repeating the analysis with these birds removed caused the relationship with malar stripe length to disappear (Table S10). However, unlike in the Eleonora's Falcon, removing these birds did not meaningfully change the relationships observed for width or darkness (Table S10), suggesting that the trends observed were not simply driven by a small number of individuals.

The results of this study show that malar stripe size and prominence vary positively with solar radiation in Peregrine Falcons, corroborating Vrettos et al. (2021), but these trends are not observed in any other falcon species. A possible reason for this discrepancy may be that Peregrine Falcons have a wider geographic distribution (and thus experience a greater diversity of solar radiation conditions over their range) than any other falcon species, and thus, if malar stripes do serve a glare-reducing function in falcons, species other than the Peregrine Falcon may simply lack sufficient variation in solar radiation conditions over their ranges to enable detection of intraspecific trends. However, solar radiation was not positively related to any of the three

malar stripe variables interspecifically, and indeed was negatively related to malar stripe characteristics in some species, suggesting that malar stripes likely do not generally serve a glare-reducing function in falcons. Similarly, other falcon species with wide geographic ranges (e.g., the Common Kestrel, American Kestrel, and Merlin) did not show any intraspecific relationships between malar stripe characteristics and solar radiation in this study, suggesting that range size is unlikely to be the reason that positive trends were not observed in species other than the Peregrine Falcon. One explanation for why malar stripe characteristics are positively related to solar radiation in Peregrine Falcons, but not other falcon species, may thus be that malar stripes do indeed serve a glare-reducing role in Peregrine Falcons, but do not serve this function in falcons generally, with Peregrine Falcon malar stripes thus representing a specialization or exaptation of a general falcon trait that originally evolved for a different purpose. While Peregrine Falcons are notable among falcons for their cosmopolitan geographic range, with breeding populations occurring on all major land masses except New Zealand (Aotearoa) and Antarctica (Ferguson-Lees and Christie 2001), they are also renowned for their unusual speed (being able to reach diving speeds over 100 km faster than other aerial chasing or stooping species (Ferguson-Lees and Christie 2001)), as well as their high degree of specialization for aerial hunting of bird prey (Ferguson-Lees and Christie 2001). Thus, Peregrine Falcons may benefit uniquely from adaptations that reduce the negative effects of solar glare on vision while hunting, or experience exceptionally strong selection for such traits, as a result of their fairly unique ecology. Thus, the solar glare hypothesis may plausibly explain intraspecific variation in malar stripe characteristics in Peregrine Falcons, despite not explaining the function or evolutionary significance of malar stripes in falcons generally.

4.2. ALTERNATIVE HYPOTHESES FOR FALCON MALAR STRIPES

The lack of trends, or negative trends, found both across falcons generally and within individual species overwhelmingly suggest that falcon malar stripes do not universally serve a glare-reducing function, at least in species other than the Peregrine Falcon. Thus, other functional hypotheses need to be considered. The fact that negative relationships with solar radiation were found for two of the malar stripe variables (length, interspecifically, and darkness, intraspecifically) directly contradicts the predictions of the solar glare hypothesis, but is consistent with the "light level-detectability" hypothesis for raptor plumage colouration (Galeotti et al. 2003; Tate et al. 2016), as well as with trends in body plumage colouration found in other raptors, such as the Black Sparrowhawk (Amar et al. 2013; Tate et al. 2016). This could potentially suggest that malar plumage in falcons serves a background-matching function, with falcons with larger and darker malar stripes or darker malar regions presumably experiencing greater crypsis in regions of lower solar radiation due to their ability to camouflage against dark skies (Galeotti et al. 2003; Amar et al. 2013; Tate et al. 2016). The fact that malar stripe width was found to be negatively related to habitat openness is also consistent with the predictions of this hypothesis, as falcons with larger malar stripes are likely less detectable to prey in the low light conditions associated with dense forest canopies or heavy vegetation cover (Galeotti et al.

2003; Amar et al. 2013; Tate et al. 2016). Indeed, the results of this study suggested that habitat and solar radiation exert a compounding influence on falcon malar plumage, with the effect of low solar radiation conditions on malar stripe width stronger between forest species, and likewise the effect of forested habitat stronger for species inhabiting regions of low solar radiation. This is consistent with light environment being the most important driver of malar plumage evolution between species. The interactions observed between solar radiation and body mass may also potentially be explained by crypsis being relatively more important for smaller species due to their need to disguise themselves from both prey and larger predators (Newman et al. 2005).

The intraspecific relationships found for the Gyrfalcon and Madagascar Kestrel were also consistent with cryptic functions for malar plumage in these species, with individuals occurring in brighter habitats exhibiting paler malar regions in order to camouflage against pale substrates or skies, while those occurring in dimmer (e.g., cloudier and/or more forested) habitats exhibit larger and/or darker malar stripes to match their darker environments (Galeotti et al. 2003; Amar et al. 2013; Tate et al. 2016). Such background-matching may be especially important in the Gyrfalcon, a highly polymorphic species whose plumage colouration varies from pure white to almost black (Ferguson-Lees and Christie 2001; Johnson and Burnham 2011), with white birds presumably experiencing greater crypsis in open tundra or bright, snowy environments, whereas darker birds experience more effective camouflage in dimmer boreal forest or taiga habitats. This is consistent with the observation that morph frequencies in the Gyrfalcon vary by geography and latitude, with white morphs dominating in northern Canada and Greenland (> 75ºN), silver and grey morphs in central to southern Greenland, Alaska, and Siberia (~67ºN), and dark grey, brown, and black morphs in Iceland and central Eurasia (Johnson and Burnham 2011). However, the fact that both the Gyrfalcon and the Madagascar Kestrel were represented by fairly small sample sizes (N = 90 and N = 177, respectively), suggest that these relationships should perhaps be interpreted with caution. Likewise, as Johnson and Burnham (2011) note, observed geographic trends in plumage colouration in Gyrfalcons may alternately be explained by plumage colour serving a thermoregulatory function, or simply by population differentiation and genetic drift within currently or historically isolated populations (Johnson and Burnham 2011). The fact that negative interspecific relationships between solar radiation and malar stripe darkness were less consistently observed when birds with uniform plumage were removed from the dataset may also suggest that these interspecific trends were spurious, and driven by species which lack clearly definable malar stripes; both this, and the fact that negative intraspecific relationships between solar radiation and malar stripe characteristics were not observed for the majority of species, may potentially provide evidence against the light environments hypothesis. Thus, further investigation is required to determine the relationships between malar plumage and solar radiation, light environments, and habitat crypsis in falcons.

However, while light environments or habitat crypsis may potentially explain the negative relationships between solar radiation, habitat openness, and malar plumage characteristics found in this study, background-matching is perhaps unlikely to explain the evolutionary significance of falcon malar stripes specifically. This is because, as Vrettos et al. (2021) argue, malar stripes cover only a small area of the body, and are thus presumably of minor importance in background-matching camouflage compared to other ventral plumage that is more conspicuous

to prey (Vrettos et al. 2021). Indeed, it does not seem intuitively plausible that selection for background-matching camouflage would result in the evolution of distinctive dark eye markings specifically (rather than overall dark plumage), especially when trends in other taxa suggest that such markings are not typically associated with species that inhabit low light environments (Ficken and Wilmot 1968; Ficken et al. 1971; Densley 1979; Ortolani 1999; Yosef et al. 2012; Josef 2017). Thus, the negative effects of solar radiation and habitat openness on malar stripe characteristics may not be due to malar stripes themselves serving a background-matching function, but rather simply a result of larger or darker malar stripes tending to occur in species with overall darker or more strongly marked plumage. Thus, more specific functional hypotheses may need to be invoked to explain the evolution and maintenance of malar stripes in falcons. One possible hypothesis is that malar stripes serve to disguise the falcon's eye, thereby reducing detectability by prey (Barlow 1972; Gavish and Gavish 1981; Josef 2017). Such a function would be consistent with the fact that dark markings around or partially incorporating the eye reduce the visibility of bird eyes to human observers (Gavish and Gavish 1981), as this means that such markings presumably have the same effect on prey species with similar visual acuity, such as birds and mammals (Gavish and Gavish 1981). The fact that I did not find any relationships between malar stripe characteristics and prey preference in this study would appear to contradict this hypothesis; however, I scored prey preference according to each species' dependence on bird prey, such that species that feed primarily on mammals or depend equally on bird and mammal prey received low scores. Thus, if the visual acuity of prey species, rather than their speed, agility, or flight ability, determines the strength of selection on falcon malar stripe characteristics, falcon species that feed on mammal prey should exhibit malar stripes of similar size and prominence to those that feed on bird prey, consistent with the lack of relationships with prey preference found in this study.

An alternate hypothesis for the function of falcon malar stripes is that they serve in visual communication or signalling, for example as aposematic devices (e.g., by enhancing the visual appearance of the eye and bill and thus enabling the bird to look larger or more threatening (Negro et al. 2007)), or as visual markers of individual identity or status (Dale 2006). For example, Negro et al. (2007) argue that falcon malar stripes may serve as aposematic signals that warn other (or larger) predators of potential aggressive or defensive behaviour and therefore deter predation or antagonistic interactions, similar to the function proposed by Newman et al. (2005) for facial masks in mid-guild mammalian carnivores (Newman et al. 2005; Negro et al. 2007). The fact that malar stripes typically occur in both adult and juvenile plumage (Ferguson-Lees and Christie 2001) may potentially corroborate this hypothesis. This use of malar stripes as intimidation devices may also be relevant to territorial displays between conspecifics, with larger or darker malar stripes potentially signalling social dominance or serving as indicators of body condition, age, and/or sex (malar stripes are typically darker in adult than in juvenile or immature plumage (Ferguson-Lees and Christie 2001), while there is also some evidence for sexual dimorphism in malar stripes in Peregrine Falcons (Zuberogoitia et al. 2009; 2013)). Malar stripe size and darkness may also serve as signals of mate quality, in keeping with the quality-signalling roles demonstrated for other melanin-based plumage characteristics in kestrels (grey tail and rump colouration correlates positively with social status, hunting skill, clutch size, and laying date in both male and female Common Kestrels (Vergara and Fargallo 2011; López-

Idiáquez et al. 2016), while the width of the black subterminal tail band correlates negatively with hatching success and food provisioning rate in male American Kestrels (Wiehn 1997)). Alternately, the warning signal of malar stripes may serve to deter potential rivals and thus reduce the frequency of potentially costly antagonistic interactions. Indeed, Dale (2006) argues that plumage colouration in territorial falcons may serve as a visual signal of identity, potentially reducing needless aggression among neighbouring heterospecifics as well as potentially facilitating mate and kin recognition (Dale 2006). Such a function for malar stripes (in which socio-sexual and behavioural traits, rather than environmental conditions or feeding ecology, may be expected to be the most important drivers of malar stripe evolution between populations or species) would be consistent with the lack of relationships between malar stripe characteristics and solar radiation in most species in this study, as well as the inconsistent evidence found for relationships between malar stripe characteristics, solar radiation, and species ecology interspecifically.

4.3. LIMITATIONS OF THE PRESENT STUDY AND DIRECTIONS FOR FUTURE RESEARCH

A potential limitation of this study is that the analysis concerned only the relationships between falcon malar plumage and solar radiation, without considering effects of other climatic variables. While Vrettos et al. (2021) found only moderate effects of climatic variables other than solar radiation, such as temperature and rainfall, on malar stripe characteristics in Peregrine Falcons, there is substantial evidence from a variety of bird taxa that plumage characteristics are affected by these climatic factors, with geographical plumage variation in many species and clades following versions of Gloger's and/or Bogert's rules (Gloger 1833; Bogert 1949; Burtt and Ichida 2004; Clusella-Trullas et al. 2007; Delhey 2018; Galván et al. 2018; Delhey 2019; Amar et al. 2019; Romano et al. 2019; Marcondes et al. 2020; Marcondes et al. 2021; Goldenberg et al. 2022). The weak negative relationships found between solar radiation and malar stripe characteristics may thus possibly be explained by underlying relationships with other climatic factors that covary with solar radiation. For example, the trend towards wider malar stripes in falcons inhabiting both regions of lower solar radiation and more forested habitats, attributed to such plumage potentially playing a role in camouflage, could instead be explained by darker plumage providing greater protection against ectoparasite or bacterial feather damage in regions of higher rainfall (Burtt and Ichida 2004; Marcondes et al. 2020), which are also characterised by greater cloud and vegetation cover (Amar et al. 2013; Tate et al. 2016). Likewise, relationships between plumage characteristics and other climatic variables (such as trends towards darker plumage in rainier or colder conditions) could potentially obscure positive relationships with solar radiation. Thus, assessing the effect of solar radiation on falcon malar stripes in conjunction with those of rainfall, humidity, and temperature, in addition to assessing the degree of correlation between malar stripe characteristics and overall body plumage, may provide more comprehensive or nuanced insight into the relative effects of different climatic conditions on falcon plumage characteristics.

4.4. CONCLUSIONS

The results of this study suggest that solar radiation is not a primary or universal driver of malar stripe characteristics in falcons, and thus that the solar glare hypothesis is unlikely to explain the function and evolutionary significance of falcon malar stripes. However, malar stripe size and prominence are positively associated with solar radiation in Peregrine Falcons, potentially indicative of malar stripes functioning as an exaptation for solar glare reduction in this species. In other falcon species, malar stripes may potentially serve as cryptic devices or function in visual signalling, although testing such hypotheses is beyond the scope of the present analysis. Likewise, the results of this study are purely correlative, and do not demonstrate any functional role for falcon malar stripes. Future studies of this nature should thus incorporate functional or experimental analyses, for example using experimental manipulation of falcon malar stripes to determine the effect of such manipulations on hunting success, detectability to prey, or behavioural responses from predators or conspecifics, in addition to investigating relationships between climatic conditions and falcon plumage characteristics more generally. Furthermore, future studies should make use of evolutionary analyses (e.g., ancestral character state reconstruction) to determine when malar stripes originally evolved in falcons, as well as the habitat conditions and behavioural ecology of the ancestral falcon species in which this trait originated. Such analyses would enhance understanding of both the functional role and evolutionary context and significance of falcon malar stripes, and thus provide valuable insight into the role of this distinctive and characteristic plumage feature.

REFERENCES

Abatzoglou, J. T., Dobrowski, S. Z., Parks, S. A., Hegewisch, K. C. 2018. TerraClimate, a high-resolution global dataset of monthly climate and climatic water balance from 1958–2015. *Scientific Data* 5:170191. DOI: 10.1038/sdata.2017.191.

Amar, A., Koeslag, A., Curtis, O. 2013. Plumage polymorphism in a newly colonized black sparrowhawk population: classification, temporal stability and inheritance patterns. *Journal of Zoology* 289:60-67. DOI: 10.1111/j.1469-7998.2012.00963.x.

Amar, A., Reynolds, C., Van Velden, J., Briggs, C. W. 2019. Clinal variation in morph frequency in Swainson's hawk across North America: no support for Gloger's ecogeographical rule. *Biological Journal of the Linnean Society*, 2019 127(2):299-309. DOI: 10.1093/biolinnean/blz037.

Averill, C. K. 1923. Black wing tips. *The Condor* 25:57–59. DOI: 10.2307/1362901.

Bachl, F., Lindgren, F., Borchers, D., Illian, J. 2019. inlabru: an R package for Bayesian spatial modelling from ecological survey data. *Methods in Ecology and Evolution* 10:760–766. DOI: 10.1111/2041-210X.13168.

Barlow, G. W. 1972. The Attitude of Fish Eye-Lines in Relation to Body Shape and to Stripes and Bars. *Copeia* 1972(1):4-12. DOI: 10.2307/1442777.

Barrowclough, G. F., Sibley, F. C. 1980. Feather Pigmentation and Abrasion: Test of a Hypothesis. *The Auk* 97(4):881-883. DOI: 10.1093/auk/97.4.881.

Bergman, G. 1982. Why are the wings of *Larus f. fuscus* so dark? *Ornis Fennica* 59:77-83.

Billerman, S. M., Keeney, B. K., Rodewald, P. G., Schulenberg T. S. (eds.). 2020. *Birds of the World*. Cornell Laboratory of Ornithology, Ithaca, New York, USA. https://birdsoftheworld.org/bow/home.

BirdLife International. 2020. IUCN Red List for birds. Downloaded from http://www.birdlife.org on 12/04/2020.

BirdLife International and Handbook of the Birds of the World. 2020. Bird species distribution maps of the world. Version 2020.1. Available at http://datazone.birdlife.org/species/requestdis.

Bivand, R., Lewin-Koh, N. 2021. maptools: Tools for Handling Spatial Objects. R package version 1.1-2, https://CRAN.R-project.org/package=maptools.

Bivand, R., Keitt, T., Rowlingson, B. 2021. rgdal: Bindings for the 'Geospatial' Data Abstraction Library. R package version 1.5-28. https://CRAN.R-project.org/package=rgdal.

Bogert, C. M. 1949. Thermoregulation in reptiles: a factor in evolution. *Evolution* 3(3):195-211. DOI: 10.1111/j.1558-5646.1949.tb00021.x.

Bolker, B. M., Brooks, M. E., Clark, C. J., Geange, S. W., Poulsen, J. R., Stevens, M. H. H. 2008. Generalized linear mixed models: a practical guide for ecology and evolution. *Trends in Ecology and Evolution* 24(3):127-135. DOI: 10.1016/j.tree.2008.10.008.

Bonser, R. C. H. 1995. Melanin and the Abrasion Resistance of Feathers. *The Condor* 97:590-591. DOI: 10.2307/1369048.

Bortolotti, G. R. 2006. Natural selection and coloration: protection, concealment, advertisement, or deception. In G. E. Hill & K. J. McGraw (eds.) *Bird coloration Vol. 2: function and evolution*. Harvard University Press, Cambridge, Massachusetts, pp. 3-35.

Burtt, E. H. 1981. The adaptiveness of animal colors. *Bioscience* 31:723–729. DOI: 10.2307/1308778.

Burtt, E. H. 1984. Colour of the upper mandible: an adaptation to reduce reflectance. *Animal Behaviour* 32(3):652-658. DOI: 10.1016/S0003-3472(84)80140-2.

Burtt, E. H. 1986. An analysis of physical, physiological, and optical aspects of avian coloration with emphasis on wood-warblers. *Ornithological Monographs* 38(38):1-126. DOI: 10.2307/40166782.

Burtt, E. H., Ichida, J. M. 2004. Gloger's Rule, Feather-Degrading Bacteria, and Color Variation Among Song Sparrows. *The Condor* 106(31):681-686. DOI: 10.1650/7383.

Caro, T., Izzo, A., Reiner, R. C., Walker, H., Stankowich, T. 2014. The function of zebra stripes. *Nature Communications* 5:3535. DOI: 10.1038/ncomms4535.

Chakarov, N., Boerner, M., Krüger, O. 2008. Fitness in common buzzards at the cross-point of opposite melanin–parasite interactions. *Functional Ecology* 22(6):1062-1069. DOI: 10.1111/j.1365-2435.2008.01460.x.

Clusella-Trullas, S., van Wyk, J. H., Spotila, J. R. 2007. Thermal melanism in ectotherms. *Journal of Thermal Biology* 32:235–245. DOI: 10.1016/j.jtherbio.2007.01.013.

Comtois, D. 2021. summarytools: Tools to Quickly and Neatly Summarize Data. R package version 1.0.0, https://CRAN.R-project.org/package=summarytools.

Cooney, C. R., Varley, Z. K., Nouri, L. O., Moody, C. J. A., Jardine, M. D., Thomas, G. H. 2019. Sexual selection predicts the rate and direction of colour divergence in a large avian radiation. *Nature Communications* 10:1773. DOI: 10.1038/s41467-019-09859-7.

Cuthill, I. C., Allen, W. L., Arbuckle, K., Caspers, B., Chaplin, G., Hauber, M. E., Hill, G. E., Jablonski, N. G., Jiggins, C. D., Kelber, A., Mappes, J., et al. 2017. The biology of color. *Science* 357(6350): eaan0221. DOI: 10.1126/science.aan0221.

Dale, J. 2006. Intraspecific Variation in Coloration. In G. E. Hill & K. J. McGraw (eds.) *Bird coloration Vol. 2: function and evolution*. Harvard University Press, Cambridge, Massachusetts, pp. 36-84.

De Broff, B. M., Pahk, P. J. 2003. The Ability of Periorbitally Applied Antiglare Products to Improve Contrast Sensitivity in Conditions of Sunlight Exposure. *Archives of Ophthalmology* 121(7): 997-1001. DOI: 10.1001/archopht.121.7.997.

Delhey, K. 2018. Darker where cold and wet: Australian birds follow their own version of Gloger's rule. *Ecography* 41(4):673-683. DOI: 10.1111/ecog.03040.

Delhey, K. 2019. A review of Gloger's rule, an ecogeographical rule of colour: definitions, interpretations and evidence. *Biological Reviews* 94(4):1294-1316. DOI: 10.1111/brv.12503.

Delhey, K., Dale, J., Valcu, M., Kempenaers, B. 2021. Migratory birds are lighter coloured. *Current Biology* 31(23):R1511-R1512. DOI: 10.1016/j.cub.2021.10.048.

Densley, M. 1979. Ross's Gulls in Alaska. *British Birds* 72:23-28.

Dinnage, R., Simonsen, A. K., Barrett, L. G., Cardillo, M., Raisbeck-Brown, N., Thrall, P. H., Prober, S. M. 2018. Larger plants promote a greater diversity of symbiotic nitrogen-fixing soil bacteria associated with an Australian endemic legume. *Journal of Ecology* 107:977-991. DOI: 10.1111/1365-2745.13083.

Dinnage, R., Skeels, A., Cardillo, M. 2020. Spatiophylogenetic modelling of extinction risk reveals evolutionary distinctiveness and brief flowering period as threats in a hotspot plant genus. *Proceedings of the Royal Society B* 287(1926): 20192817. DOI: 10.1098/rspb.2019.2817.

Dormann, C. F., McPherson, J. M., Araújo, M. B., Bivand, R., Bolliger, J., Carl, G., Davies, R. G., Hirzel, A., Jetz, W., Kissling, W. D., Kühn, I., Ohlemüller, R., Peres-Neto, P. R., Reineking, B., Schröder, B., Schurr, F. M., Wilson, R. 2007. Methods to account for spatial autocorrelation in the analysis of species distributional data: a review. *Ecography* 30:609-628. DOI: 10.1111/j.2007.0906-7590.05171.x.

Dunning, J. B. 2008. *CRC Handbook of Avian Body Masses*, 2nd ed. CRC Press, Boca Raton, Florida. DOI: 10.1201/9781420064452.

Ellis, H. I. 1984. Energetics of free-ranging seabirds. In G. C. Whittow & H. Rahn (eds.), *Seabird Energetics.* Springer US, New York, pp. 203-234. DOI: 10.1007/978-1-4684-4859-7_10.

Ferguson-Lees, J., Christie, D. A. 2001. *Raptors of the world*. A&C Black, London.

Ferns, P. N., Hinsley, S. A. 2004. Immaculate tits: Head plumage pattern as an indicator of quality in birds. *Animal Behaviour* 67(2):261-272. DOI: 10.1016/j.anbehav.2003.05.006.

Ficken, R. W., Matthiae, P. E., Horwich, R. 1971. Eye Marks in Vertebrates: Aids to Vision. *Science* 173(4000):936-939. DOI: 10.1126/science.173.4000.936.

Ficken, R. W., Wilmot, L. B. 1968. Do Facial Eye-stripes Function in Avian Vision? *The American Midland Naturalist* 79(2):522-523. DOI: 10.2307/2423199.

Fuchs, J., Johnson, J. A., Mindell, D. P. 2015. Rapid diversification of falcons (Aves: Falconidae) due to expansion of open habitats in the Late Miocene. *Molecular Phylogenetics and Evolution* 82:166-182. DOI: 10.1016/j.ympev.2014.08.010.

Galeotti, P., Rubolini, D., Dunn, P. O., Fasola, M. 2003. Colour polymorphism in birds: causes and functions. *Journal of Evolutionary Biology* 16(4):635-646. DOI: 10.1046/j.1420-9101.2003.00569.x.

Galván, I., Rodríguez-Martínez, S., Carrascal, L. M. 2018. Dark pigmentation limits thermal niche position in birds. *Functional Ecology* 32:1531–1540. DOI: 10.1111/1365-2435.13094.

Galván, I., Sanz, J. J. 2007. The cheek plumage patch is an amplifier of dominance in great tits. *Biology Letters* 4(1):12-15. DOI: 10.1098/rsbl.2007.0504.

Gangoso, L., Grande, J. M., Ducrest, A.-L., Figuerola, J., Bortolotti, G. R., Andrés, J. A., Roulin, A. 2011. MC1R-dependent, melanin-based colour polymorphism is associated with cell-mediated response in the Eleonora's falcon. *Journal of Evolutionary Biology* 24(9):2055-2063. DOI: 10.1111/j.1420-9101.2011.02336.x.

Gavish, L., Gavish, B. 1981. Patterns that Conceal a Bird's Eye. *Zeitschrift für Tierpsychologie* 56(3):193-204. DOI: 10.1111/j.1439-0310.1981.tb01296.x.

Gelman, A., Jakulin, A., Pittau, M. G., Su, Y.-S. 2008. A weakly informative default prior distribution for logistic and other regression models. *The Annals of Applied Statistics* 2:1360–1383. DOI: 10.1214/08-AOAS191.

Gloger, C. W. L. 1833. Abänderungsweise der einzelnen, einer Veränderung durch das Klima unterworfenen Farben. In C. W. L. Gloger (ed.) *Das Abändern der Vögel durch Einfluss des Klimas* [*The Evolution of Birds Through the Impact of Climate*] (in German). August Schulz, Breslau, pp. 11-24.

Goldenberg, J., Bisschop, K., D'Alba, L., Shawkey, M. D. 2022. The link between body size, colouration and thermoregulation and their integration into ecogeographical rules: a critical appraisal in light of climate change. *Oikos* 2022: e09152. DOI: 10.1111/oik.09152.

Gomes, A. C., Silva, R., Cardoso, G. C. (2018). Plumage pigmentation patterns of diurnal raptors in relation to colour ornamentation and ecology. *Journal of Ornithology* 159:793-804. DOI: 10.1007/s10336-018-1550-3.

Gorelick, N., Hancher, M., Dixon, M., Ilyushchenko, S., Thau, D., Moore, R. 2017. Google Earth Engine: Planetary-scale geospatial analysis for everyone. *Remote Sensing of Environment* 202(1):18-27. DOI: 10.1016/j.rse.2017.06.031.

Graul, W. D. 1973. Possible Functions of Head and Breast Markings in Charadriinae. *The Wilson Bulletin* 85(1):60-70.

Heppner, F. 1970. The metabolic significance of differential absorption of radiant energy by black and white birds. *The Condor* 72:50–59. DOI: 10.2307/1366474.

Hijmans, R. J. 2022. raster: Geographic Data Analysis and Modeling. R package version 3.5-21, https://CRAN.R-project.org/package=raster.

Hirsch, J. 1982. Falcon visual sensitivity to grating contrast. *Nature* 300(5887):57-58. DOI: 10.1038/300057a0.

Hockey, P. A. R., Dean, W. R. J., Ryan, P. G. 2005. *Roberts Birds of Southern Africa*, VIIth ed. The Trustees of the John Voelcker Bird Book Fund, Cape Town.

Hustler, K. 1983. Breeding Biology of the Peregrine Falcon in Zimbabwe. *Ostrich* 54(3):161-171. DOI: 10.1080/00306525.1983.9634466.

Illian, J. B., Sørbye, S. H., Rue, H. 2012. A toolbox for fitting complex spatial point process models using integrated nested Laplace approximation (INLA). *The Annals of Applied Statistics* 6(4):1499–1530. DOI: 10.1214/11-AOAS530.

Jenkins, A. 2000. Factors affecting breeding success of Peregrine and Lanner Falcons in South Africa. *Ostrich* 71(3-4):385-392. DOI: 10.1080/00306525.2000.9639837.

Johnson, J. A., Burnham, K. K. 2011. Population Differentiation and Adaptive Selection on Plumage Color Distributions in Gyrfalcons. In R. T. Watson, T. J. Cade, M. Fuller, G. Hunt, and E. Potapov (eds.) *Gyrfalcons and Ptarmigan in a Changing World, Volume I*. The Peregrine Fund, Boise, Idaho, USA, pp. 71-90. DOI: 10.4080/gpcw.2011.0108.

Jones, M. P., Pierce Jr, K. E. and Ward, D. 2007. Avian vision: a review of form and function with special consideration to birds of prey. *Journal of Exotic Pet Medicine* 16(2): 69-87. DOI: 10.1053/j.jepm.2007.03.012.

Josef, M. 2017. Peri-Ocular Eye Patterning (POEP): More than Meets the Eye. *Open Journal of Animal Sciences* 7(3):356-363. DOI: 10.4236/ojas.2017.73027.

Lebow, C. 2020.Glare Reduction by Dark Facial Markings and Bills in Birds. Electronic Theses and Dissertations 287. https://scholarworks.sfasu.edu/etds/287.

Lei, B., Amar, A., Koeslag, A., Gous, T. A., Tate, G. J. 2013. Differential haemoparasite intensity between black sparrowhawk (*Accipiter melanoleucus*) morphs suggests an adaptive function for polymorphism. PLoS One 8(12): e81607. DOI: 10.1371/journal.pone.0081607.

Leighton, G. R. M., Hugo, P. S., Roulin, A., Amar, A. 2016. Just Google it: assessing the use of Google Images to describe geographical variation in visible traits of organisms. *Methods in Ecology and Evolution* 7(9). DOI: 10.1111/2041-210X.12562.

Li, D., Dinnage, R., Nell, L. A., Helmus, M. R., Ives, A. R. 2020. phyr: An r package for

phylogenetic species-distribution modelling in ecological communities. *Methods in Ecology and Evolution* 11(11):1455-1463. DOI: 10.1111/2041-210X.13471.

Lindgren, F., Rue, H. 2015. Bayesian Spatial Modelling with R-INLA. *Journal of Statistical Software* 63(19):1-25. DOI: 10.18637/jss.v063.i19.

Lindgren, F., Rue, H., Lindström, J. 2011. An explicit link between Gaussian fields and Gaussian Markov random fields: the stochastic partial differential equation approach. J*ournal of the Royal Statistical Society: Series B (Statistical Methodology)* 73:423–498. DOI: 0.1111/j.1467-9868.2011.00777.x.

López-Idiáquez, D., Vergara, P., Fargallo, J. A., Martínez-Padilla, J. 2016. Female plumage coloration signals status to conspecifics. *Animal Behaviour* 121:101-106. DOI: 10.1016/j.anbehav.2016.08.020.

Marcondes, R. S., Stryjewski, K. F., Brumfield, R. T. 2020. Testing the simple and complex versions of Gloger's rule in the Variable Antshrike (*Thamnophilus caerulescens*, Thamnophilidae). *The Auk* 137(3):ukaa026. DOI: 10.1093/auk/ukaa026.

Marcondes, R. S., Nations, J. A., Seeholzer, G. F., Brumfield, R. T. 2021. Rethinking Gloger's Rule: Climate, Light Environments, and Color in a Large Family of Tropical Birds (Furnariidae). *The American Naturalist* 197(5). DOI: 10.1086/713386.

Mazerolle, M. J. 2020. AICcmodavg: Model selection and multimodel inference based on (Q)AIC(c). R package version 2.3-1. https://cran.r-project.org/package=AICcmodavg,

McClure, C. J., Lepage, D., Dunn, L., Anderson, D. L., Schulwitz, S. E., Camacho, L., et al. 2020. Towards reconciliation of the four world bird lists: Hotspots of disagreement in taxonomy of raptors. *Proceedings of the Royal Society B* 287(1929):20200683. DOI: 10.1098/rspb.2020.0683.

McPherson, S., Sumasgutner, P., Downs, C. T. 2021. South African raptors in urban landscapes: a review. Ostrich 92(1):41-57. DOI: 10.2989/00306525.2021.1900942.

Mitkus, M., Potier, S., Martin, G. R., Duriez, O., Kelber, A. 2018. Raptor vision. In S. M. Sherman (ed.) *Oxford Research Encyclopedia of Neuroscience*. Oxford University Press, Oxford. DOI: 10.1093/acrefore/9780190264086.013.232.

Mosher, J. A., Henny, C. J. 1976. Thermal adaptiveness of plumage color in Screech Owls. *The Auk* 93:614–619. DOI: 10.1093/auk/93.3.614.

Negro, J. J., Bortolotti, G. R., Sarasola, J. H. 2007. Deceptive plumage signals in birds: manipulation of predators or prey? *Biological Journal of the Linnean Society* 90:467-477. DOI: 0.1111/j.1095-8312.2007.00735.x.

Newman, C., Buesching, C. D., Wolff, J. O. 2005. The Function of Facial Masks in "Midguild" Carnivores. *Oikos* 108(3):623-633. DOI: 10.1111/j.0030-1299.2005.13399.x.

Ortolani, A. 1999. Spots, stripes, tail tips and dark eyes: Predicting the function of carnivore colour patterns using the comparative method. *Biological Journal of the Linnaean Society* 67:433-476. DOI: 10.1111/j.1095-8312.1999.tb01942.x.

Paradis, E., Schliep, K. 2019. ape 5.0: an environment for modern phylogenetics and evolutionary analyses in R. *Bioinformatics* 35:526-528. DOI: 10.1093/bioinformatics/bty633.

Pebesma, E. 2018. Simple Features for R: Standardized Support for Spatial Vector Data. *The R Journal* 10(1):439-446. DOI: 10.32614/RJ-2018-009.

Pebesma, E., Bivand, R. 2005. S Classes and Methods for Spatial Data: the sp Package. *R News* 5(2):9-13.

Pedersen, T. L. 2020. patchwork: The Composer of Plots. R package version 1.1.1, https://CRAN.R-project.org/package=patchwork.

Pedersen, T. L., Crameri, F. 2020. scico: Colour Palettes Based on the Scientific Colour-Maps. R package version 1.2.0, https://CRAN.R-project.org/package=scico.

Peterson, B. G., Carl, P. 2019. PerformanceAnalytics: Econometric Tools for Performance and Risk Analysis. R package version 2.0.4, https://CRAN.R-project.org/package=PerformanceAnalytics.

Pérez-Rodríguez, L., Jovani, R., Stevens, M. 2017. Shape matters: Animal colour patterns as signals of individual quality. *Proceedings of the Royal Society B* 284(1849):20162446. DOI:10.1098/rspb.2016.2446.

Pinheiro, J., Bates, D., R Core Team. 2022. nlme: Linear and Nonlinear Mixed Effects Models. R package version 3.1-153, https://CRAN.R-project.org/package=nlme.

Potier, S., Leuvin, M., Pfaff, M., Kelber, M. 2020. How fast can raptors see? *Journal of Experimental Biology* 223: jeb209031. DOI: 10.1242/jeb.209031.

Price, T., Pavelka, M. 2002. Evolution of a colour pattern: History, development, and selection. *Journal of Evolutionary Biology* 9(4):451-470. DOI: 10.1046/j.1420-9101.1996.9040451.x.

R Core Team. 2022. R: a language and environment for statistical computing. R Foundation for Statistical Computing, Vienna.

Redding, D. W., Lucas, T., Blackburn, T., Jones, K. E. 2017. Evaluating Bayesian spatial methods for modelling species distributions with clumped and restricted occurrence data. PLoS ONE 12(11): e0187602..1371/journal.pone.0187602.

Rensch, B. 1936. Some problems of geographical variation and species-formation. *Proceedings of the Linnean Society of London* 150:275– 285. DOI: 10.1111/j.1095-8312.1938.tb00182k.x.

Revell, L. J. 2012. phytools: An R package for phylogenetic comparative biology (and other things). *Methods in Ecology and Evolution* 3:217-223. DOI:10.1111/j.2041-210X.2011.00169.x.

Rogalla, S., D'Alba, L, Verdoodt, A., Shawkey, M. D. 2019. Hot wings: thermal impact of wing coloration on surface temperature during bird flight. *Journal of the Royal Society Interface* 16:20190032. DOI: 10.1098/rsif.2019.0032.

Romano, A., Sechaud, R., Hirzel, A. A., Roulin, A. 2019. Climate-driven evolution of plumage colour in a cosmopolitan bird. *Global Ecology and Biogeography* 28:496-507. DOI: 10.1111/geb.12870.

Roulin, A. 2004. The evolution, maintenance and adaptive function of genetic colour polymorphism in birds. *Biological Reviews* 79(4):815-848. DOI: 10.1017/S1464793104006487.

Roulin, A., Randin, C. 2015. Gloger's rule in North American Barn Owls. *The Auk* 132(2):321-332. DOI: 10.1642/AUK-14-167.1.

Rue, H., Martino, S., Chopin, N. 2009. Approximate Bayesian inference for latent Gaussian models by using integrated nested Laplace approximations. *Journal of the Royal Statistical Society: Series B (Statistical Methodology)* 71(2):319-392. DOI: 10.1111/j.1467-9868.2008.00700.x.

San-Jose, L. M., Séchaud, R., Schalcher, K., Judes, C., Questiaux, A., Oliveira-Xavier, A., Gémard, C., Almasi, B., Béziers, P., Kelber, A., Amar, A., Roulin, A. 2019. Differential fitness effects of moonlight on plumage colour morphs in barn owls. *Nature Ecology & Evolution* 3:1331-1340. DOI: 10.1038/s41559-019-0967-2.

Sheard, C., Neate-Clegg, M. H., C., Alioravainen, N., Jones, S. E. I., Vincent, C., MacGregor, H. E. A., Bregman, T. P., Claramunt, S., Tobias, J. A. 2020. Ecological drivers of global gradients in avian dispersal inferred from wing morphology. *Nature Communications* 11:2463. DOI: 10.1038/s41467-020-16313-6.

Simmons, R. E., Jenkins, A. R., Brown, C. J. 2008. A review of the population status and threats to Peregrine Falcons throughout Namibia. In J. Sielicki and T. Mizera (eds.) *Peregrine Falcon populations – status and perspectives in the 21st century.* Turul Publishing Ltd., Warsaw, pp. 597-606.

Simpson, D., Rue, H., Riebler, A., Martins, T. G., Sørbye, S. H. 2017. Penalising model component complexity: A principled, practical approach to constructing priors. Statistical Science 32:1–28. DOI: 10.1214/16-STS576.

Tate, G. J., Bishop, J. M., Amar, A. 2016. Differential foraging success across a light level spectrum explains the maintenance and spatial structure of colour morphs in a polymorphic bird. *Ecology Letters* 19(6):679-686. DOI: 10.1111/ele.12606.

Tobias, J. A., Sheard, C., Seddon, N., Meade, A., Cotton, A. Nakagawa, S. 2016. Territoriality, social bonds, and the evolution of communal signalling in birds. *Frontiers in Ecology and Evolution* 4:74. DOI:10.3389/fevo.2016.00074.

Tobias, J. A., Sheard, C., Pigot, A. L., Devenish, A. J. M., Yang, J., Sayol, F., Neate-Clegg, M. H. C., Alioravainen, N., Weeks, T. L., Barber, R. A., Walkden, P. A. et al. 2022. AVONET: morphological, ecological and geographical data for all birds. *Ecology Letters* 25(3):581-597. DOI: 10.1111/ele.13898.

Töpfer, T. Gedeon, K., Pröhl, T. 2019. New breeding records and observations of the Peregrine Falcon *Falco peregrinus minor* from Ethiopia. Scopus 39(1):60-63.

van de Pol, M., Wright, J. 2009. A simple method for distinguishing within- versus between-subject effects using mixed models. *Animal Behaviour* 77:753-758. DOI: 10.1016/j.anbehav.2008.11.006.

Vergara, P., Fargallo, J. A. 2011. Multiple coloured ornaments in male common kestrels: different mechanisms to convey quality. *Naturwissenschaften* 98:289–298. DOI 10.1007/s00114-011-0767-2.

Vrettos, M., Amar, A., Reynolds, C. 2021. Malar stripe size and prominence in peregrine falcons vary positively with solar radiation: support for the solar glare hypothesis. *Biology Letters* 17(6): 20210116. DOI: 10.1098/rsbl.2021.0116.

Ward, J. M., Blount, J. D., Ruxton, G. D., Houston, D. C. 2002. The adaptive significance of dark plumage for birds in desert environments. *Ardea* 90:311–323.

White, C. M, Boyce D.A. 1988. An overview of Peregrine Falcon subspecies. In T. Cade, J. H. Enderson, C. G. Thelander & C. M. White (eds.) *Peregrine Falcon populations: Their management and recovery*. The Peregrine Fund, Boise, Idaho, pp. 789-812.

Wickham, H. 2016. ggplot2: Elegant Graphics for Data Analysis. Springer-Verlag, New York.

Wickham, H., François, R., Henry, L., Müller, K. 2018. dplyr: A Grammar of Data Manipulation. R package version 1.0.7, https://CRAN.R-project.org/package=dplyr.

Wickham, H., Girlich, M. 2022. tidyr: Tidy Messy Data. R package version 1.2.0, https://CRAN.R-project.org/package=tidyr.

Wiehn, J. 1997. Plumage Characteristics as an Indicator of Male Parental Quality in the American Kestrel. *Journal of Avian Biology* 28(1):47-55. DOI: 10.2307/3677093.

Wilke, C. O. 2021. ggridges: Ridgeline Plots in 'ggplot2'. R package version 0.5.3, https://CRAN.R-project.org/package=ggridges.

Yosef, R., Zduniak, P., Tryjanowski, P. 2012. Unmasking Zorro: functional importance of the facial mask in the Masked Shrike (*Lanius nubicus*). *Behavioural Ecology* 23(3): 615-618. DOI: 10.1093/beheco/ars005.

Yu, G., Smith, D., Zhu, H., Guan, Y., Lam, T. T. 2017. ggtree: an R package for visualization and annotation of phylogenetic trees with their covariates and other associated data. *Methods in Ecology and Evolution* 8(1):28-36. DOI:10.1111/2041-210X.12628.

Zink, R. M., Remsen, J. V. 1986. Evolutionary processes and patterns of geographic variation in birds. In R. F. Johnston (ed.). *Current Ornithology 4.* Plenum Press, New York, pp. 1-69.

Zuberogoitia, I., Azkona, A., Zabala, J., Astorkia, L., Castillo, I., Iraeta, A., Martínez, J. A., Martínez, J. E. 2009. Phenotypic variations of Peregrine Falcon in subspecies distribution border. In J. Sielicki and T. Mizera (eds.) *Peregrine Falcon populations – status and perspectives in the 21st century.* Turul Publishing Ltd., Warsaw, pp. 295-308.

Zuberogoitia, I., Martínez, J. E., Zabala, J. 2013. Individual recognition of territorial peregrine falcons Falco peregrinus: a key for long-term monitoring programmes. *Munibe (Ciencias Naturales-Natur Zientziak)* 61:117-127.

SUPPLEMENTARY MATERIAL

Additional notes on the statistical models

Dinnage et al. (2020) describe full mathematical details of the spatiophylogenetic modelling approach using INLA. However, the models that I used in this study differed from those developed by Dinnage et al. (2020) in that they were fit to observation-level data, rather than species-level data aggregated from multiple observations of each species. As such, my approach differed in that I did not aggregate the spatial random effect for each species across all observation points for the species, and instead used the default INLA method, in which the spatial effects are represented by an A matrix with N_{obs} rows (where N_{obs} is the number of observations) and N_{mesh} columns (where N_{mesh} is the number of spatial mesh points). My approach also differed in that I included both random intercept and slope terms for each species, in addition to partitioning the solar radiation predictor term into a within-species and a between-species term (van de Pol and Wright 2009; Dinnage et al. 2018). The full mathematical equations of the model formulae I used can thus be written as follows:

$$y_{\text{ij}} \sim \text{N}(\mu,\ \sigma^2)$$

$$\mu_{\text{phylo}}[\text{j}] \sim \text{MVN}(0,\ \sigma^2{}_{\text{phylo}}\, V_{\text{phylo}})$$

i) Simple models:

$$y[\text{ij}] = \beta_0 + \beta_1(x_{\text{solar}}[\text{ij}] - \bar{x}_{\text{solar}}[\text{j}]) + \beta_2\bar{x}_{\text{solar}}[\text{j}] + \beta_3 x_{\text{distortion1}}[\text{ij}] \ldots + \beta_7 x_{\text{distortion5}}[\text{ij}] + \mu_0[\text{j}] + \mu_1[\text{j}](x_{\text{solar}}[\text{ij}] - \bar{x}_{\text{solar}}[\text{j}]) + \mu_{\text{phylo}}[\text{j}] + f\,(s_m[\text{ij}]) + e_0[\text{ij}]$$

ii) Additive models:

$$y[\text{ij}] = \beta_0 + \beta_1(x_{\text{solar}}[\text{ij}] - \bar{x}_{\text{solar}}[\text{j}]) + \beta_2\bar{x}_{\text{solar}}[\text{j}] + \beta_3 x_{\text{distortion1}}[\text{ij}] \ldots + \beta_7 x_{\text{distortion5}}[\text{ij}] + \beta_8 x_{\text{trait}}[\text{j}] + \mu_0[\text{j}] + \mu_1[\text{j}](x_{\text{solar}}[\text{ij}] - \bar{x}_{\text{solar}}[\text{j}]) + \mu_{\text{phylo}}[\text{j}] + f\,(s_m[\text{ij}]) + e_0[\text{ij}]$$

iii) Interactive models (within species):

$$y[\mathrm{ij}] = \beta_0 + \beta_1(x_{\mathrm{solar}}[\mathrm{ij}] - \bar{x}_{\mathrm{solar}}[\mathrm{j}]) + \beta_2\bar{x}_{\mathrm{solar}}[\mathrm{j}] + \beta_3 x_{\mathrm{distortion1}}[\mathrm{ij}] \ldots + \beta_7 x_{\mathrm{distortion5}}[\mathrm{ij}] + \beta_8 x_{\mathrm{trait}}[\mathrm{j}] + \beta_9(x_{\mathrm{solar}}[\mathrm{ij}] - \bar{x}_{\mathrm{solar}}[\mathrm{j}])x_{\mathrm{trait}}[\mathrm{j}] + \mu_0[\mathrm{j}] + \mu_1[\mathrm{j}](x_{\mathrm{solar}}[\mathrm{ij}] - \bar{x}_{\mathrm{solar}}[\mathrm{j}]) + \mu_{\mathrm{phylo}}[\mathrm{j}] + f(s_m[\mathrm{ij}]) + e_0[\mathrm{ij}]$$

iv) Interactive models (between species):

$$y[\mathrm{ij}] = \beta_0 + \beta_1(x_{\mathrm{solar}}[\mathrm{ij}] - \bar{x}_{\mathrm{solar}}[\mathrm{j}]) + \beta_2\bar{x}_{\mathrm{solar}}[\mathrm{j}] + \beta_3 x_{\mathrm{distortion1}}[\mathrm{ij}] \ldots + \beta_7 x_{\mathrm{distortion5}}[\mathrm{ij}] + \beta_8 x_{\mathrm{trait}}[\mathrm{j}] + \beta_{10}\bar{x}_{\mathrm{solar}}[\mathrm{j}]x_{\mathrm{trait}}[\mathrm{j}] + \mu_0[\mathrm{j}] + \mu_1[\mathrm{j}](x_{\mathrm{solar}}[\mathrm{ij}] - \bar{x}_{\mathrm{solar}}[\mathrm{j}]) + \mu_{\mathrm{phylo}}[\mathrm{j}] + f(s_m[\mathrm{ij}]) + e_0[\mathrm{ij}]$$

where β_0 is the intercept, $\beta_1(x_{\mathrm{solar}}[\mathrm{ij}] - \bar{x}_{\mathrm{solar}}[\mathrm{j}])$ is the effect of the within-species solar radiation predictor term β_1 on the response at observation *i* in species *j*, $\beta_2\bar{x}_{\mathrm{solar}}[\mathrm{j}]$ is the effect of the between-species solar radiation predictor term β_2 on the response for species *j*, $\beta_{k+2}x_{\mathrm{distortion}k}[\mathrm{ij}]$ is the effect of the *k*th head angle/plumage distortion predictor term on the response at observation *i* in species *j*, $\beta_8 x_{\mathrm{trait}}[\mathrm{j}]$ is the effect of the species-level trait predictor term β_8 on the response for species *j*, $\beta_9(x_{\mathrm{solar}}[\mathrm{ij}] - \bar{x}_{\mathrm{solar}}[\mathrm{j}])x_{\mathrm{trait}}[\mathrm{j}]$ is effect of the interaction term between the trait predictor and the within-species solar radiation predictor at observation *i* in species *j*, $\beta_{10}\bar{x}_{\mathrm{solar}}[\mathrm{j}]x_{\mathrm{trait}}[\mathrm{j}]$ is the effect of the interaction term between the trait predictor and the between-species solar radiation predictor for species *j*, $\mu_0[\mathrm{j}]$ is the random intercept term for species *j*, $\mu_1[\mathrm{j}](x_{\mathrm{solar}}[\mathrm{ij}] - \bar{x}_{\mathrm{solar}}[\mathrm{j}])$ is the random slope term describing the species-dependent effect of solar radiation on the response at observation *i* in species *j*, $\mu_{\mathrm{phylo}}[\mathrm{j}]$ is the phylogenetic effect, $f(s_m[\mathrm{ij}])$ is a function describing the spatial effect for the *m*th latitude/ longitude coordinate pair at observation *i* in species *j*, and $e_0[\mathrm{ij}]$ is the error associated with observation *i* in species *j*. The phylogenetic effect is described by a multivariate normal distribution with mean 0 and variance $\sigma^2_{\mathrm{phylo}}V_{\mathrm{phylo}}$, in which $\sigma^2_{\mathrm{phylo}}$ is a scaling factor and V_{phylo} is the standardised phylogenetic covariance matrix. The mean and variance of the observations *ij* are given by μ and σ^2, respectively. The spatial random effect term estimates the spatial Matérn covariance function across a spatial mesh using a stochastic partial differential equation (SPDE) approach, full mathematical details of which are provided by Lindgren et al. (2011).

I chose a spatial mesh that gave appropriate coverage across the datapoints and provided the maximum spatial resolution, while still being large enough to prevent spatial overfitting (Dinnage et al. 2020). This mesh was generated through trial and error, by modifying the mesh

parameters used by Dinnage et al. (2020) until a suitable mesh was generated. Since I was working with global-scale data, and thus a two-dimensional, planar mesh structure was not appropriate for modelling the spatial effect as it did not account for the curvature of the Earth's surface or accurately model spatial distances between coordinate points, I also converted the planar mesh structure used by Dinnage et al. (2020) to a three-dimensional, spherical mesh by reprojecting the latitude/longitude coordinate points onto a sphere, using the R package inlabru (Bachl et al. 2019). I did not use the meshbuilder function in the INLA package (Lindgren and Rue 2015) to generate or modify the spatial mesh, as this function is currently not available for use with spherical meshes.

Following Dinnage et al. (2020), I used the default INLA prior (a weak Gaussian prior with mean = 0 and variance = 100) for all fixed effect parameters. For the phylogenetic scaling parameter σ^2_{phylo}, I used the same weakly informative prior used by Dinnage et al. (2020), a Penalized Complexity ('pcprior') distribution with parameters 1 and 0.1 (indicating an exponential distribution with ~10% of its probability distribution > 1), based on the recommendations of Simpson et al. (2017) and Gelman et al. (2008). For the spatial random effect, I followed Dinnage et al. (2020) in using a 'pcprior' with 10% of its density < 2 decimal degrees for the range parameter κ, and a 'pcprior' with 10% of its density > 1 for the variation parameter σ (Dinnage et al. 2020). Illian et al. (2012) recommend choosing priors on κ which place most of the prior density on values greater than the observed covariance range of the fixed environmental covariates, preventing the model from overfitting the spatial effect (Illian et al. 2012). This is because, as κ represents the spatial range at which the covariance between datapoints decays to near-zero values, specifying a prior on κ that is substantially smaller than the observed spatial covariance range of the environmental covariates can cause the spatial effect to fit on too fine a scale, and thus 'explain away' variation in the response that is actually driven by the covariates (Illian et al. 2012). I found that a prior range of 2 decimal degrees was sufficient to prevent spatial overfitting in my models, and that rerunning the analysis with prior values > 2 (e.g., 5, 10, 15, and 20 decimal degrees) produced virtually identical results, as the estimated spatial ranges for all malar stripe variables were considerably greater than 2 (see Results). For the α parameter, which controls the smoothness of the Matérn covariance function, I used a fixed value of 3/2 (rather than 2, as used by Dinnage et al. (2020)), as the non-random distribution of my data necessitated the use of a smaller smoothing parameter to prevent spatial overfitting due to the function estimating large, negative SPDE values in regions containing no observations (H. Rue and F. Lindgren, *pers. comm.*, 2022).

Table S1. Photograph selection process for each species (including whether observations were clipped to only include the breeding/resident range, whether distance-constrained sampling was performed, and whether observations were filtered by date to exclude wintering migrant birds), along with whether the species was coded as having uniform plumage.

Species	Clipped to Resident/ Breeding Range	Distance-constrained sampling	Filtered by Date	Uniform Plumage
African Hobby (*Falco cuvierii)*	No	No	No	No
American Kestrel (*Falco sparverius*)	Yes	Yes	Yes	No
Amur Falcon (*Falco amurensis*)	Yes	No	No	M = Yes F = No
Aplomado Falcon (*Falco femoralis*)				No
Australian Hobby (*Falco longipennis*)	Yes	Yes	No	No
Australian Kestrel (*Falco cenchroides*)	Yes	Yes	No	No
Banded Kestrel (*Falco zoniventris*)	No	No	No	No
Barbary Falcon (*Falco (peregrinus) pelegrinoides)*	Yes	No	No	Yes
Bat Falcon (*Falco rufigularis*)	No	Yes	No	No
Black Falcon (*Falco subniger*)	No	No	No	Yes
Brown Falcon (*Falco berigora*)	No	Yes	No	No
Common Kestrel (*Falco tinnunculus*)	Yes	Yes	Yes	No
Dickinson's Kestrel (*Falco dickinsoni*)	No	No	No	Yes
Eleonora's Falcon (*Falco eleonorae*)	Yes (Buffer Added)	No	No	Mixed
Eurasian Hobby (*Falco subbuteo*)	Yes	Yes	Yes	No
Fox Kestrel (*Falco alopex*)	No	No	No	Yes
Greater Kestrel (*Falco rupicoloides*)	No	No	No	Yes
Grey Falcon (*Falco hypoleucos*)	No	No	No	Yes
Grey Kestrel (*Falco ardosiaceus*)	No	No	No	Yes
Gyrfalcon (*Falco rusticolus*)	Yes	Yes	Yes	No
Laggar Falcon (*Falco jugger*)	No	No	No	No
Lanner Falcon (*Falco biarmicus*)	Yes	No	No	No
Lesser Kestrel (*Falco naumanni*)	Yes	No	Yes	No
Madagascar Kestrel (*Falco newtoni*)	No	No	No	No
Mauritius Kestrel (*Falco punctatus*)	No	No	No	No
Merlin (*Falco columbarius*)	Yes	Yes	Yes	No
New Zealand Falcon (Kārearea) (*Falco novaeseelandiae*)	No	No	No	No
Orange-breasted Falcon (*Falco deiroleucus*)	No	No	No	No
Oriental Hobby (*Falco severus*)	Yes			No
Peregrine Falcon (*Falco peregrinus*)	Yes	Yes	Yes	No
Prairie Falcon (*Falco mexicanus*)	Yes	Yes	Yes	No
Red-footed Falcon (*Falco vespertinus*)	Yes	No	No	M = Yes F = No
Red-necked Falcon (*Falco chicquera*)	No	No	No	No
Rock Kestrel (*Falco rupicolus*)	No	No	No	No
Saker Falcon (*Falco cherrug*)	Yes	Yes	Yes	No
Seychelles Kestrel (*Falco araeus*)	No	No	No	No
Sooty Falcon (*Falco concolor*)	Yes (Buffer Added)	No	No	Yes
Spotted Kestrel (*Falco moluccensis*)	No	No	No	No
Taita Falcon (*Falco fasciinucha*)	No	No	No	No

Table S2. Ranges and dates for which photographs were filtered to exclude wintering migrant birds, for species in which breeding and resident populations overlap in range.

Species	Ranges Filtered (BirdLife International maps)	Non-Filtered Subspecies	Migrant Breeding Season	Date Range Excluded
American Kestrel (*Falco sparverius*)	Resident range	*F. s. aequatorialis*, *F. s. brevipennis*, *F. s. caribaearum*, *F. s. cearae*, *F. s. caucae*, *F. s. dominicensis*, *F. s. fernandensis*, *F. s. isabellinus*, *F. s. nicaraguensis*, *F. s. ochraceus*, *F. s. paulus*, *F. s. peninsularis*, *F. s. peruvianus*, *F. s. sparverioides*, *F. s. tropicalis*	Apr-Jul (N hemisphere), Oct-Mar (S hemisphere)	Jan-Mar, Aug-Dec (N hemisphere), Apr-Sep (S hemisphere)
Common Kestrel (*Falco tinnunculus*)	Resident range	*F. t. alexandri*, *F. t. archeri*, *F. t. canariensis*, *F. t. dacotiae*, *F. t. interstinctus*, *F. t. neglectus*, *F. t. objurgatus*, *F. t. rufescens*, *F. t. rupicolaeformis*	Mar-Aug	Jan-Feb, Sep-Dec
Eurasian Hobby (*Falco subbuteo*)	Resident range	-		
Gyrfalcon (*Falco rusticolus*)	Resident range	-		
Lesser Kestrel (*Falco naumanni*)	Resident range	-		
Merlin (*Falco columbarius*)	Resident range	*F. c. richardsonii*, *F. c. suckleyi*	May-Aug	Jan-Apr, Sep-Dec
Peregrine Falcon (*Falco peregrinus*)	Resident, passage, and wintering ranges	*F. p. brookei*, *F. p. cassini*, *F. p. ernesti*, *F. p. fruitii*, *F. p. macropus*, *F. p. madens*, *F. p. minor*, *F. p. nesiotes*, *F. p. peregrinator*, *F. p. radama*, *F. p. submelanogenys*	Mar-Aug	Jan-Feb, Sep-Dec
Prairie Falcon (*Falco mexicanus*)	Resident range		Mar-Jul	Jan-Feb, Aug-Dec
Saker Falcon (*Falco cherrug*)	Resident range	-	Mar-Aug	Jan-Feb, Sep-Dec

Table S3. Physical and plumage characteristics used to sex adult birds and identify juvenile/immature individuals for removal from the dataset, for species in which age and sex classes are visually separable. Diagnostic characteristics are based on identification guides provided in Ferguson-Lees and Christie (2001) and Birds of the World (Billerman et al. 2020).

Species	Sexes Separable	Male	Female	Non-adults Separable	Juvenile/Immature
African Hobby (*Falco cuvierii*)	No	-	-	Yes	Breast and belly heavily streaked or blotched black (not finely streaked as in ad.)
American Kestrel (*Falco sparverius*)	Yes	Back, shoulders and wing coverts grey; breast plain or lightly spotted black; tail unbarred except for one to few black subterminal bars on the underside	Back and wing coverts chestnut-brown (not grey), barred dark brown; breast streaked or barred brown; tail barred dark brown with wide black or dark brown subterminal bar	Yes	M appearing intermediate between M and F ad. plumage; F as ad. but lacking wide subterminal bar on tail feathers 2-5 (subterminal bar not wider than other tail bars)
Amur Falcon (*Falco amurensis*)	Yes	Uniform slate-grey, malar stripe not clearly defined	White/pale cream with black barring on the breast and belly, distinct dark cap, and clearly defined malar stripe	Yes	As F but with vertical streaking (not horizontal barring) on breast and belly; back and cap scaled dark brown (not dark grey); bare parts yellow (never orange or red)
Aplomado Falcon (*Falco femoralis*)	No	-	-	No	-
Australian Hobby (*Falco longipennis*)	No	-	-	No	-
Australian Kestrel (*Falco cenchroides)*	Yes	Crown grey	Crown chestnut or brown	No	-
Banded Kestrel (*Falco zoniventris*)	No	-	-	Yes	Browner above than ad.; tail bars brown/buff/rufous (not white)
Barbary Falcon (*Falco (peregrinus) pelegrinoides)*	No	-	-	Yes	Back, cap, and malar stripe grey-brown (not black or slate-grey); cheeks, breast, and belly cream or rufous-buff

Table S3. cont.

Bat Falcon (*Falco rufigularis*)	No	-	-	No	
Black Falcon (*Falco subniger*)	No	-	-	Yes	Uniform dark brown or black (darker than ad., often lacking lighter patches or variegation); mantle edged pale cream
Brown Falcon (*Falco berigora*)	No	-	-	No	-
Common Kestrel (*Falco tinnunculus*)	Yes	Head grey; crown unstreaked; cheeks may be paler or streaked grey	Head variably brown/rufous; crown streaked darker brown or rufous; cheeks buff, occasionally washed grey	No	-
Dickinson's Kestrel (*Falco dickinsoni*)	No	-	-	Yes	Slight brown wash on flanks and underparts; fine white barring on flanks; bare parts grey-green or green-yellow (not yellow as in ad.)
Eleonora's Falcon (*Falco eleonorae*)	Yes	Cere yellow	Cere blue	Yes	Fringed cream to rufous above (not plain black as in ad.)
Eurasian Hobby (*Falco subbuteo*)	No	-	-	No	-
Fox Kestrel (*Falco alopex*)	No	-	-	Yes	Eye dark brown/black (not pale brown or yellow as in ad.)
Greater Kestrel (*Falco rupicoloides*)	No	-	-	Yes	Eye dark brown/black (not pale brown or yellow as in ad.)
Grey Falcon (*Falco hypoleucos)*	No	-	-	Yes	Back, cap, and upper wing darker grey than ad., paler below; breast finely streaked darker grey; more clearly defined cap and malar stripe than ad.
Grey Kestrel (*Falco ardosiaceus*)	No	-	-	Yes	Paler grey than ad., with more defined streaking on the cheeks, breast, and belly; slight brown wash on flanks and upperparts; bare parts grey-green or green-yellow (not yellow as in ad.)
Gyrfalcon (*Falco rusticolus*)	No	-	-	No	-

Table S3. cont.

Laggar Falcon (*Falco jugger*)	No	-	-	No	-
Lanner Falcon (*Falco biarmicus*)	No	-	-	Yes	Back, cap, and malar stripe dark brown (not black or slate-grey); breast and belly heavily streaked or blotched black or dark brown (not lightly spotted as in ad. F); cheeks cream (not white as in ad.)
Lesser Kestrel (*Falco naumanni*)	Yes	Head uniform grey, crown and cheeks unstreaked	Head variably brown/rufous; crown streaked darker brown or rufous; cheeks buff	No	-
Madagascar Kestrel (*Falco newtoni)*	No	-	-	No	-
Mauritius Kestrel (*Falco punctatus*)	No	-	-	No	-
Merlin (*Falco columbarius*)	Yes	Blue-grey above; fine rufous streaking on breast, belly, and flanks	Dark brown to rufous above; strong brown streaking or blotching on breast, belly, and flanks	No	-
New Zealand Falcon (Kārearea) (*Falco novaeseelandiae*)	No	-	-	No	-
Orange-breasted Falcon (*Falco deiroleucus*)	No	-	-	Yes	Browner-black above than ad.; breast bars edged buff
Oriental Hobby (*Falco severus*)	No	-	-	No	-
Peregrine Falcon (*Falco peregrinus*)	No	-	-	Yes	Back, cap and malar stripe dark brown (not black or slate-grey); breast and belly streaked or blotched black or dark brown (not barred as in ad.); cheeks, breast, and belly cream (not white); bare parts grey, bluish, or greenish (not yellow as in ad.)
Prairie Falcon (*Falco mexicanus*)	No	-	-	Yes	Cheeks, throat, and breast cream-buff (not white as in ad.); bare parts blue-grey (not yellow as in ad.)

Table S3. cont.

Red-footed Falcon (*Falco vespertinus*)	Yes	Uniform slate-grey, malar stripe not clearly defined	Head and underparts pale orange-buff; cheeks often lighter cream or white; lores and malar stripe black (sometimes with rufous 'shadow stripe')	Yes	Grey-brown above, cream or buff below with white collar and dark brown or black streaking on the breast, belly, and flanks; defined cap, hood, and malar stripe
Red-necked Falcon (*Falco chicquera*)	No	-	-	Yes	Darker above than ad.; crown and nape dark brown (not rufous), with buff patches on lower hindneck; breast, belly, and flanks barred dark brown (not black); washed rufous below with fine streaking on upper breast
Rock Kestrel (*Falco rupicolus*)	No	-	-	No	-
Saker Falcon (*Falco cherrug*)	No	-	-	Yes	More heavily streaked below than ad.; in light morph, cheeks, throat, and breast cream-buff (not white as in ad.); bare parts blue-grey (not yellow as in ad.)
Seychelles Kestrel (*Falco araeus*)	No	-	-	Yes	Head chestnut-brown (not grey as in ad.); more heavily marked above; breast and belly lightly spotted; tail rufous-tinged (not grey) and tipped with buff or cream (not white)
Sooty Falcon (*Falco concolor*)	No	-	-	Yes	Dark grey-brown above, cream below with grey-brown streaking on the breast, belly, and flanks; clearly-defined cap, hood, and malar stripe contrasting with cream/buff cheeks and throat
Spotted Kestrel (*Falco moluccensis*)	No	-	-	No	-
Taita Falcon (*Falco fasciinucha)*	No	-	-	No	-

Table S4. Breeding season information for each species, along with whether solar radiation data were extracted for the March-August period (boreal summer) or the September-February period (austral summer). Breeding seasons are based on information provided in Ferguson-Lees and Christie (2001) and Birds of the World (Billerman et al. 2020).

Species	Breeding Season	Months for Which Solar Radiation Data Extracted (Observations > 10° N)	Months for Which Solar Radiation Data Extracted (Observations < 10° S)	Months for Which Solar Radiation Data Extracted (Observations 10° N – 10° S)
African Hobby (*Falco cuvierii*)	Feb-Jun (W Africa), Dec-Jun (E Africa to Uganda and W Kenya), Aug-Dec (E Africa from W Kenya), Sep-Jan (S Africa from Zambia)	Mar-Aug	Sep-Feb	Mar-Aug to 0° N, Sep-Feb from 0° N
American Kestrel (*Falco sparverius*)	Mar-Jul (N America), Dec-May (C America & northern S America), Oct-Mar (southern S America)	Mar-Aug	Sep-Feb	Mar-Aug to 0° N, Sep-Feb from 0° N
Amur Falcon (*Falco amurensis*)	May-Aug	Mar-Aug	-	-
Aplomado Falcon (*Falco femoralis*)	Feb-Aug (N & C America), Sep-Jan (S America from Argentina)	Mar-Aug	Sep-Feb	Mar-Aug to 0° N, Sep-Feb from 0° N
Australian Hobby (*Falco longipennis*)	Jul-Jan	-	Sep-Feb	Sep-Feb
Australian Kestrel (*Falco cenchroides*)	Sep-Dec	-	Sep-Feb	Sep-Feb
Banded Kestrel (*Falco zoniventris*)	Sep-Dec	-	Sep-Feb	Sep-Feb
Barbary Falcon (*Falco (peregrinus) pelegrinoides*)	Feb-Jul	Mar-Aug	-	Mar-Aug
Bat Falcon (*Falco rufigularis*)	Feb-Jun (S America to 4° N), Aug-Dec (S America from Brazil)	Mar-Aug	Sep-Feb	Mar-Aug to 4° N, Sep-Feb from 4° N
Black Falcon (*Falco subniger*)	Jul-Dec	-	Sep-Feb	-
Brown Falcon (*Falco berigora*)	Sep-Jan (Australia), Apr-Nov (New Guinea)	-	Sep-Feb	Mar-Aug to 0° N, Sep-Feb from 0° N
Common Kestrel (*Falco tinnunculus*)	Mar-Aug (Eurasia & N Africa), Apr-Sep (E Africa)	Mar-Aug	-	Mar-Aug

Table S4. cont.

Dickinson's Kestrel (*Falco dickinsoni*)	Jul-Oct (E Africa), Sep-Dec (S Africa)	-	Sep-Feb	Sep-Feb
Eleonora's Falcon (*Falco eleonorae*)	Jul-Sep	Mar-Aug	-	-
Eurasian Hobby (*Falco subbuteo*)	Jun-Aug	Mar-Aug	-	-
Fox Kestrel (*Falco alopex*)	Mar-Nov	Mar-Aug	-	Mar-Aug
Greater Kestrel (*Falco rupicoloides*)	Apr-Aug (E Africa to Tanzania), Jul-Apr (S Africa)	Mar-Aug	Sep-Feb	Mar-Aug
Grey Falcon (*Falco hypoleucos*)	Aug-Dec	-	Sep-Feb	-
Grey Kestrel (*Falco ardosiaceus*)	Mar-Jun (E Africa to Uganda), Aug-Dec (S Africa from Kenya)	Mar-Aug	Sep-Feb	Mar-Aug to 0° N, Sep-Feb from 0° N
Gyrfalcon (*Falco rusticolus*)	Apr-Aug	Mar-Aug	-	-
Laggar Falcon (*Falco jugger*)	Jan-May	Mar-Aug	-	-
Lanner Falcon (*Falco biarmicus*)	Jan-Jul (Eurasia & N & W Africa), Jun-Oct and Dec-Mar (E Africa), May-Feb (S Africa)	Mar-Aug	Sep-Feb	Sep-Feb
Lesser Kestrel (*Falco naumanni*)	May-Jul	Mar-Aug	-	-
Madagascar Kestrel (*Falco newtoni*)	Sep-Jan	-	Sep-Feb	Sep-Feb
Mauritius Kestrel (*Falco punctatus*)	Aug-Nov	-	Sep-Feb	-
Merlin (*Falco columbarius*)	Apr-Aug	Mar-Aug	-	-
New Zealand Falcon (Kārearea) (*Falco novaeseelandiae*)	Sep-Feb	-	Sep-Feb	-
Orange-breasted Falcon (*Falco deiroleucus*)	Mar-Jun (C & northern S America), Jan-Apr (central S America), dry season in S of range	Mar-Aug	Sep-Feb	Mar-Aug to 0° N, Sep-Feb from 0° N
Oriental Hobby (*Falco severus*)	May-Aug	Mar-Aug	-	Mar-Aug
Peregrine Falcon (*Falco peregrinus*)	Mar-Aug (Arctic to N temperate), Jun-Feb (tropics), Jul-Jan (S temperate)	Mar-Aug	Sep-Feb	Sep-Feb
Prairie Falcon (*Falco mexicanus*)	Mar-Jul	Mar-Aug	-	-
Red-footed Falcon (*Falco vespertinus*)	Apr-Aug	Mar-Aug	-	-
Red-necked Falcon (*Falco chicquera*)	Feb-Jul (Asia & N/W Africa), Jul-Nov (E & S Africa)	Mar-Aug	Sep-Feb	Sep-Feb

Table S4. cont.

Rock Kestrel (*Falco rupicolus*)	Aug-Nov	-	Sep-Feb	-
Saker Falcon (*Falco cherrug*)	Mar-Aug	Mar-Aug	-	-
Seychelles Kestrel (*Falco araeus*)	Aug-Dec	-	Sep-Feb	Sep-Feb
Sooty Falcon (*Falco concolor*)	Jul-Oct	Mar-Aug	-	-
Spotted Kestrel (*Falco moluccensis*)	Mar-Oct	Mar-Aug	Sep-Feb	Mar-Aug
Taita Falcon (*Falco fasciinucha*)	Apr-Sep (E Africa), Jul-Dec (S Africa)	-	Sep-Feb	Mar-Aug

Table S5. Numerical scoring systems for the non-biometric species trait data used in this study, along with data sources.

Trait variable	Score					Source
	1	2	3	4	5	
Prey	Predominantly or entirely non-bird prey (mammals, reptiles, amphibians, and/or insects)	Generalist feeder; both bird and non-bird prey in equal or varying proportions	Predominantly non-bird prey outside the breeding season, but predominantly or exclusively bird prey during the breeding season	Predominantly or exclusively bird prey	-	Ferguson-Lees and Christie (2001); score for the Rock Kestrel based on Roberts Birds of Southern Africa, VIIth ed. (Hockey et al. 2005)
Hunting Style	Predominantly or exclusively non-aerial hunting methods (hovering, perch/still-hunting, quartering, terrestrial stalking, etc.); may occasionally hawk insects	Occasionally uses aerial hunting methods, or uses aerial hunting methods in conjunction with other, non-aerial methods; may rely predominantly on hawking	Largely aerial hunting methods, but occasionally non-aerial methods; may rely partly or largely on hawking	Predominantly or exclusively aerial hunting methods (aerial chasing, tail-chasing, or stooping)	-	Ferguson-Lees and Christie (2001); score for the Rock Kestrel based on Roberts Birds of Southern Africa, VIIth ed. (Hockey et al. 2005)
Habitat	Forest dependency listed as "High"	Forest dependency listed as "Medium"	Forest dependency listed as "Low"	Forest dependency listed as "Does not normally occur in forest"; habitat description contains forest, open woodland, plantations, or forest edge	Forest dependency listed as "Does not normally occur in forest"; habitat description does not contain any forest types	Ferguson-Lees and Christie (2001), BirdLife International (2020); score for the Rock Kestrel based on Roberts Birds of Southern Africa, VIIth ed. (Hockey et al. 2005)

Table S6. Marginal posterior means, standard deviations, and 95% credible intervals of the solar radiation parameters in the simple, additive, and interactive INLA models for each malar stripe variable in the full dataset (N = 10906), along with the standard deviations of the phylogenetic and spatial random effects in all models. Fixed effects which demonstrated a substantial effect on the response (95% credible intervals do not or only marginally overlap zero) are bolded.

Model	**Phylogenetic Random Effect (SD)**				**Spatial Random Effect (SD)**				**Solar Radiation (Within Species)**				**Solar Radiation (Between Species)**			
	Mean	**SD**	**0.025**	**0.975**	**Mean**	**SD**	**0.025**	**0.975**	**Mean**	**SD**	**0.025**	**0.975**	**Mean**	**SD**	**0.025**	**0.975**
Length																
Solar Radiation Only	0.462	0.827	0.350	0.634	0.056	0.013	0.033	0.084	-0.032	0.038	-0.108	0.042	-0.043	0.071	-0.184	0.097
Solar Radiation + Body Mass	0.420	0.664	0.430	0.689	0.073	0.014	0.048	0.104	-0.035	0.042	-0.177	0.046	-0.033	0.076	-0.183	0.117
Solar Radiation + HWI	0.432	0.743	0.325	0.642	0.051	0.019	0.025	0.099	-0.033	0.038	-0.109	0.043	-0.035	0.072	-0.179	0.108
Solar Radiation + Prey	0.416	0.660	0.298	0.646	0.057	0.018	0.032	0.101	-0.033	0.039	-0.110	0.044	-0.039	0.074	-0.185	0.107
Solar Radiation + Habitat	0.435	0.740	0.327	0.659	0.071	0.016	0.041	0.105	-0.031	0.037	-0.104	0.041	-0.039	0.073	-0.183	0.105
Solar Radiation * Body Mass (Within Species)	0.455	0.828	0.345	0.604	0.053	0.016	0.029	0.092	-0.028	0.042	-0.112	0.054	-0.025	0.082	-0.188	0.137
Solar Radiation * Body Mass (Between Species)	0.440	0.767	0.328	0.612	0.056	0.013	0.031	0.083	-0.032	0.038	-0.107	0.043	-0.101	0.084	-0.266	0.064
Solar Radiation * HWI (Within Species)	0.464	0.777	0.337	0.639	0.056	0.018	0.031	0.100	-0.037	0.042	-0.120	0.046	-0.026	0.071	-0.165	0.113
Solar Radiation * HWI (Between Species)	0.471	0.827	0.353	0.651	0.056	0.013	0.031	0.083	-0.032	0.038	-0.109	0.043	-0.004	0.081	-0.164	0.154
Solar Radiation * Prey (Within Species)	0.423	0.674	0.308	0.611	0.053	0.015	0.030	0.087	-0.036	0.039	-0.113	0.040	-0.038	0.072	-0.182	0.104

Table S6. cont.

Solar Radiation * Prey (Between Species)	0.411	0.669	0.297	0.604	0.072	0.017	0.042	0.107	-0.032	0.037	-0.104	0.041	-0.017	0.076	-0.168	0.133
Solar Radiation * Habitat (Within Species)	0.469	0.774	0.338	0.655	0.053	0.015	0.030	0.089	-0.031	0.039	-0.108	0.045	-0.040	0.077	-0.193	0.111
Solar Radiation * Habitat (Between Species)	0.418	0.797	0.327	0.558	0.071	0.016	0.042	0.105	-0.033	0.038	-0.108	0.042	-0.047	0.074	-0.192	0.098
Width																
Solar Radiation Only	0.538	0.976	0.409	0.729	0.241	0.038	0.175	0.324	-0.028	0.035	-0.097	0.041	**-0.177**	**0.074**	**-0.323**	**-0.033**
Solar Radiation + Body Mass	0.546	1.000	0.420	0.750	0.231	0.033	0.180	0.307	-0.027	0.035	-0.096	0.041	**-0.206**	**0.081**	**-0.366**	**-0.046**
Solar Radiation + HWI	0.542	0.978	0.414	0.750	0.242	0.035	0.182	0.321	-0.028	0.035	-0.096	0.040	**-0.173**	**0.075**	**-0.322**	**-0.026**
Solar Radiation + Prey	0.518	0.889	0.384	0.734	0.241	0.035	0.182	0.318	-0.027	0.035	-0.096	0.041	**-0.171**	**0.075**	**-0.319**	**-0.024**
Solar Radiation + Habitat	0.507	0.883	0.380	0.718	0.233	0.033	0.180	0.309	-0.028	0.035	-0.097	0.041	-0.140	0.076	-0.291	0.010
Solar Radiation * Body Mass (Within Species)	0.541	0.975	0.412	0.746	0.249	0.036	0.186	0.329	-0.023	0.035	-0.092	0.045	**-0.207**	**0.082**	**-0.368**	**-0.047**
Solar Radiation * Body Mass (Between Species)	0.545	0.996	0.420	0.756	0.234	0.032	0.181	0.307	-0.027	0.035	-0.096	0.041	**-0.233**	**0.089**	**-0.409**	**-0.057**
Solar Radiation * HWI (Within Species)	0.545	0.988	0.417	0.753	0.236	0.033	0.182	0.312	-0.036	0.036	-0.108	0.035	**-0.174**	**0.075**	**-0.322**	**-0.026**
Solar Radiation * HWI (Between Species)	0.562	1.025	0.430	0.766	0.235	0.033	0.181	0.312	-0.028	0.035	-0.096	0.041	**-0.159**	**0.082**	**-0.321**	**0.000**

Table S6. cont.

Solar Radiation * Prey (Within Species)	0.523	0.904	0.389	0.736	0.236	0.032	0.183	0.309	-0.030	0.036	-0.100	0.040	**-0.171**	**0.075**	**-0.319**	**-0.025**
Solar Radiation * Prey (Between Species)	0.506	0.850	0.371	0.727	0.241	0.035	0.182	0.319	-0.027	0.035	-0.096	0.041	**-0.162**	**0.083**	**-0.325**	**0.000**
Solar Radiation * Habitat (Within Species)	0.520	0.896	0.386	0.729	0.234	0.033	0.181	0.309	-0.029	0.035	-0.099	0.040	**-0.140**	**0.077**	**-0.292**	**0.011**
Solar Radiation * Habitat (Between Species)	0.337	0.450	0.214	0.556	0.253	0.040	0.182	0.340	-0.028	0.035	-0.096	0.040	**-0.183**	**0.071**	**-0.323**	**-0.043**
Darkness																
Solar Radiation Only	0.533	1.029	0.421	0.714	0.224	0.027	0.176	0.283	**-0.084**	**0.042**	**-0.168**	**-0.002**	-0.100	0.071	-0.241	0.040
Solar Radiation + Body Mass	0.541	1.030	0.422	0.716	0.221	0.027	0.176	0.280	**-0.084**	**0.042**	**-0.168**	**-0.001**	-0.131	0.079	-0.287	0.025
Solar Radiation + HWI	0.536	1.016	0.417	0.709	0.230	0.030	0.176	0.293	**-0.084**	**0.042**	**-0.168**	**-0.002**	-0.108	0.074	-0.253	0.036
Solar Radiation + Prey	0.514	0.963	0.399	0.695	0.228	0.030	0.174	0.290	**-0.084**	**0.043**	**-0.169**	**-0.001**	-0.095	0.073	-0.239	0.047
Solar Radiation + Habitat	0.519	0.960	0.398	0.689	0.232	0.032	0.173	0.298	**-0.085**	**0.042**	**-0.169**	**-0.002**	-0.069	0.076	-0.220	0.081
Solar Radiation * Body Mass (Within Species)	0.541	1.029	0.422	0.716	0.221	0.026	0.175	0.278	**-0.076**	**0.041**	**-0.158**	**0.005**	-0.132	0.079	-0.288	0.024
Solar Radiation * Body Mass (Between Species)	0.533	1.007	0.413	0.706	0.226	0.028	0.176	0.287	**-0.084**	**0.043**	**-0.169**	**-0.001**	**-0.175**	**0.087**	**-0.347**	**-0.005**
Solar Radiation * HWI (Within Species)	0.536	1.032	0.423	0.721	0.225	0.028	0.176	0.285	**-0.088**	**0.044**	**-0.176**	**-0.001**	-0.106	0.073	-0.252	0.037

Table S6. cont.

Solar Radiation * HWI (Between Species)	0.537	1.031	0.423	0.719	0.229	0.030	0.175	0.291	**-0.084**	**0.042**	**-0.168**	**-0.002**	-0.096	0.081	-0.258	0.062
Solar Radiation * Prey (Within Species)	0.518	0.963	0.400	0.697	0.230	0.029	0.177	0.291	**-0.086**	**0.044**	**-0.173**	**-0.001**	-0.096	0.073	-0.240	0.047
Solar Radiation * Prey (Between Species)	0.530	0.980	0.408	0.713	0.224	0.027	0.176	0.284	**-0.084**	**0.043**	**-0.168**	**-0.001**	-0.107	0.080	-0.265	0.050
Solar Radiation * Habitat (Within Species)	0.525	0.997	0.411	0.705	0.221	0.026	0.176	0.279	**-0.083**	**0.043**	**-0.169**	**0.001**	-0.069	0.076	-0.219	0.079
Solar Radiation * Habitat (Between Species)	0.519	0.971	0.402	0.697	0.223	0.027	0.176	0.283	**-0.085**	**0.042**	**-0.169**	**-0.002**	-0.085	0.076	-0.237	0.065

Table S7. Marginal posterior means, standard deviations, and 95% credible intervals of the solar radiation parameters in the simple, additive, and interactive INLA models for each malar stripe variable in a subset of the dataset with birds with uniform plumage removed (N = 9668), along with the standard deviations of the phylogenetic and spatial random effects in all models. Fixed effects which demonstrated a substantial effect on the response (95% credible intervals do not or only marginally overlap zero) are bolded.

Model	**Phylogenetic Random Effect (SD)**				**Spatial Random Effect (SD)**				**Solar Radiation (Within Species)**				**Solar Radiation (Between Species)**			
	Mean	**SD**	**0.025**	**0.975**	**Mean**	**SD**	**0.025**	**0.975**	**Mean**	**SD**	**0.025**	**0.975**	**Mean**	**SD**	**0.025**	**0.975**
Length																
Solar Radiation Only	0.359	0.477	0.228	0.573	0.091	0.024	0.047	0.139	-0.036	0.055	-0.144	0.071	0.054	0.082	-0.110	0.216
Solar Radiation + Body Mass	0.309	0.398	0.192	0.549	0.090	0.020	0.056	0.134	-0.037	0.053	-0.141	0.066	0.081	0.087	-0.092	0.253
Solar Radiation + HWI	0.354	0.463	0.222	0.569	0.092	0.025	0.047	0.141	-0.037	0.055	-0.145	0.071	0.067	0.083	-0.098	0.231
Solar Radiation + Prey	0.319	0.416	0.201	0.588	0.091	0.022	0.056	0.143	-0.035	0.053	-0.140	0.068	0.062	0.085	-0.107	0.230
Solar Radiation + Habitat	0.352	0.493	0.230	0.549	0.089	0.029	0.037	0.144	-0.036	0.055	-0.145	0.072	0.020	0.087	-0.152	0.190
Solar Radiation * Body Mass (Within Species)	0.325	0.391	0.193	0.566	0.089	0.021	0.054	0.134	-0.026	0.051	-0.127	0.075	0.084	0.088	-0.091	0.258
Solar Radiation * Body Mass (Between Species)	0.304	0.423	0.199	0.501	0.090	0.020	0.057	0.136	-0.034	0.052	-0.138	0.069	-0.018	0.090	-0.195	0.158
Solar Radiation * HWI (Within Species)	0.368	0.512	0.240	0.579	0.094	0.026	0.048	0.146	-0.046	0.055	-0.155	0.062	0.072	0.083	-0.093	0.235
Solar Radiation * HWI (Between Species)	0.363	0.536	0.247	0.574	0.090	0.033	0.033	0.155	-0.035	0.053	-0.141	0.070	0.093	0.092	-0.092	0.272
Solar Radiation * Prey (Within Species)	0.328	0.442	0.211	0.576	0.091	0.027	0.043	0.144	-0.039	0.055	-0.148	0.069	0.057	0.086	-0.113	0.226

Table S7. cont.

Solar Radiation * Prey (Between Species)	0.351	0.473	0.226	0.612	0.091	0.026	0.045	0.142	-0.036	0.054	-0.144	0.071	0.060	0.089	-0.117	0.235
Solar Radiation * Habitat (Within Species)	0.337	0.471	0.222	0.576	0.092	0.022	0.051	0.136	-0.037	0.055	-0.145	0.070	0.017	0.091	-0.165	0.195
Solar Radiation * Habitat (Between Species)	0.351	0.444	0.215	0.575	0.091	0.023	0.049	0.138	-0.036	0.055	-0.144	0.072	0.030	0.092	-0.153	0.210
Width																
Solar Radiation Only	0.560	0.905	0.402	0.823	0.270	0.037	0.207	0.373	-0.009	0.043	-0.094	0.076	-0.169	0.092	-0.352	0.011
Solar Radiation + Body Mass	0.566	0.912	0.405	0.832	0.270	0.036	0.208	0.351	-0.009	0.043	-0.094	0.076	**-0.204**	**0.102**	**-0.406**	**-0.004**
Solar Radiation + HWI	0.558	0.895	0.399	0.832	0.268	0.036	0.207	0.348	-0.009	0.043	-0.094	0.076	-0.163	0.094	-0.351	0.021
Solar Radiation + Prey	0.544	0.845	0.381	0.812	0.270	0.037	0.206	0.352	-0.009	0.043	-0.094	0.077	-0.155	0.095	-0.343	0.033
Solar Radiation + Habitat	0.495	0.728	0.335	0.764	0.262	0.036	0.203	0.344	-0.010	0.043	-0.094	0.075	-0.126	0.098	-0.317	0.068
Solar Radiation * Body Mass (Within Species)	0.552	0.915	0.402	0.803	0.268	0.042	0.192	0.357	-0.002	0.044	-0.088	0.084	**-0.206**	**0.101**	**-0.405**	**-0.007**
Solar Radiation * Body Mass (Between Species)	0.545	0.880	0.392	0.811	0.246	0.030	0.197	0.312	-0.009	0.043	-0.094	0.076	**-0.241**	**0.114**	**-0.467**	**-0.016**
Solar Radiation * HWI (Within Species)	0.558	0.905	0.401	0.825	0.261	0.035	0.204	0.342	-0.022	0.044	-0.110	0.066	-0.162	0.094	-0.349	0.021
Solar Radiation * HWI (Between Species)	0.593	1.000	0.436	0.849	0.269	0.036	0.209	0.349	-0.009	0.043	-0.094	0.075	-0.128	0.100	-0.328	0.067

Table S7. cont.

Solar Radiation * Prey (Within Species)	0.530	0.814	0.369	0.807	0.268	0.036	0.207	0.347	-0.012	0.044	-0.099	0.075	-0.156	0.095	-0.345	0.031
Solar Radiation * Prey (Between Species)	0.550	0.840	0.381	0.830	0.273	0.038	0.206	0.357	-0.009	0.043	-0.093	0.076	-0.164	0.099	-0.360	0.032
Solar Radiation * Habitat (Within Species)	0.499	0.727	0.336	0.782	0.259	0.035	0.203	0.341	-0.011	0.044	-0.097	0.076	-0.127	0.099	-0.321	0.069
Solar Radiation * Habitat (Between Species)	0.047	0.020	0.018	0.306	0.274	0.038	0.208	0.356	-0.010	0.043	-0.094	0.075	**-0.197**	**0.091**	**-0.377**	**-0.017**
Darkness																
Solar Radiation Only	0.353	0.495	0.233	0.586	0.383	0.041	0.307	0.468	-0.100	0.060	-0.219	0.018	-0.140	0.089	-0.320	0.032
Solar Radiation + Body Mass	0.355	0.505	0.236	0.579	0.379	0.040	0.305	0.463	-0.100	0.059	-0.218	0.017	-0.160	0.090	-0.340	0.015
Solar Radiation + HWI	0.356	0.496	0.234	0.597	0.373	0.038	0.308	0.457	-0.099	0.060	-0.217	0.018	-0.149	0.091	-0.334	0.026
Solar Radiation + Prey	0.361	0.502	0.237	0.598	0.370	0.038	0.307	0.455	-0.099	0.060	-0.218	0.017	-0.137	0.091	-0.320	0.039
Solar Radiation + Habitat	0.347	0.468	0.223	0.588	0.372	0.038	0.307	0.456	-0.100	0.060	-0.219	0.017	-0.116	0.095	-0.309	0.067
Solar Radiation * Body Mass (Within Species)	0.368	0.521	0.244	0.595	0.365	0.038	0.301	0.449	-0.088	0.058	-0.203	0.026	-0.161	0.091	-0.341	0.016
Solar Radiation * Body Mass (Between Species)	0.390	0.566	0.262	0.609	0.349	0.029	0.299	0.412	-0.099	0.060	-0.219	0.019	**-0.211**	**0.097**	**-0.403**	**-0.020**
Solar Radiation * HWI (Within Species)	0.353	0.488	0.231	0.597	0.374	0.039	0.306	0.458	-0.112	0.063	-0.237	0.011	-0.151	0.091	-0.336	0.024

Table S7. cont.

Solar Radiation * HWI (Between Species)	0.351	0.465	0.223	0.610	0.384	0.044	0.302	0.473	-0.099	0.060	-0.219	0.019	-0.181	0.110	-0.405	0.027
Solar Radiation * Prey (Within Species)	0.345	0.468	0.223	0.611	0.379	0.039	0.310	0.462	-0.098	0.061	-0.219	0.021	-0.141	0.092	-0.326	0.036
Solar Radiation * Prey (Between Species)	0.340	0.458	0.219	0.592	0.372	0.037	0.309	0.454	-0.098	0.060	-0.218	0.020	-0.150	0.090	-0.332	0.025
Solar Radiation * Habitat (Within Species)	0.343	0.458	0.219	0.587	0.375	0.038	0.308	0.459	-0.099	0.061	-0.219	0.021	-0.115	0.095	-0.308	0.069
Solar Radiation * Habitat (Between Species)	0.296	0.366	0.179	0.555	0.369	0.046	0.301	0.477	-0.100	0.060	-0.219	0.017	-0.141	0.098	-0.341	0.046

Table S8. Marginal posterior means, standard deviations, and 95% credible intervals of the species trait parameters in the additive and interactive INLA models for each malar stripe variable in a subset of the dataset with birds with uniform plumage removed (N = 9668). Fixed effects which demonstrated a substantial effect on the response (95% credible intervals do not or only marginally overlap zero) are bolded.

Variable	Variable Type	Mean	SD	0.025	0.975
Length					
Body Mass	Fixed	0.159	0.133	-0.105	0.418
+ Interaction Term (Within Species)		0.141	0.132	-0.123	0.398
+ Interaction Term (Between Species)		**0.345**	**0.140**	**0.067**	**0.620**
HWI	Fixed	-0.117	0.115	-0.344	0.110
+ Interaction Term (Within Species)		-0.114	0.114	-0.339	0.111
+ Interaction Term (Between Species)		-0.114	0.113	-0.337	0.110
Prey	Fixed	0.060	0.146	-0.227	0.348
+ Interaction Term (Within Species)		0.061	0.146	-0.227	0.350
+ Interaction Term (Between Species)		0.073	0.151	-0.224	0.369
Habitat	Fixed	0.100	0.100	-0.096	0.298
+ Interaction Term (Within Species)		0.105	0.105	-0.100	0.313
+ Interaction Term (Between Species)		0.123	0.124	-0.121	0.367
Width					
Body Mass	Fixed	-0.126	0.155	-0.431	0.179
+ Interaction Term (Within Species)		-0.132	0.152	-0.432	0.168
+ Interaction Term (Between Species)		-0.049	0.188	-0.421	0.322
HWI	Fixed	-0.067	0.143	-0.349	0.216
+ Interaction Term (Within Species)		-0.061	0.143	-0.343	0.222
+ Interaction Term (Between Species)		-0.058	0.145	-0.343	0.229
Prey	Fixed	0.136	0.168	-0.192	0.469
+ Interaction Term (Within Species)		0.134	0.167	-0.194	0.466
+ Interaction Term (Between Species)		0.140	0.170	-0.193	0.475
Habitat	Fixed	-0.155	0.120	-0.396	0.077
+ Interaction Term (Within Species)		-0.154	0.122	-0.399	0.082
+ Interaction Term (Between Species)		**-0.524**	**0.112**	**-0.743**	**-0.303**
Darkness					
Body Mass	Fixed	-0.123	0.130	-0.379	0.134
+ Interaction Term (Within Species)		-0.149	0.127	-0.400	0.102
+ Interaction Term (Between Species)		-0.021	0.151	-0.318	0.278
HWI	Fixed	0.088	0.118	-0.144	0.323
+ Interaction Term (Within Species)		0.101	0.120	-0.134	0.340
+ Interaction Term (Between Species)		0.092	0.120	-0.143	0.329
Prey	Fixed	0.011	0.138	-0.263	0.284
+ Interaction Term (Within Species)		0.018	0.141	-0.259	0.298
+ Interaction Term (Between Species)		0.004	0.137	-0.265	0.274
Habitat	Fixed	-0.071	0.104	-0.276	0.136
+ Interaction Term (Within Species)		-0.076	0.106	-0.285	0.134
+ Interaction Term (Between Species)		-0.153	0.122	-0.392	0.090

Table S9. Marginal posterior means, standard deviations, and 95% credible intervals of the interaction terms between the solar radiation parameters and species trait variables in the interactive INLA models for each of the malar stripe variables in a subset of the dataset with birds with uniform plumage removed (N = 9668). Terms for which a substantial interaction was found (95% credible intervals do not or only marginally overlap zero) are bolded.

Interaction Term	Mean	SD	0.025	0.975
Length				
Solar Radiation (Within Species) * Body Mass	**-0.090**	**0.045**	**-0.179**	**-0.003**
Solar Radiation (Between Species) * Body Mass	**0.122**	**0.048**	**0.028**	**0.218**
Solar Radiation (Within Species) * HWI	0.040	0.052	-0.063	0.144
Solar Radiation (Between Species) * HWI	-0.066	0.109	-0.280	0.152
Solar Radiation (Within Species) * Prey	-0.023	0.056	-0.135	0.087
Solar Radiation (Between Species) * Prey	-0.032	0.106	-0.245	0.173
Solar Radiation (Within Species) * Habitat	0.008	0.050	-0.090	0.105
Solar Radiation (Between Species) * Habitat	-0.035	0.097	-0.226	0.155
Width				
Solar Radiation (Within Species) * Body Mass	-0.053	0.037	-0.126	0.020
Solar Radiation (Between Species) * Body Mass	0.039	0.055	-0.072	0.148
Solar Radiation (Within Species) * HWI	0.044	0.042	-0.038	0.127
Solar Radiation (Between Species) * HWI	-0.119	0.129	-0.371	0.136
Solar Radiation (Within Species) * Prey	-0.027	0.044	-0.115	0.059
Solar Radiation (Between Species) * Prey	0.043	0.114	-0.184	0.266
Solar Radiation (Within Species) * Habitat	0.008	0.039	-0.069	0.086
Solar Radiation (Between Species) * Habitat	**0.462**	**0.091**	**0.283**	**0.641**
Darkness				
Solar Radiation (Within Species) * Body Mass	**-0.099**	**0.049**	**-0.197**	**-0.003**
Solar Radiation (Between Species) * Body Mass	0.068	0.052	-0.035	0.169
Solar Radiation (Within Species) * HWI	0.044	0.059	-0.070	0.161
Solar Radiation (Between Species) * HWI	0.062	0.120	-0.171	0.303
Solar Radiation (Within Species) * Prey	0.011	0.060	-0.108	0.128
Solar Radiation (Between Species) * Prey	0.145	0.105	-0.063	0.353
Solar Radiation (Within Species) * Habitat	-0.017	0.053	-0.122	0.089
Solar Radiation (Between Species) * Habitat	0.117	0.094	-0.068	0.303

a)

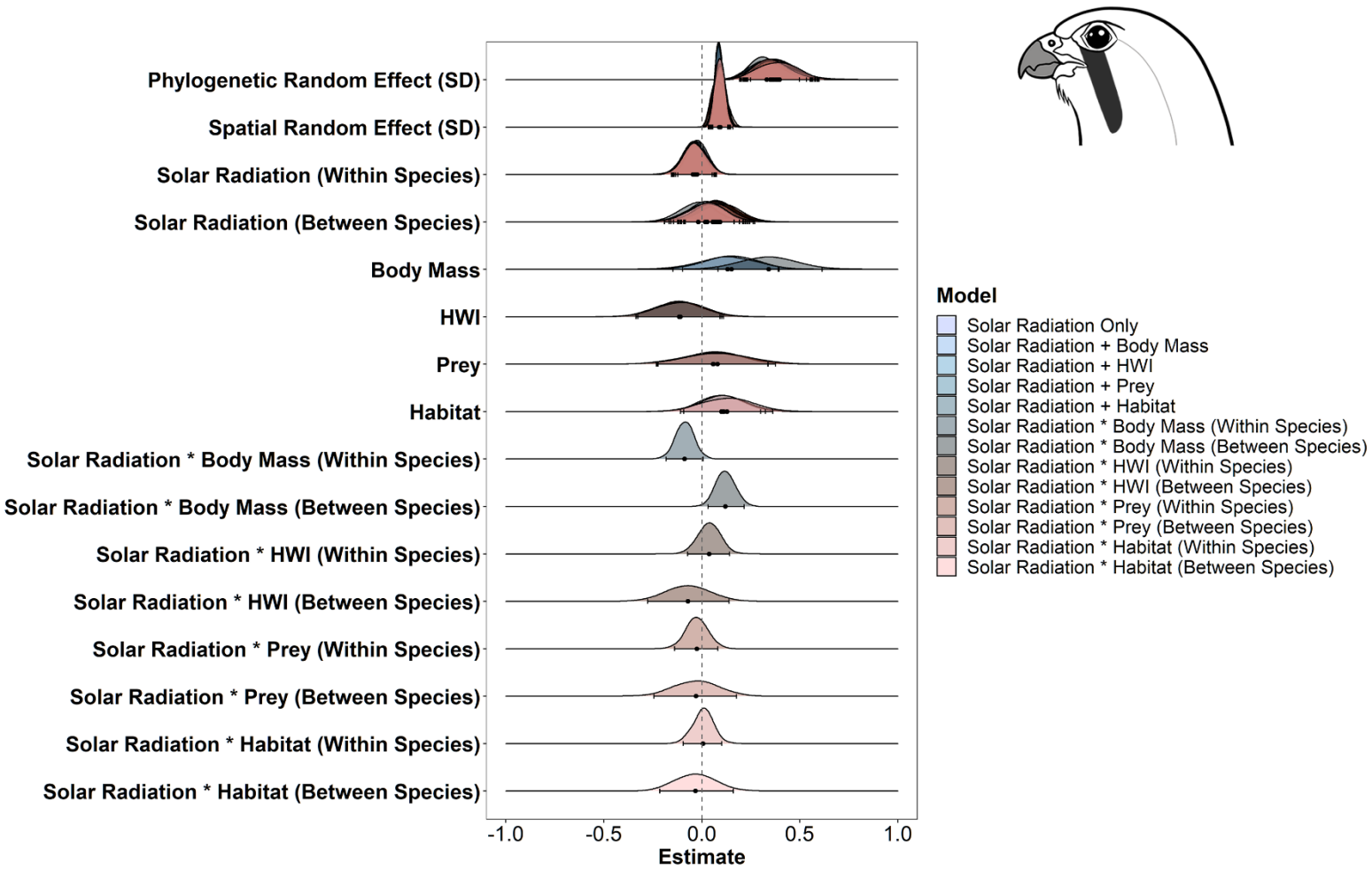

Figure S1a. Marginal posterior probability distributions of the fixed effects and the standard deviations of the phylogenetic and spatial random effects in the INLA models for malar stripe length in a subset of the dataset with birds with uniform plumage removed (N = 9668), colour coded according to model specification. Since all fixed effect variables were standardized prior to model fitting, these coefficients are comparable to one another. Plots were created using the R package phyr (Li et al. 2020).

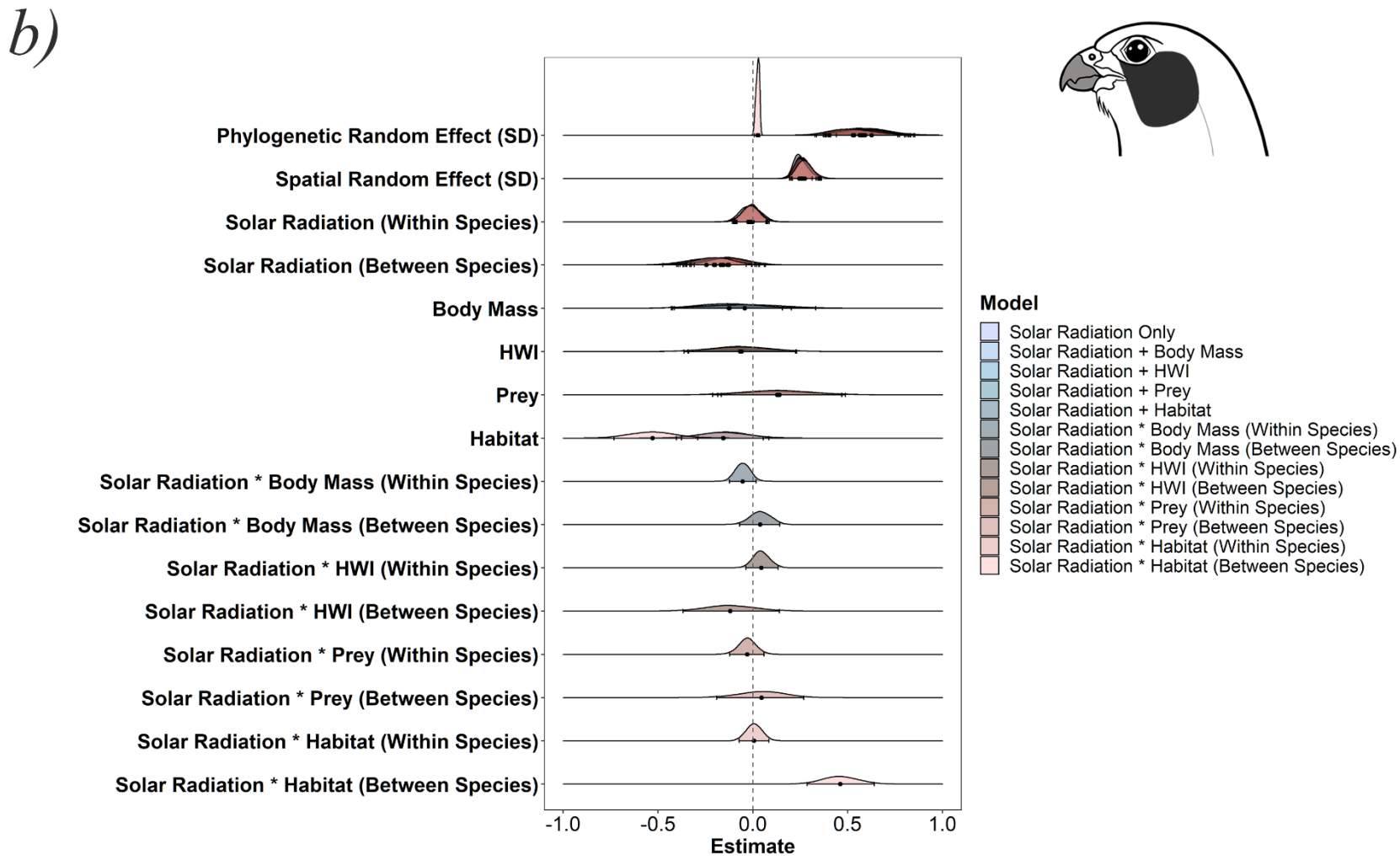

Figure S1b. Marginal posterior probability distributions of the fixed effects and the standard deviations of the phylogenetic and spatial random effects in the INLA models for malar stripe width in a subset of the dataset with birds with uniform plumage removed (N = 9668), colour coded according to model specification. Since all fixed effect variables were standardized prior to model fitting, these coefficients are comparable to one another. Plots were created using the R package phyr (Li et al. 2020).

c)

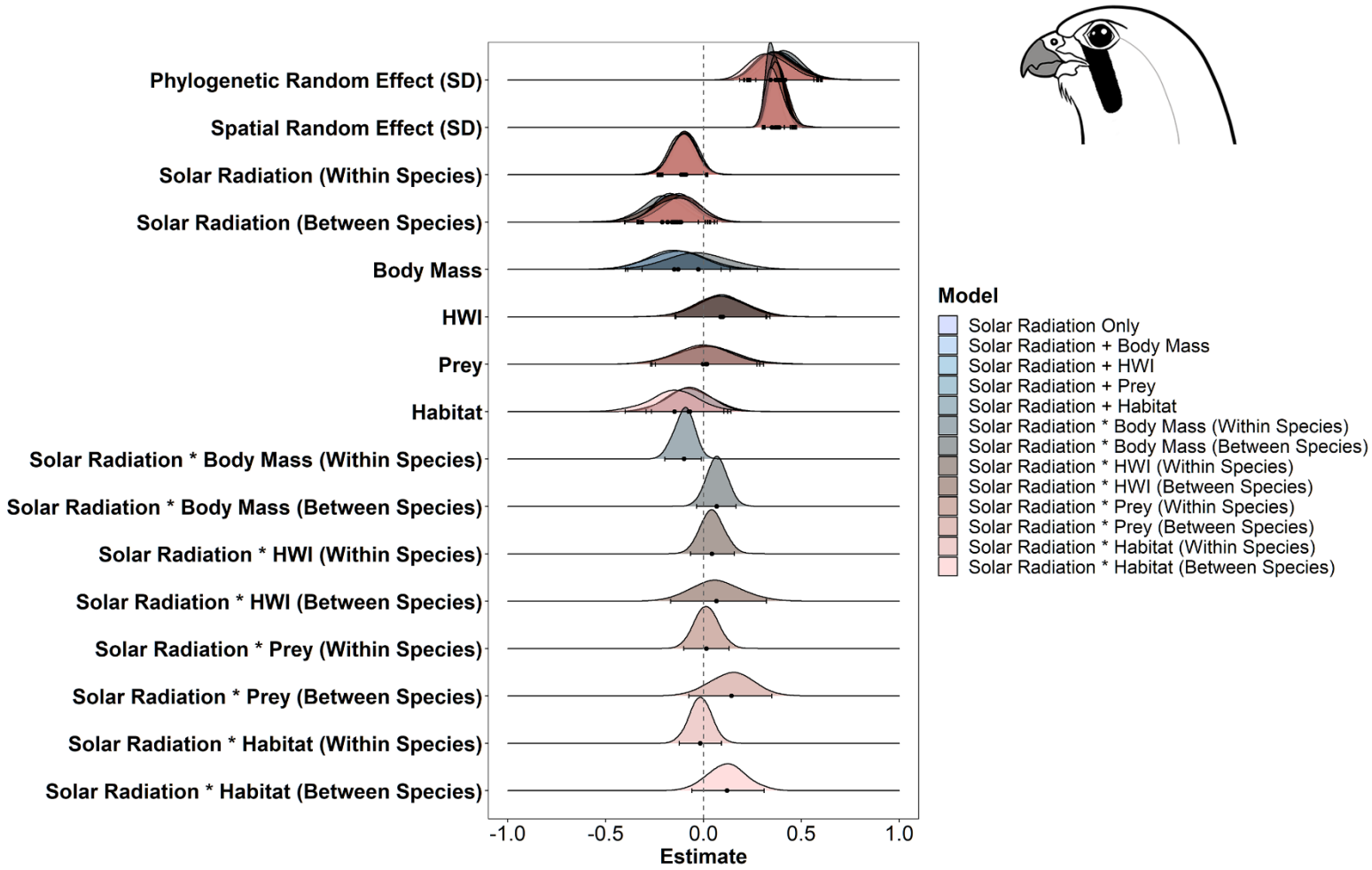

Figure S1c. Marginal posterior probability distributions of the fixed effects and the standard deviations of the phylogenetic and spatial random effects in the INLA models for malar stripe darkness in a subset of the dataset with birds with uniform plumage removed (N = 9668), colour coded according to model specification. Since all fixed effect variables were standardized prior to model fitting, these coefficients are comparable to one another. Plots were created using the R package phyr (Li et al. 2020).

Table S10. Results of GLS models analysing the relationships between malar stripe characteristics and solar radiation in the Gyrfalcon and the Eleonora's Falcon, with birds with zero scores for all variables removed from the analysis (N = 86 and N = 111, respectively). Species and variables for which evidence for a relationship was found ($p < 0.05$, 95% confidence interval does not overlap zero) are bolded.

Model	Log Likelihood	Residual standard error	Residual df	Solar Radiation					
				Mean	SE	95% CI Lower	95% CI Upper	t	p
Gyrfalcon									
Length	-111.039	0.880	79	0.137	0.099	-0.071	0.346	1.289	0.201
Width	**-114.380**	**0.915**	**79**	**-0.292**	**0.111**	**-0.509**	**-0.075**	**-2.638**	**0.010**
Darkness	**-111.070**	**0.888**	**79**	**-0.299**	**0.107**	**-0509**	**-0.089**	**-2.791**	**0.007**
Eleonora's Falcon									
Length	-152.609	0.957	104	-0.039	0.098	-0.154	0.232	0.395	0.693
Width	-156.158	0.988	104	0.061	0.102	-0.138	0.260	0.601	0.549
Darkness	-147.341	0.940	104	0.200	0.103	-0.001	0.402	1.948	0.054